AUTONOMOUS UNIVERSITY OF MADRID
FACULTY OF SCIENCES
DEPARTMENT OF MOLECULAR BIOLOGY

Characterization and targeting of the NF-κB pathway in non-Hodgkin lymphoma

By

Lina Odqvist

Doctoral Thesis
Madrid 2013

INDEX

TABLE OF CONTENTS

PUBLICATIONS

ARTICLES

NIK controls classical and alternative NF-κB activation and is necessary for the survival of human T cell lymphoma cells

Odqvist L, Sánchez-Beato M, Montes-Moreno S, Martín-Sánchez E, Pajares R, Sánchez-Verde L, Ortiz-Romero PL, Rodriguez J, Rodríguez-Pinilla SM, Iniesta-Martínez F, Solera-Arroyo J, Ramos-Asensio R, Flores T, Menarguez Palanca J, García Bragado F, Domínguez Franjo P, Piris MA.

Clinical Cancer Research. 2013 May1;16(9):2319-30.

Simultaneous pan-PI3K and MEK inhibition as a potential therapeutic strategy in peripheral T cell lymphomas

Martin-Sanchez E, Rodriguez-Pinilla SM, Sanchez-Beato M, Lombardia L, Dominguez-Gonzalez B, Romero D, Odqvist L, Garcia-Sanz P, Wozniak MB, Kurz G, Blanco C, Mollejo M, Alves FJ, Menarguez J, Gonzalez-Palacios F, Rodriguez-Peralto JL, Ortiz-Romero PL, Garcia JF, Bischoff JR, Piris MA.

Haematologica. 2013 Jan;98(1):57-64.

EBV-positive diffuse large B-cell lymphoma of the elderly is an aggressive post-germinal center B-cell neoplasm characterized by prominent nuclear factor-kB activation

Montes-Moreno S, Odqvist L, Diaz-Perez JA, Lopez AB, de Villambrosía SG, Mazorra F, Castillo ME, Lopez M, Pajares R, García JF, Mollejo M, Camacho FI, Ruiz-Marcellán C, Adrados M, Ortiz N, Franco R, Ortiz-Hidalgo C, Suarez-Gauthier A, Young KH, Piris MA.

Modern Pathology. 2012 Jul;25(7):968-82.

Nanog regulates proliferation during early fish development

Camp E, Sánchez-Sánchez AV, García-España A, Desalle R, Odqvist L, Enrique O'Connor J, Mullor JL.

Stem Cells. 2009 Sep;27(9):2081-91.

SUMMARY

SUMMARY

NF-κB is a family of transcription factors responsible for the regulation of hundreds of genes controlling key cellular processes such as proliferation, apoptosis and inflammation. The activation of NF-κB is an Achilles heel of many lymphoid malignancies. Therefore, a lot of effort is being made in investigating its regulatory mechanisms and exploring its therapeutic potentials. In this doctoral thesis, we have investigated the NF-κB pathway in non-Hodgkin lymphomas, with the aim of characterizing its expression and clinical impact in human lymphomas and identifying putative molecular targets able to interfere with its activation and lymphoma cell survival.

Abnormal NF-κB activation has been linked to Diffuse Large B-cell Lymphoma (DLBCL) and has been described to play a key role in the pathogenesis of a specific molecular subtype of this malignancy, the ABC-DLBCL. In the first part of this work, we evaluated the expression of NF-κB by immunohistochemistry in a large series of DLBCL cases. The five different family members showed a heterogeneous and intricate expression pattern, but most remarkably, NF-κB signaling was found to be a prominent feature not only in ABC-DLBCL, but also in GCB-DLBCL, a subtype of DLBCL previously described to lack NF-κB activation. Furthermore, c-Rel expression was observed as a common feature in DLBCL and was able to identify a subset of patients with enhanced overall survival.

Peripheral T-cell lymphomas (PTCL) are highly aggressive tumors with a current lack of effective therapies, partly due to its unknown molecular pathology. In the second part of this work, we investigated the function of the NF-κB–inducing kinase (NIK) in NF-κB signaling and its potential as a molecular target in T-cell lymphomas. We showed that the NF-κB pathway was activated in a subset of PTCLs associated with poor overall survival. NIK was overexpressed in a number of PTCL cell lines and primary samples and a role for NIK as a critical regulator of both classical and alternative NF-κB activation was unveiled. Using genetic silencing, we demonstrated a pivotal role for NIK in the survival of these tumor cells as NIK depletion led to a dramatic induction of apoptosis in NIK-overexpressing cells. The knockdown of NIK led to a modulation of several key factors in cancer cell survival and apoptosis evasion and had also an impact on other important survival pathways, apart from NF-κB, in PTCL pathogenesis. The results of this part of the study indicate that NIK could be a promising therapeutic target in these aggressive malignancies.

ABBREVIATIONS

ABBREVIATIONS

ABC Activated B-cell-like
AITL Angioimmunoblastic T-cell lymphoma
ALCL Anaplastic large cell lymphoma
ALK Anaplastic lymphoma kinase
APC Allophycocyanin
API2 Apoptosis inhibitor 2
ATCC American Type Culture Collection
ATL Adult T-cell leukemia/lymphoma
BAFF B-cell activating factor
BAFFR B-cell activating factor receptor
BCL2 B-cell lymphoma 2
BCL2L1 BCL2-like 1
BCL6 B-cell lymphoma 6
BCR B-cell receptor
BIRC Baculoviral IAP Repeat-Containing protein
BLIMP1 B lymphocyte-induced maturation protein
BSA Bovine Serum Albumin
BTK Bruton tyrosine kinase
CARD11 Caspase recruitment domain family, member 11
CFLAR CASP8 and FADD-like apoptosis regulator
c-Flip Cellular FLICE-like inhibitory protein
c-IAP Cellular inhibitors of apoptosis
CD Cluster of differentiation
cDNA Complementary DNA
CDKN2A Cyclin-dependent kinase inhibitor 2A
CHOP Cyclophosphamide, Hydroxy doxorubicin, Oncovin and Prednisone
CNIO Spanish National Cancer Research Centre
ConA Concanavalin A
cRNA Complementary RNA
Cy3 Cyanine 3-conjugated dUTP
Cy5 Cyanine 5-conjugated dUTP
CYLD Cylindromatosis
CXCL13 Chemokine (C-X-C motif) ligand 13
DAB Diaminobenzidine
DAPI 4',6-diamidino-2-phenylindole
DLBCL Diffuse Large B Cell Lymphoma
DMEM Dulbecco´s modified eagle medium
DMSO Dimethyl Sulphoxide
DNA Deoxyribonucleic acid
dNTP 2'-Deoxyribonucleoside-5'-triphosphate
DSMZ Deutsche Sammlung von Mikroorganismen und Zellkulturen
ECACC European Collection of Cell Cultures
EBER Epstein-Barr Virus encoded RNA
EBV Epstein-Barr virus
ECOG Eastern Cooperative Oncology Group
ELISA Enzyme-Linked Immunosorbent Assay
ERK Extracellular signal-regulated kinase
FAM 6-carboxyfluorescein
FBS Fetal Bovine Serum
FDR False Discovery Rate
FITC fluorescein isothiocyanate
Fn14 Fibroblast growth factor-inducible response protein 14
FL Follicular Lymphoma
FOXP1 forkhead box protein P1
GCB Germinal center B-cell-like
GCET1 Germinal center B-cell transcript 1
GEP Gene Expression Profiling
GFP Green fluorescent protein
GSEA Gene Set Enrichment Analysis
GUSB Glucuronidase beta
HHV6B Human herpes virus 6B
HL Hodgkin Lymphoma
HRP Horseradish peroxidase
HTLV1 Human T-lymphotropic virus-1

HUMV Hospital Universitario Marqués de Valdecilla

IARC International Agency of Cancer Research

IκB Inhibitory of kappa B

IKK Inhibitor of kappa B kinase

IL Interleukin

IL1R Interleukin 1 receptor

IMDM Iscove´s modified Dulbecco´s medium

IPI International prognostic index

IRAK4 Interleukin-1 receptor-associated kinase 4

ITK IL2-inducible T-cell kinase

JAK Janus kinase

JNK c-jun N-terminal kinase

KLF2 Kruppel-like factor 2

LB Luria-Bertani

LDH Lactate dehydrogenase

LMP1 Latent membrane protein 1

LTβR Lymphotoxin beta receptor

MALT Mucosa associated lymphoid tissue

MAPK Mitogen-activated protein kinase

MCL Mantle Cell Lymphoma

MCL1 Myeloid cell leukemia sequence 1

MEK MAPK/ERK kinase

MEKK3 MAPK/ERK kinase kinase 3

MF Mycosis Fungoides

MHC Major histocompatibility complex

miR MicroRNA

MMLV-RT Moloney Murine Leukemia Virus Reverse Transcriptase

mRNA Messenger RNA

MUM1 Multiple myeloma oncogene 1

MYC V-myc avian myelocytomatosis viral oncogene homolog

Myd88 Myeloid differentiation primary response 88

NEMO NF-κB essential modulator

NES Normalized enrichment score

NFAT Nuclear factor of activated T-cells

NF-κB Nuclear Factor Kappa B

NFKBIA Nuclear factor of kappa light polypeptide gene enhancer in B-cells inhibitor alpha

NHL Non-Hodgkin Lymphoma

NIK NF-κB–inducing kinase

NK Natural killer

NOS Not otherwise specified

NTC Non-template control

PARP Poly (ADP-ribose) polymerase 1

PBS Phosphate Buffered Saline

PBS-T Phosphate Buffered Saline with Tween

PCR Polymerase Chain Reaction

PD-1 Programmed death 1

PE Phycoerythrin

PFA Paraformaldehyde

PI Propidium Iodide

PI3K Phosphatidylinositol 3-kinase

PMSF Phenylmethylsulfonyl fluoride

PTCL Peripheral T-cell lymphoma

PTEN Phosphatase and tensin homolog

PRDM1 PR domain containing 1, with ZNF domain

RANK Receptor activator for NF-κB

R-CHOP Rituximab, Cyclophosphamide, Hydroxy doxorubicin, Oncovin and Prednisone

REL V-rel avian reticuloendotheliosis viral oncogene homolog

RELA V-rel avian reticuloendotheliosis viral oncogene homolog A

RELB **V**-rel avian reticuloendotheliosis viral oncogene homolog B

RHD REL homology domain

RIP Receptor-interacting protein
RIPA Radio immunoprecipitation assay
RNA Ribonucleic acid
rpm Revolutions per minute
RPMI Roswell Park Memorial Institute
RT Reverse Transcription
RT-qPCR Reverse transcription quantitative Polymerase chain reaction
SDS Sodium Dodecyl Sulfate
shRNA Short Hairpin RNA
siIKK siRNA against IKK
siKLF2 siRNA against KLF2
siNIK siRNA against NIK
siNTC Non-template control siRNA
siRNA Short/small interference RNA
siSTAT3 siRNA against STAT3
SMZL Splenic Marginal Zone Lymphoma
SS Sézary syndrome
STAT3 Signal transducer and activator of transcription 3
SYK Spleen tyrosine kinase
TAD Transactivation domain
TAK1 Transforming growth factor-beta-activated kinase 1
TALL1 TNF- and APOL-related leukocyte expressed ligand 1
TBS Tris Buffered Saline
TCR T-cell receptor
Th17 T helper 17
TIA-1 T-cell-restricted intracellular antigen-1
TLR Toll-like receptor
TMA Tissue Microarray
TNF Tumor necrosis factor
TNFR Tumor necrosis factor receptor
TNFAIP3 Tumor necrosis factor, alpha-induced protein 3
TNFRSF13B Tumor necrosis factor receptor superfamily member 13B
TP53 Tumor protein p53
TRAF TNF receptor-associated factors
VEGF-A Vascular endothelial growth factor A
WHO World Health Organization
XBP1 X-box binding protein 1
YAP1 Yes-associated protein 1
18S Human 18S ribosomal RNA

1. INTRODUCTION

1.1 Lymphomas

1.1.1 General features

Lymphoma is a cancer of the lymphatic system. It arises from malignant transformation and uncontrolled proliferation of B, T or NK cells, leading to the formation of tumors in several parts of the body, including lymph nodes, spleen, blood, bone marrow or other organs. The term lymphoma describes a heterogeneous group of neoplasms including over 60 entities, presenting different clinical course, treatment response and prognosis. A proper lymphoma classification is important for accurate clinical practice and treatment strategies. The World Health Organization (WHO) classification of neoplasms of the hematopoietic and lymphoid tissues (Swerdlow et al. 2008) describes the most recent classification system, which is used worldwide for the diagnosis of these tumors. Lymphomas are stratified according to their cell lineage and their derivation from immature or mature lymphocytes. Many lymphomas recapitulate stages of normal lymphocyte differentiation so that classification can to some extent be made according to the corresponding normal stage. Classification criteria are based on morphology, immunophenotype, genetic abnormalities and molecular and clinical features (Puente et al. 2011).

There are two major categories of lymphomas: Hodgkin lymphoma (HL, the first lymphoma to be described by Thomas Hodgkin in 1832) and non-Hodgkin lymphoma (NHL). NHL represents almost 90% of all lymphomas and accounts for around 3% of all cancers in Europe, where 7 individuals out of 100 000 get the disease each year (Data from the International Agency of Cancer Research, IARC, Globocan 2008). NHL can be further stratified into B or T/NK cell neoplasms, where B cell lymphomas account for nearly 85% of all NHL.

In this section, the lymphoma types relevant for the work of this doctoral thesis, diffuse large B cell lymphoma and peripheral T cell lymphoma, will be described.

1.1.2 Diffuse large B-cell lymphoma

1.1.2.1 General features

Diffuse large B-cell lymphoma (DLBCL) is the most common type of lymphoma in adults, accounting for 30 to 40% of all non-Hodgkin lymphomas in the United States as well as in Spain (Morton et al. 2006; Novelli et al. 2013). It is a form of mature B-cell lymphoma characterized by a diffuse growth pattern of neoplastic large B lymphocytes with large nuclei. The median age of diagnosis is in the 7th decade but children and young adults may also be affected (Swerdlow et al. 2008). Patients are often asymptomatic and the disease is often detected as a rapidly enlarging tumor mass at either nodal or extranodal sites. DLBCL is a molecularly and clinically heterogeneous entity and both morphologic and molecular variants have been described (Swerdlow et al. 2008).

1.1.2.2 Molecular characteristics and pathogenesis

Based on gene expression profiling, two different molecular subtypes of DLBCL are recognized according to the putative cell of origin; the activated B-cell-like (ABC) subtype, and the germinal center B-cell-like (GCB) subtype (Alizadeh et al. 2000; Lenz et al. 2008). These subtypes reflect distinct differentiation stages of normal B-cell development and differ in their clinical presentation, cure rates and oncogenic pathways (Staudt et al. 2005). GCB-DLBCLs express genes defining B cells of the germinal center, whereas the gene expression profile of ABC-DLBCL suggests that this subtype arises from post-germinal center B cells that are arrested in their differentiation process towards plasma cells. More recently, the distinction into ABC and GCB subtypes has been performed with high accuracy using immunohistochemistry of CD10, multiple myeloma oncogene 1 (MUM1) and B-cell lymphoma 6 (BCL6) (named Hans´algorithm (Hans et al. 2004)) or germinal center B-cell trascript 1 (GCET1), CD10, BCL6, MUM1 and forkhead box protein P1 (FOXP1) (Choi´s algorithm (Choi et al. 2009)).

During the germinal-center reaction, somatic hypermutation and class-switch recombination are two processes which induce modification in the B-cell immunoglobulin DNA in order to produce high affinity antibodies. These genetic modifications are necessary for normal immune response, but they can also be a source of DNA damage that can become pathologic

in lymphomas. A range of different genetic alterations has been described in DLBCL. Four recent reports using next generation sequencing of the DLBCL exome, reveal extensive genetic heterogeneity and >30 genetic lesions per case (Morin et al. 2011; Pasqualucci et al. 2011; Lohr et al. 2012; Zhang et al. 2013). Some of these are common between different molecular subtypes, and others are subtype-specific. *BCL6* gene translocation (involving 3q27) is the most common translocation reported in DLBCL, occurring in approximately 30% of patients (Pasqualucci et al. 2003). BCL6 is a repressor of transcription and a master regulator of the germinal-center phenotype where it represses genes involved in differentiation of plasma cells, cell cycle, apoptosis, and response to DNA damage (Lenz et al. 2010). Other frequent gene alterations in DLBCL affect chromatin modification (with approximately 40% of cases harboring alterations in histone methyltransferases or histone acetyltransferases) and immune recognition by T cells (Pasqualucci et al. 2011). In the GCB subtype, specific genetic lesions such as t(14;18) translocations (giving rise to immunoglobulin-driven BCL2 expression), V-myc avian myelocytomatosis viral oncogene homolog *(MYC)* translocations, V-rel avian reticuloendotheliosis viral oncogene homolog *(REL)* amplifications, phosphatase and tensin homolog *(PTEN)* deletions, and tumor protein 53 (*TP53)* mutations are recurrent (Rosenwald et al. 2002; Lenz et al. 2008). The ABC subtype is characterized by prominent NF-κB activation (Davis et al. 2001), which can partly be explained by frequent genetic lesions in mediators of NF-κB signaling (Compagno et al. 2009) (described in detail in the NF-κB section below). Inactivating lesions in PR domain containing 1 (*PRDM1*, the gene encoding B-lymphocyte maturation protein 1 (BLIMP1), a master regulator of plasma cell differentiation) is also a common feature of ABC-DLBCL (Mandelbaum et al. 2010).

Additionally, the oncogenic virus Epstein-Barr virus (EBV) has been associated with the etiology of DLBCL in a subgroup of patients. EBV is a ubiquitous human γ-herpesvirus, which infects primarily B cells, where it stays as a latent infection throughout the life of the individual (Kutok et al. 2006). EBV can transform B cells *in vitro* (Kaye et al. 1993) and even though EBV infections are harmless in the vast majority of individuals, latent EBV infections have been associated with several B-cell malignancies (Saha et al. 2011). EBV-positive DLBCL associated with advanced age was included as a separate entity of DLBCL in the WHO classification system of hematological malignancies 2008 (Swerdlow et al. 2008).

1.1.2.3 Treatment and prognosis

DLBCL is an aggressive lymphoma but can potentially be cured using anthracyclin-based chemotherapy, such as a combination of cyclophosphamide, doxorubicin, vincristine, and prednisone (CHOP). The addition of the anti-CD20 monoclonal antibody, Rituximab, to CHOP (R-CHOP), has significantly improved the prognosis in DLBCL and is today the standard treatment for DLBCL. Still, the cure rate of DLBCL is only 40-50% (Coiffier 2007; Coiffier et al. 2010; Lenz et al. 2010). The overall survival of patients of the ABC subtype is significantly inferior than that of patients with GCB subtype (Alizadeh et al. 2000; Lenz et al. 2010).

1.1.3 Peripheral T-cell lymphoma

1.1.3.1 General Features

Peripheral T-cell lymphomas (PTCLs), also called mature T-cell lymphomas, comprise a variety of malignancies that arise from abnormal growth of post-thymic mature T lymphocytes. Lymphomas derived from natural killer (NK) cells are also generally grouped under this category. The vast majority of T-cell lymphomas falls under the category PTCL, since they arise from mature lymphocytes in the peripheral lymphoid tissue (lymph nodes, spleen, mucosa-associated lymphoid tissue). T-cell lymphomas arising from immature T cells in the central lymphoid tissue (bone marrow and thymus) are called immature T cell lymphomas and will not be described in this work. PTCL is a heterogeneous group of over 20 malignant entities that are generally associated with a very poor prognosis and treatment response (Swerdlow et al. 2008). Classification of PTCL is challenging and does not well predict therapeutic strategies. The WHO 2008 classification of mature T- and NK-cell neoplasms is based mainly on morphology and immunophenotype and the subtypes are listed in Table 1.1. PTCLs account for approximately 12% of all NHL in Western countries (Piccaluga et al. 2011). Relative frequencies of PTCL subtypes from a study of an international adult population of 1314 patients (Vose et al. 2008) are shown in Figure 1.1.

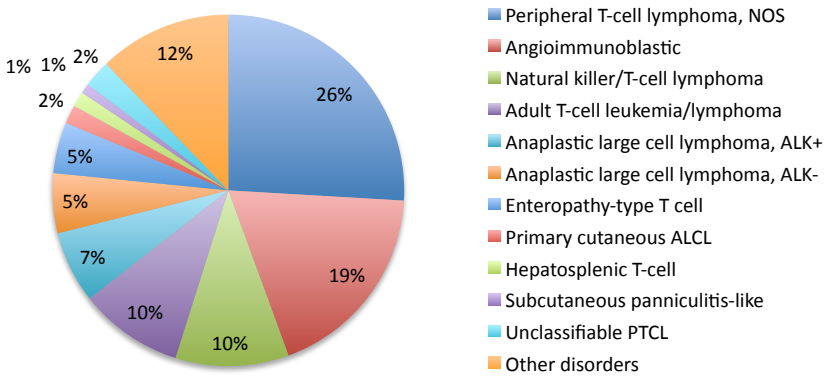

Figure 1.1 Relative frequencies of PTCL subtypes

Relative distribution of different PTCL subtypes in an international population of 1314 patients. Data extracted from Vose J et al., 2008. NOS = not otherwise specified, ALK = anaplastic lymphoma kinase, ALCL = anaplastic large cell lymphoma, PTCL = peripheral T-cell lymphoma.

The incidence of these neoplasms varies in different geographic regions and racial populations, where PTCL-NOS, AITL and ALCL are relatively more common in North America and Europe, while NK-TCL and ATLL are more frequent in Asia (Vose et al. 2008). In general, PTCLs have a higher incidence in Asia and South/Central America (Rudiger et al. 2002; Swerdlow et al. 2008; de Leval et al. 2011), partly overlapping with the endemicity of certain viruses, such as human T-lymphotropic virus-1 (HTLV1) and Epstein-Barr virus (EBV), described as risk factors for some subtypes of T-cell lymphoma (Swerdlow et al. 2008; Foss et al. 2011). A brief description of the PTCL subtypes used in this thesis project; peripheral T-cell lymphoma - not otherwise specified (PTCL-NOS), angioimmunoblastic T-cell lymphoma (AITL), anaplastic large cell lymphoma (ALCL) and cutaneous T-cell lymphoma), can be found in Table 1.2.

1.1.3.2 Molecular characteristics and pathogenesis

The molecular pathogenesis of PTCL is still largely unknown. The heterogeneous background of these malignancies, the low incidence, and a lack of experimental models contribute to the poor understanding of the biology of these disorders. Apart from chromosomal translocations involving the anaplastic lymphoma kinase (*ALK*) gene in ALCL, few recurrent genetic disorders are reported that can help explaining the pathogenesis of PTCL. ALK is a

tyrosine kinase receptor of the insulin receptor superfamily and its expression is normally absent in lymphoid cells (Morris et al. 1994). A constitutively active ALK has been shown to induce cell transformation and is involved in a complex signaling network including activation of signal transducer and activator of transcription 3 (STAT3), phosphatidylinositol 3-kinase / v-akt murine thymoma viral oncogene homolog (PI3K/AKT) and RAS/ Extracellular signal-regulated kinase (ERK) pathways (Ferreri et al. 2012). The (2;5)(p23;q35) translocation is the most common alteration giving rise to nucleophosmin (NPM)-ALK fusion protein, but variant ALK fusion partners have also been described and they all lead to an overexpression and activation of the ALK protein (Ferreri et al. 2012). Gene expression analysis of PTCL has shown distinct molecular profiles in different subtypes of PTCL as well as within PTCL subtypes (Piccaluga et al. 2007; Piccaluga et al. 2007; Iqbal et al. 2010). Results from these studies indicated NF-κB activation and abnormal methylation patterns in a group of PTCL (Martinez-Delgado et al. 2005; Costello et al. 2010).

Table 1.1 WHO classification of Mature T-cell and NK-cell neoplasms
(Swerdlow et al., 2008)

T cell prolymphocytic leukemia
Chronic lymphoproliferative disorder of NK-cells *
Aggressive NK cell leukaemia
Systemic EBV-positive T-cell lymphoproliferative disease of childhood
Hydroa vacciniforme-like lymphoma
Adult T-cell leukaemia/lymphoma
Extranodal NK/T cell lymphoma, nasal type
Enteropathy-associated T-cell lymphoma
Hepatosplenic T-cell lymphoma
Subcutaneous panniculitis-like T-cell lymphoma
Mycosis fungoides
Sézary syndrome
Primary cutaneous CD30 positive T-cell lymphoproliferative disorders
Lymphomatoid papulosis
Primary cutaneous anaplastic large cell lymphoma
Primary cutaneous gamma-delta T-cell lymphoma
Primary cutaneos CD8 positive aggressive epidermotropic cytotoxic T-cell lymphoma *
Primary cutaneous CD4 positive small/medium T-cell lymphoma *
Peripheral T-cell lymphoma, NOS
Angioimmunoblastic T-cell lymphoma
Anaplastic large cell lymphoma, ALK positive
Anaplastic large cell lymphoma, ALK negative *

* represents provisional entities

Molecular pathways that have been reported to be activated in T-cell lymphomas are the PI3K/AKT pathway, NF-κB pathway, Notch pathway, Janus kinase (JAK)/STAT pathway and the Mitogen-activated protein kinase (MAPK) pathway (Zhao 2010; Martin-Sanchez et al. 2013). The presence of viral infections, such as EBV, human T lymphotropic virus (HTLV) and human herpes virus 6B (HHV6B) in association with some T or NK lymphomas has led to the suggestion that these viruses might be involved in the etiology of PTCL (Quintanilla-Martinez et al. 2000; Swerdlow et al. 2008; Foss et al. 2011). Further information of the genetic and molecular aberrations of PTCL is summarized in Table 1.2.

1.1.3.3 Treatment and prognosis of PTCL

The heterogeneous nature of PTCL tumors is also reflected in the clinical outcome of these patients. In general terms, PTCLs are aggressive malignancies with a dismal prognosis. Figure 1.2 shows the overall survival curves of different PTCL entities.

Up to date, with the exception of some cutaneous T-cell lymphomas that can be treated with topical administration of corticoids, alkylating agents, bexarotene or ultraviolet radiation (Wilcox 2011), no PTCL-specific or subtype-specific treatment strategy is available. PTCLs have in the past been grouped as a minority together with aggressive B-cell lymphomas in clinical trials, resulting in the use of treatment strategies adapted for B-cell lymphomas. The standard therapy for PTCLs today is CHOP (cyclophosphamadide, doxorubicin, vincristine and prednisone) or CHOP-like regimens that add anthracyclines, in spite of reports showing that it is largely ineffective (Savage 2011). Although without optimal treatment outcome, ALCL is the only aggressive PTCL subtype where a significant group of patients can be cured using CHOP-based therapies (Armitage 2012). High-Dose Chemotherapy and Autologous Stem Cell Transplantation HDC/ASCT is also performed in eligible patients with refractory PTCL (Dearden et al. 2011).

Today, therapeutic trials for the different PTCL subtypes are beginning, with the hope of finding more effective treatments. Early phase clinical trials combining CHOP with different agents such as etoposide, the proteasome inhibitor Bortezomib or monoclonal antibodies for CD52 (alemtuzumab) or VEGF-A (bevacizumab), are being performed and other novel chemotherapy combinations including gemcitabine have shown variable response (Dearden et al. 2011; Savage 2011; Armitage 2012). Other new treatment strategies that have been evaluated in early phase clinical trials in PTCLs include Pralatrexate (a novel folate analog),

Bendamustine (alkylating agent), HDAC inhibitors (inhibitors of histone deacetylases), Lenalidomide (immunosuppressive agent), Aurora A kinase inhibitors, and Bortezomib (Savage 2011). More extensive studies are though needed in order to decide their clinical advantage. The lack of knowledge of the biological background of PTCL and the rarity of the

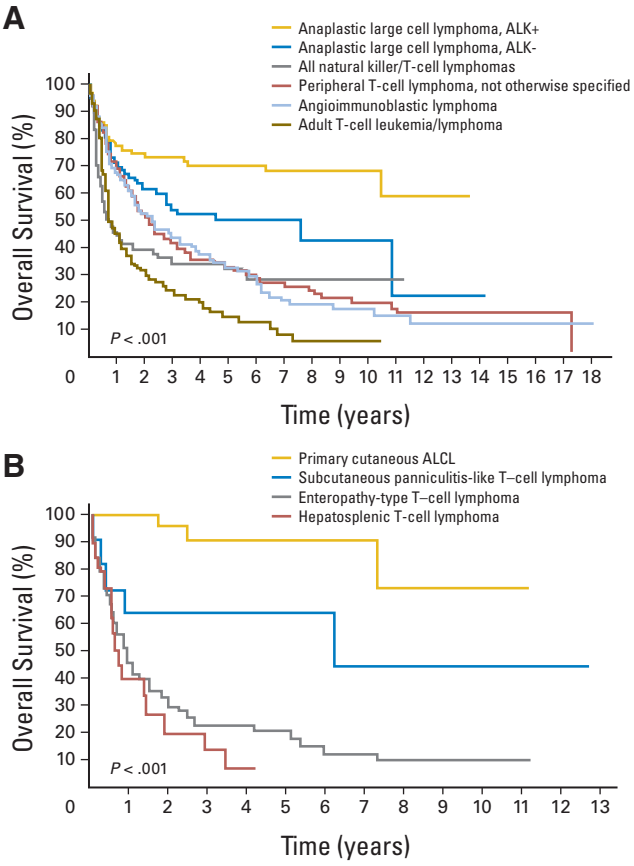

disease, have complicated the development of effective targeted therapies.

Figure 1.2 Kaplan-Meir curves of overall survival of patients with different subtypes of PTCL.
A) Overall survival patients with the most common type of T cell lymphomas. B) Overall survival of patients with less common subtypes. Reproduced from Vose J et al. 2008.

As in B-cell lymphomas, the International Prognostic Index (IPI) is commonly used as a prognostic tool in PTCL and is inversely related to survival (Armitage 2012). The IPI is calculated taking into account the Ann Arbor stage, lactate dehydrogenase (LDH)-levels, performance status (Eastern Cooperative Oncology Group, ECOG), number of extranodal sites, and age at diagnosis (Swerdlow et al. 2008). Apart from the IPI, several other markers have been suggested to predict survival in PTCL, including p53, Ki67, CD30 and EBV infection (Pescarmona et al. 2001; Rudiger et al. 2002; Foss et al. 2011).

Table 1.2 Characteristics of the most common types of PTCL

PTCL subtype	Clinical Manifestations	Morphology	Immunophenotype	Pathogenesis and genetic alterations
Peripheral T-cell lymphoma, not otherwise specified (PTCL-NOS)	PTCL-NOS describes a heterogeneous category, which doesn't fulfill the criteria to be classified into any other specific PTCL entity. Patients present enlarged lymph nodes and often advanced disease involving bone marrow, liver, spleen and extranodal tissues. Most patients are adults.	Diffuse infiltrates of atypical intermediate/large cells with irregular nuclei. Proliferation is usually high and T-cell associated antigens are variably expressed.	Predominantly CD4+/CD8- phenotype and loss of pan-T markers such as CD5 and CD7 with maintained CD2 expression. Frequently TCRß+ and clonal rearrangement of T-cell receptor (TCR) genes. Some cases present CD30 expression. (Rodriguez-Abreu et al. 2008; de Leval et al. 2011)et al 2011)	Complex karyotypes. Some recurrent chromosomal alterations, such as t(5;9)(q33;q22), involving *ITK* and *SYK* tyrosine kinases (Zettl et al. 2004; Streubel et al. 2006). Gene expression profiling revealed deregulation in proliferation, apoptosis, cell adhesion and matrix remodeling and a subset of cases have a gene expression profile characteristic of AITL. PTCL-NOS is a molecularly heterogeneous entity, probably containing several molecular subgroups. (Iqbal et al. 2010).
Angio-immunoblastic T-cell lymphoma (AITL)	Acute or subacute systemic illness with generalized lymphadenopathy. Fever, weight loss and presense of hepatomegaly, splenomegaly and skin rash are common (de Leval et al. 2010). AITL affects mainly middle-aged and elderly.	Polymorphous infiltrate of medium-sized T cells with pale cytoplasm, involving lymph nodes. Proliferation of high endothelial venules (HEV). Often EBV-positive B cells. (Zhou et al. 2007; Vose et al). 2008)	CD4+ with presence of reactive CD8+ T-cell. Pan T-cell antigens (CD3, CD2 and CD5). T_{FH}-markers (CD10, CXCL13;PD-1). Frequently Clonal rearrangement of TCR (Tan et al. 2006; de Leval et al. 2010)	The viruses EBV and HHV6B have been suggested to play a role in the malignant transformation of these cells (Dunleavy et al. 2007; Foss et al. 2011), and some recurrent cytogenetic abnormalities have been reported, such as trisomy or chromosomes 3, 5 and 21, gain of X and loss of 6q (de Leval et al. 2011).
Anaplastic large cell lymphoma (ALCL)	ALCL, ALK+ is more frequent in children and young adults and has a male predominance. Advanced stage disease with lymphadenopathy, fever, and both nodal and extranodal involvement. ALCL, ALK- occurs in older patients and present worse clinical outcome. (Vose et al. 2008; Fornari et al. 2009)	Variable proportion of hallmark large cells with abundant cytoplasm and eccentric, horseshoe- or kidney-shaped nuclei.	CD30-positive. Loss of T-cell markers (CD3, CD2, CD5 and CD43) can occur frequently in both ALK+ and ALK- tumors (Bonzheim et al. 2004), and most cases are positive for cytotoxic associated antigens such as TIA1, granzyme B and perforin (Iqbal et al. 2010).	Translocations involving *ALK* in ALCL, ALK+, with frequent secondary chromosomal imbalances (Morris et al. 1994; Salaverria et al. 2008). A few recurrent alterations in ALCL, ALK-, such as gain of 1q and 6p21(Salaverria et al. 2008). ALK+ and ALK- ALCL have different chromosomal alterations and gene expression profile, probably indicating different underlying molecular mechanisms of these entities (Lamant et al. 2007).
Cutaneous T cell lymphomas: Mycosis fungoides (MF) and Sézary syndrome (SS)	MF has an indolent clinical course and arises as skin patches, which can later disseminate and form tumors. SS is an aggressive, leukemic form presenting erythroderma, generalized lymphadenopathy with neoplastic T-cells in skin, lymph nodes and peripheral blood.	Stage-dependent. Skin infiltration of small to medium-sized T lymphocytes with cerebriform nuclei.	The immunophenotype is commonly CD2+, CD3+, TCRß+, CD5+, CD4+ and CD8-, but loss of several T-cell antigens is also reported (Robson 2010; Wong et al. 2011).	Complex karyotype with few recurrent alterations. CD28- and microenvironment-dependence and altered cytokine profile (McCusker et al. 1997; Berger et al. 2005; Wong et al. 2011). Viral infections possibly involved, but no clear evidences are reported (Hwang et al. 2008). Constitutive STAT3 activation and inactivation of CDKN2A/p16INK4A and PTEN have been described in MF (Navas et al. 2000; Scarisbrick et al. 2000; Wong et al. 2011)

Note: Information extracted from WHO classification of hematological tumors (swerdlow et al. 2008) , if not otherwise specified. Abbreviations : ALK = Anaplastic lymphoma kinase, TCR = T cell receptor, TCRß = T cell receptor beta chain, TIA = T-cell-restricted intracellular antigen 1, ITK = IL2-inducible T-cell kinase, SYK = Spleen tyrosine kinase, STAT3 = Signal *transducer and activator of*

1.2 The NF-κB family of transcription factors

Nuclear factor-kappa B (NF-κB) was first discovered in 1986 by David Baltimore and his group as a transcription factor that binds to the enhancer of the kappa light chain gene in B cells (Sen et al. 1986). The NF-κB transcription factors were then identified as major regulators of innate and adaptive immunity as well as inflammation (Li et al. 2002). After several observations that the NF-κB pathway was deregulated in numerous diseases such as cancer, diabetes and inflammatory disorders, the function and regulation of these transcription factors have been studied extensively.

The NF-κB family of transcription factors include 5 members in mammals: NF-κB1 (p50 and its precursor p105), NF-κB2 (p52 and its precursor p100), RelA (also named p65), RelB, and c-Rel. All of them are characterized by a Rel Homology Domain (RHD) in their N-terminal (Hoffmann et al. 2006). The RHD is responsible for homo- and hetero-dimerization of the transcription factors, and specific DNA binding. Whereas RelA, RelB and c-Rel contain a C-terminal transcription activation domain (TAD), p100/p52 and p105/p50 lack this domain and must therefore heterodimerize with other factors in order to positively regulate transcription(Hayden et al. 2008). Although several dimers are possible, RelB preferentially dimerize with p100/p52, while RelA and c-Rel usually form heterodimers with p50/p105 (Vallabhapurapu et al. 2009).

Latent NF-κB transcription factors are expressed in most mammalian cell types and can regulate inducible gene transcription in response to a broad range of stimuli. NF-κB regulates the expression of hundreds of genes involved in cellular processes such as inhibition of apoptosis (Beg et al. 1996), stimulation of cell proliferation (Joyce et al. 2001) and promotion of cell migration and invasion (Huang et al. 2001). NF-κB dimers bind to DNA sequences called κB sites (5´-GGGRNWYYCC-3´, where N is any base, R is purine, W is adenine or thymine, and Y is pyrimidine) in the promoter and enhancer regions of target genes. Target-gene selectivity is achieved at several levels, including dimer composition, post-translational modifications, chromatin barriers, and synergy between NF-κB and other transcription factors and auxiliary proteins (Smale 2011). The expression of genes regulated by NF-κB is essential to a normal development and function of the immune system (Hayden et al. 2011), skeletal system (Novack 2011) and epithelium (Wullaert et al. 2011). Up to date, the majority of NF-κB research has been focused on its function in immunology and its role

in cancer. Much of our knowledge of the biological role of NF-κB has come from a range of different murine knockout models. NF-κB has multiple roles in regulating normal development and function of the immune system, including the development of lymphoid structures, the differentiation of myeoloid and lymphoid cells and proliferation and survival of lymphocytes (reviewed in Hayden et al. 2011, Vallabhapurapu et al. 2009 and Hoffmann et al. 2006). The role of NF-κB in cancer will be described below.

1.2.1 The NF-κB signaling pathway

In most cell types, the NF-κB dimers are held inactive in the cytoplasm by specific inhibitors, called inhibitory kappa B proteins (IκBs). These IκB proteins, including IκBα, IκBβ and IκBε, contain characteristic ankyrin repeats in their structure, which bind to the RHD of the NF-κB dimers and prevent their nuclear translocation. In the C-terminal of p100 and p105, these ankyrin repeats are also present, which confer IκB functions to the full length of these transcription factors (Karin et al. 2000). The phosphorylation of p100 or p105 leads to proteasomal partial degradation to form p52 and p50, which lack the C-terminal inhibitory domain. Inducing stimuli, such as tumor necrosis factor (TNF)-receptor or antigen-receptor activation, gives rise to the activation of the IκB kinase (IKK) complex, responsible for the phosphorylation of IκB, leading to its subsequent ubiquitination and degradation. The IKK complex contains two kinase subunits, IKKα and IKKβ, and one regulatory subunit, IKKγ (also called NEMO). Specific IKK subunits have preferences for particular IκBs, which in turn have certain predilections for specific NF-κB dimers, although the patterns of these preferences are not fully understood. The release of the NF-κB dimers from the IκB proteins, permits their nuclear translocation, DNA-binding and transcription of target genes (Hayden et al. 2008).

The NF-κB signaling has been broadly divided into two major signaling pathways: the classical (also called canonical) NF-κB pathway, and the alternative (or non-canonical) pathway (Figure 1.3). The classical pathway relies on inducible degradation of IκBs and nuclear translocation of dimers containing p50, RelA or c-Rel (Vallabhapurapu et al. 2009). Canonical NF-κB is dependent on the kinase activity of the IKKβ subunit (Li et al. 1999). The alternative pathway, which was identified by Michael Karin and colleages in 2001 (Senftleben et al. 2001), is independent of IKKβ and NEMO and relies on the kinase activity

of IKKα and the NF-κB-inducing kinase, NIK, leading to the inducible processing of p100 and liberation of preferentially p52/RelB dimers (Sun 2011).

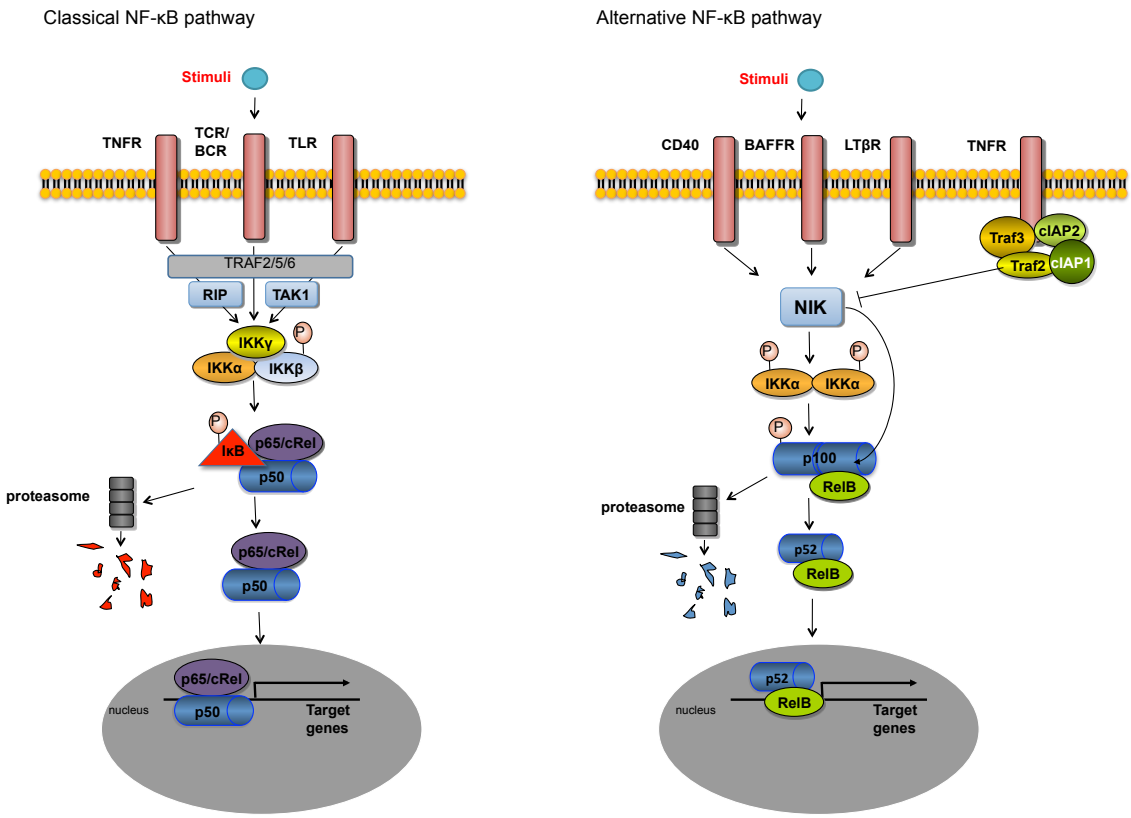

Figure 1.3 Classical and alternative NF-κB signaling cascades

Prototypic schemes of classical (to the left) and alternative (to the right) NF-κB pathways. In the classical pathway, receptor stimulation leads to the phosphorylation of the IKK complex (IKKβ phosphorylation is essential) which in turn phosphorylates IκB. Phosphorylated IκB is targeted for proteasomal degradation, liberating the p50-p65/c-Rel dimer, allowing their nuclear translocation. In the alternative pathway, receptor engagement leads to the recruitment and decomposition of the TRAF2-TRAF3-cIAP1/2 complex which is responsible for NIK degradation in resting cells. NIK accumulation gives rise to IKKα and p100 phosphorylation with subsequent p100 proteasomal processing and nuclear translocation of p52/RelB heterodimers.

A diverse set of stimuli can activate the NF-κB pathway through the engagement of a range of different receptors. The mechanism by which the IKK complex is activated is complicated and depends on the receptor and cell type. The classical arm of the NF-κB pathway can be activated by numerous stimuli and receptors, including TNF-receptors, Toll-like receptors, IL-

1R and antigen receptors (T-cell receptor, TCR, and B-cell receptor, BCR) (Hayden et al. 2012). Upon binding of a ligand to the receptor, signaling proceeds by the binding of several adapter proteins to the receptor. Of these, the receptor-interacting proteins (RIPs) are particularly important for classical NF-κB activation. The adapter proteins facilitate the recruitment of other adapter proteins with E3 ubiquitin ligase activity, the TNF receptor-associated factors (TRAFs). TRAF can then ubiquitinate RIP and recruit the IKK complex to the receptor complex where the recruitment of kinases that can activate the kinase activity of IKK is facilitated (for review, see Vallabhapurapu et al. 2009). For IKK phosphorylation, the kinases transforming growth factor-beta-activated kinase 1 (TAK1) and MAPK/ERK kinase kinase 3 (MEKK3) or autophosphorylation have been suggested (Wang et al. 2001; Yang et al. 2001).

The activation of the alternative arm has so far only been linked to a handful of signals. These include members of the TNF receptor superfamily such as B-cell activating factor receptor (BAFFR), lymphotoxin β receptor (LTβR), CD40 and receptor activator for NF-κB (RANK), Fn14 and CD30 (Claudio et al. 2002; Coope et al. 2002; Dejardin et al. 2002; Saitoh et al. 2003; Sun 2011). Additionally, it is known that both the classical and alternative pathway can be activated by oncogenic viruses, such as EBV and HTLV-1 (Xiao et al. 2001; Atkinson et al. 2003; Luftig et al. 2004). In the alternative NF-κB pathway, the stimulation of TNF receptors gives rise to the activation of the NF-κB-inducing kinase (NIK). NIK is a kinase that is essential for the activation of the alternative pathway (Xiao et al. 2001). NIK activates IKKα, which leads to the phosphorylation of p100, resulting in its polyubiquitination mediated by the ubiquitin ligase β-TrCP, and its subsequent proteasomal processing to p52. Nuclear accumulation of mainly p52/RelB heterodimers is observed after activation of the alternative pathway (reviewed in Razani et al. 2011 and Sun 2011). It has been suggested that NIK is regulated by a receptor-associated multi-protein complex consisting of TRAF2, TRAF3 and the cellular inhibitors of apoptosis 1 and 2 (c-IAP1 and c-IAP2, also called BIRC2 and BIRC3). These proteins target NIK for ubiquitin-dependent degradation. Receptor activation leads to degradation of TRAF3, which prevents the association of NIK to the complex resulting in NIK stabilization and activation (Zarnegar et al. 2008).

Figure 1.3 represents prototypic alternative and classical NF-κB signaling cascades. The two pathways are thought to give rise to the transcription of distinct sets of target genes and also display different kinetics. The classical pathway is fast acting, responding within minutes

after stimulation, whereas the alternative pathway responds more slowly and is dependent of protein synthesis for its activation (Hoffmann et al. 2006; Liang et al. 2006). However, the fact that both pathways can be activated at the same time and in cases by the same receptors, the existence of crosstalk between the pathways, and the influence of numerous known and unknown regulators, makes the gene expression induced by either one of the two pathways hard to characterize. Biologically, the canonical pathway is largely responsible for the regulation of inflammation and the control of lymphoid cell proliferation and apoptosis during the immune response, and the alternative pathway is more associated with the regulation of the development of the lymphoid organs (Bonizzi et al. 2004).

1.2.2 The NF-κB-inducing kinase (NIK)

NIK, encoded by the gene *MAP3K14*, was discovered in 1997 as a kinase mediating NF-κB activation downstream TNF and IL-1 receptors (Malinin et al. 1997). NIK knockout mice (NIK-/-) (Yin et al. 2001) or mice harboring an inactivating point mutation in NIK (aly/aly mice) (Shinkura et al. 1999), however, showed no defects in TNFα-induced NF-κB activation. On the other hand, p100 processing was blocked and NIK was later identified as the kinase necessary for p100 processing and activation of the IKKα-dependent alternative NF-κB pathway (Senftleben et al. 2001; Xiao et al. 2001). Both NIK-/- and aly/aly mice showed lack of lymph nodes and Peyer´s patches, disorganized splenic and thymic structures, and poor antibody response upon immunization. They also presented defects in B-cell proliferation and function (Yamada et al. 2000), reduced number of CD4+CD5+ regulatory T cells (Tregs) (Kajiura et al. 2004) and impairment in the differentation to Th17 T cells (Jin Blood 2009).
Hence, NIK is suggested to be important for proper lymphoid organogenesis, lymphocyte differentiation and function, as well as controlling autoimmunity. NIK also plays a role in bone microenvironment where it is needed for p100 processing downstream RANKL for proper osteoclast differentiation (Novack et al. 2003).

NIK is a serine/threonine kinase belonging to the mitogen-activating protein kinase kinase kinase (MAP3K) family (Figure 1.4). NIK binds to and activates IKKα by phosphorylation of IKKα residue Ser-176 (Ling et al. 1998). Although with lower affinity, NIK has also been reported to interact with and activate IKKβ (Woronicz et al. 1997; Delhase et al. 1999). Activated IKKα binds and phosphorylates its substrate p100, leading to its ubiquitination, partial proteasomal degradation and loss of its C-terminal region (containing the IκB –like

domain), forming p52. It appears that NIK not only activates IKKα, but also assist in docking p100 to IKKα (Xiao et al. 2004). Moreover, it has also been reported that NIK can directly phosphorylate p100 (Xiao et al. 2001).

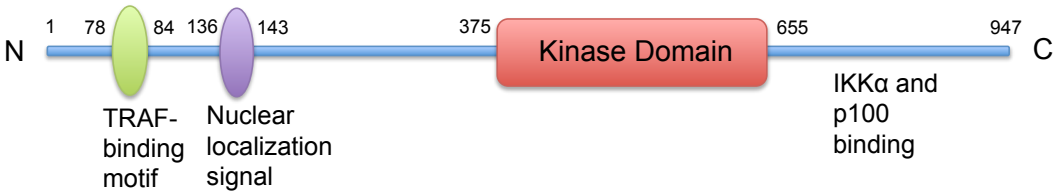

Figure 1.4 Schematic diagram of human NIK protein

Human NIK is a 947-amino acid protein with a molecular weight of 104 kD. In its N-terminal there is a TRAF-binding motif and a nuclear localization signal, whereas the binding of IKKα and p100 occurs in the C-terminal region. NIK has a core kinase domain with flanked N- and C-terminal regions that are conserved between species but differ from other serine/threonine kinases.

Signals from a subset of TNFR family members have been reported to induce NIK-dependent NF-κB activation. These include CD40, BAFFR, LTβR, RANK, Fn14, and CD27 (Claudio et al. 2002; Pham et al. 2011; Yin et al. 2001; Coope et al. 2002; Saitoh et al. 2003; Ramakrishnan et al. 2004). NIK is an unstable protein and has a rapid turnover in nonstimulated cells due to a constant ubiquitination-dependent proteasomal degradation (Liao et al. 2004). Controlling NIK protein stability has appeared as a central mechanism for regulating alternative NF-κB signaling. Upon stimulation of one of the receptors above mentioned, NIK is stabilized and the accumulation of NIK protein leads to its activation and induction of p100 processing (Figure 1.5). The mechanism of receptor-induced NIK stabilization has recently been revealed in several studies. TRAF3 was first shown to interact with the N-terminal domain of NIK and to target its ubiquitination and degradation and has been identified as a major negative regulator of NIK stability (Liao et al. 2004). TRAF3 knockout mice (TRAF3-/-) exhibit NIK stabilization and activation of the alternative NF-κB pathway, while TRAF3 overexpression induces NIK proteasomal degradation (Liao et al. 2004; He et al. 2006). It was later demonstrated that TRAF3 is a part of a multi-subunit ubiquitin ligase complex composed by TRAF2, TRAF3, cIAP1 and cIAP2, where TRAF3 serves as and adapter molecule and cIAP1 and CIAP2 are the E3 ubiquitin ligases responsible for NIK ubiquitination and degradation in unstimulated cells (Varfolomeev et al. 2007). Deletion of TRAF2, TRAF3 or

cIAP1/2 leads to increased NIK accumulation and p100 processing (Vallabhapurapu et al. 2008; Zarnegar et al. 2008). The stimulation of CD40 or BAFFR starts an ubiquitination cascade within the TRAF2/3-cIAP1/2 complex, terminating in the polyubiquitination and degradation of TRAF3, and liberation of NIK from the ubiquitin ligase complex (Hostager et al. 2003; Vallabhapurapu et al. 2008).

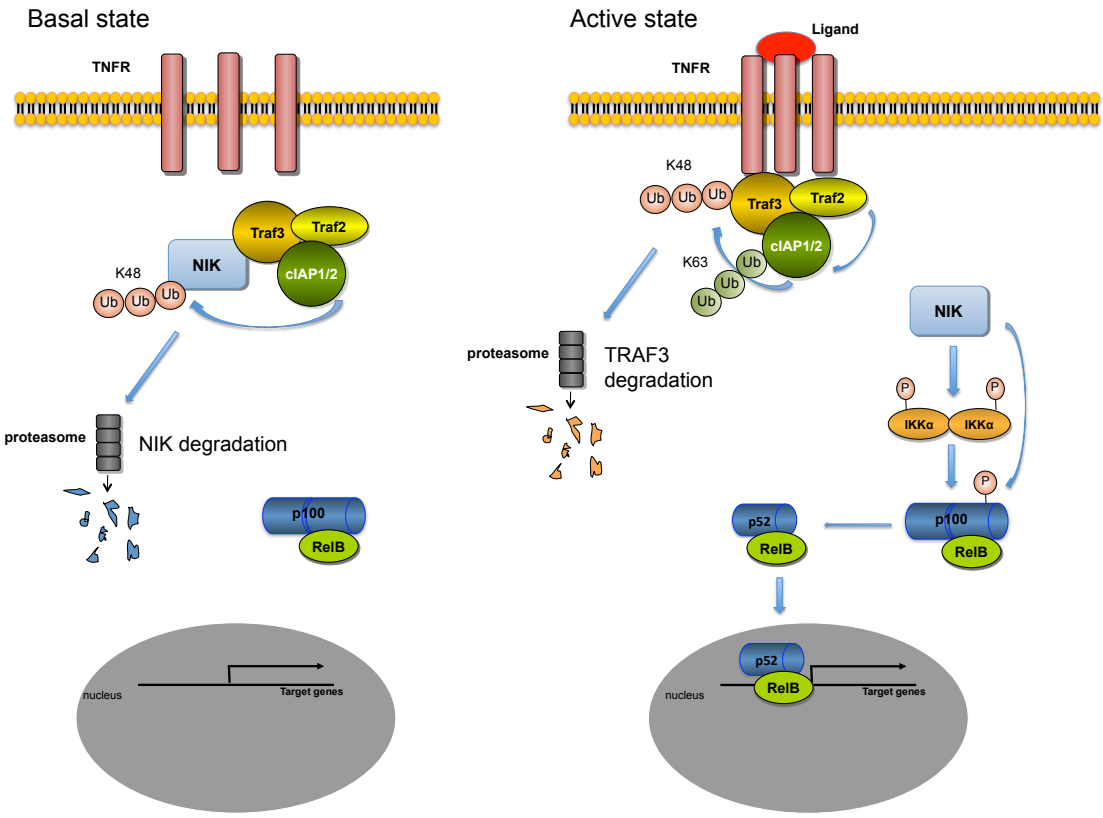

Figure 1.5. NIK activation by protein degradation and stabilization

The proposed model of NIK regulation. In a nonstimulated cell (to the left), NIK is continuously degraded by the proteasome due to K48-linked ubiquitination targeted by the TRAF2/TRAF3/cIAP1/2-complex. p100/RelB dimers are retained in the cytoplasm. Upon receptor stimulation (to the right), the TRAF2/TRAF3/cIAP1/2-complex is recruited to the receptor where TRAF2 activates cIAP1/2 through K63-linked ubiquitination. cIAP1/2 in turn target TRAF3 for degradation. The resultant TRAF3 degradation allows for the accumulation of NIK and phosphorylation of IKKα and p100 with subsequent nuclear translocation of p52/RelB dimers.

Apart from protein stabilization, NIK may also require phosphorylation in its activation loop for kinase activity. Since NIK protein accumulation without additional stimuli is sufficient for

NIK-dependent activation of NF-κB, it has been suggested that accumulation of NIK dimers leads to autophosphorylation of NIK, or that some constitutitive cellular kinase is responsible for the phosphorylation of NIK, although the precise mechanism is unknown (Lin et al. 1998; Razani et al. 2011). On the contrary, two recent studies exploring the structure of NIK, show no evidence of NIK phosphorylation and suggest that NIK exhibit a constitutively active kinase domain without the requirement of phosphorylation (de Leon-Boenig et al. 2012; Liu et al. 2012).

NIK is essential for the processing of p100 to p52 and activation of the alternative pathway, but its role in the classical pathway has been debated. Whether NIK is involved in classical pathway activation or not, seems to be cell type and receptor specific, but how this specificity works is still to be defined (Xiao et al. 2001; Thu et al. 2010). Stabilization of NIK has been reported to induce classical NF-κB activation through IKKβ activation (Annunziata et al. 2007; Zarnegar et al. 2008). However NIK is not strictly necessary for classical pathway activation and seems to be required only in response to certain ligands (Thu et al. 2010).

Although the major function of NIK appears to be the regulation of NF-κB activation, there are a few studies reporting that NIK has substrates involved in other signaling pathways. As a member of the MAP3K family, NIK has been reported to be involved in the activation of MEK1/2 and ERK1/2 in the process of neural differentiation (Foehr et al. 2000). STAT3 and c-jun N-terminal kinase (JNK) are other suggested targets (Akiba et al. 1998; Nadiminty et al. 2007).

Since the discovery of NIK as a core regulator of the alternative NF-κB pathway and the awareness of its involvement malignancies (described in the following section), a rapidly increasing number of publications are emerging trying to decipher its function both in the immune system and in cancer.

1.2.3 NIK and NF-κB in tumorigenesis

A number of different tumors have been linked to an aberrant NF-κB activation. Constitutive NF-κB activation has been observed in both solid tumors (breast, pancreas, prostate, renal, lung and liver cancer to mention a few) and hematological malignancies (described below). If we have a look at the numerous target genes of NF-κB, it is not hard to realize why. The

genes induced upon NF-κB activation are involved in several central processes of tumorigenesis, including proliferation, survival, angiogenesis, inflammation, metastasis and suppression of apoptosis (Figure 1.6) (Baud et al. 2009).

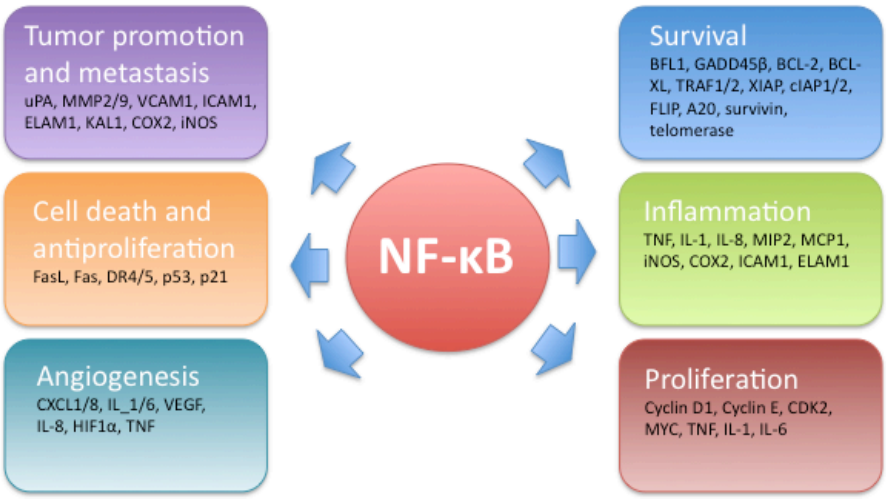

Figure 6. NF-κB target genes involved in cancer development and progression.

NF-κB target genes are involved in several key processes important for tumorigenesis, such as survival, inflammation, proliferation, angiogenesis, metastasis and apoptosis. Adapted from Baud and Karin et al., 2008.

In solid tumors, NF-κB activation may be the result of exposure to pro-inflammatory stimuli from the tumor microenvironment (DiDonato et al. 2012). In lymphoid malignancies on the other hand, constitutive NF-κB signaling can be a result of oncogenic activating mutations in different components of the NF-κB pathway. Many subtypes of lymphomas are characterized by aberrant NF-κB activation, including both B- and T-cell lymphomas as well as Hodgkin lymphomas (Jost et al. 2007). Several lymphomas depend on NF-κB activation for proliferation and survival and NF-κB targeting has therefore been suggested as a therapeutic potential in these tumors (Staudt 2010). One of the earliest notions suggesting that NF-κB had oncogenic properties, was the identification of *NFKB2* gene rearrangements in B- and T-cell lymphomas, giving rise to a truncated p100 protein lacking the IκB-like domain (Neri et al. 1991; Chang et al. 1995). In Hodgkin lymphoma and DLBCL, amplifications of the locus

encoding c-Rel (*REL*) occur in a significant number of patients (Martin-Subero et al. 2002; Barth et al. 2003; Lenz et al. 2008).

Aside from *NFKB2* and *REL* aberrations, most genetic lesions affecting NF-κB signaling occur in members acting upstream in the signaling cascade. A hallmark of the ABC subtype of DLBCL is constitutive NF-κB activation and a disruption of this activation in induces apoptosis in DLBCL cell lines (Davis et al. 2001). Several recurrent genetic aberrations affecting NF-κB signaling have been described in over 50% of ABC-DLBCL (Compagno et al. 2009). Oncogenic mutations in Caspase recruitment domain family, member 11 (*CARD11)* or mutations in *CD79* are involved in the activation of NF-κB downstream BCR and has been proposed to account for the NF-κB activation in about a third of ABC-DLBCL patients (Lenz et al. 2008; Davis et al. 2010; Staudt 2010). Another frequent genetic alteration in ABC-DLBCL is inactivating mutation or deletion of tumor necrosis factor alpha inducing protein 3 (*TNFAIP3*, encoding the protein A20), observed in approximately 30% of the patients (Compagno et al. 2009). A20 is a deubiquitinase that acts as a negative regulator of NF-κB activation (Lin et al. 2008). Frequent TNFAIP3 deletions or inactivating mutations have also been detected in Hodgkin lymphoma (Schmitz et al. 2009) and several subtypes of non-Hodgkin lymphomas including mantle cell lymphoma, mucosa-associated lymphoid tissue (MALT) lymphoma, follicular lymphoma and PTCL (Honma et al. 2009; Braun et al. 2011). A20 deletions have been shown to have functional relevance in lymphomagenesis since overexpression of A20 leads to apoptosis and silencing of A20 is associated with resistance to apoptosis in lymphoma cell lines (Compagno et al. 2009; Honma et al. 2009). Morevoer, a recurrent oncogenic mutation in myeloid differentiation primary response 88 *(MYD88*), encoding for an adaptor protein involved in NF-κB signaling downstream TLRs and interleukin receptors, was recently described in DLBCL, MALT lymphoma, Waldenström's macroglobulinemia (Lymphoplasmacytic lymphoma) and chronic lymphocytic leukemia (Ngo et al. 2011; Landau et al. 2013; Varettoni et al. 2013). Other mutations described that give rise to an activation of NF-κB include translocations involving *MALT1* in MALT lymphoma (Lucas et al. 2001), mutations of the deubiquitin ligase cylindromatosis (CYLD) in multiple myeloma (Annunziata et al. 2007) and inactivating mutations of the genes for IκBα and IκBε in Hodgkin lymphoma (Cabannes et al. 1999; Emmerich et al. 2003).

An activated alternative NF-κB pathway with NIK overexpression or stabilization has been described in several lymphomas, such as DLBCL, Hodgkin lymphoma, Adult T-cell leukemia

(ATL), MALT-lymphoma and multiple myeloma (Keats et al. 2007; Saitoh et al. 2008; Pham et al. 2011; Rosebeck et al. 2011; Ranuncolo et al. 2012). NIK has additionally been reported to be important in the biology of other tumors, such as pancreatic cancer and melanoma (Thu et al. 2012; Doppler et al. 2013). Both mutations in the members of the ubiquitin ligase complex responsible for NIK degradation, or excessive upstream receptor signaling have been described as causes of constitutive NIK and NF-κB activation in lymphomas. The alternative NF-κB pathway has been shown to play an important role in the pathogenesis of multiple myeloma, a neoplasm affecting the plasma cells, where numerous genetic alterations with the common mechanism of NIK stabilization and/or NF-κB activation are described (Annunziata et al. 2007; Keats et al. 2007). Frequent inactivating mutations or deletions of members of the NIK degradation complex (*TRAF2, TRAF3* or *BIRC2/3*) have been reported as well as activating mutations in upstream receptors *LTBR, CD40* and *TACI* and mutations in *NFKB1* and *NFKB2*. Amplifications or translocations of NIK locus (*MAP3K14*) has also been reported in a few multiple myeloma and Hodgkin lymphoma cases (Keats et al. 2007; Otto et al. 2012). The API2-MALT1 fusion protein expressed in MALT-lymphoma, was recently described to induce proteolytic cleavage of NIK with subsequent NIK stabilization and alternative pathway activation (Rosebeck et al. 2011). In support of NIK having oncogenic properties, NIK overexpression can transform rat fibroblast and a B-cell-specific NIK overexpression in mice, or particularly, mice overexpressing a form of NIK lacking its TRAF3-bindig domain, gives rise to a dramatic accumulation of mature B cells (Saitoh et al. 2008; Sasaki et al. 2008).

Other triggers of NF-κB activation in lymphomas are oncogenic viruses, such as EBV and HTLV, which are associated with several lymphomas and are suggested to play a role in their pathogenesis (Vallabhapurapu et al. 2009).

The frequent activation and occurrence of genetic aberrations affecting the NF-κB pathway in lymphomas (Figure 1.7), highlight the importance of this pathway in the pathogenesis of these malignancies and encourage researchers to explore this pathway for effective therapeutic targeting. However, still, there is a lack of specific NF-κB inhibitors to properly study its potential as therapeutic target. Clinical benefit has been achieved in multiple myeloma and refractory B cell lymphoma using the proteasome inhibitor Bortezomib (Staudt 2010; DiDonato et al. 2012). Although inhibition of NF-κB has been attributed to the mechanism of action of Bortezomib, the proteasome targets a tremendous number of

proteins and cannot be considered NF-κB-specific. IKKβ is the component of the NF-κB pathway that has been most efficiently targeted. A range of different IKKβ inhibitors are available and have shown antitumor effect in experimental models. Nevertheless, up to date, there is no clinically approved specific NF-κB inhibitor (DiDonato et al. 2012).

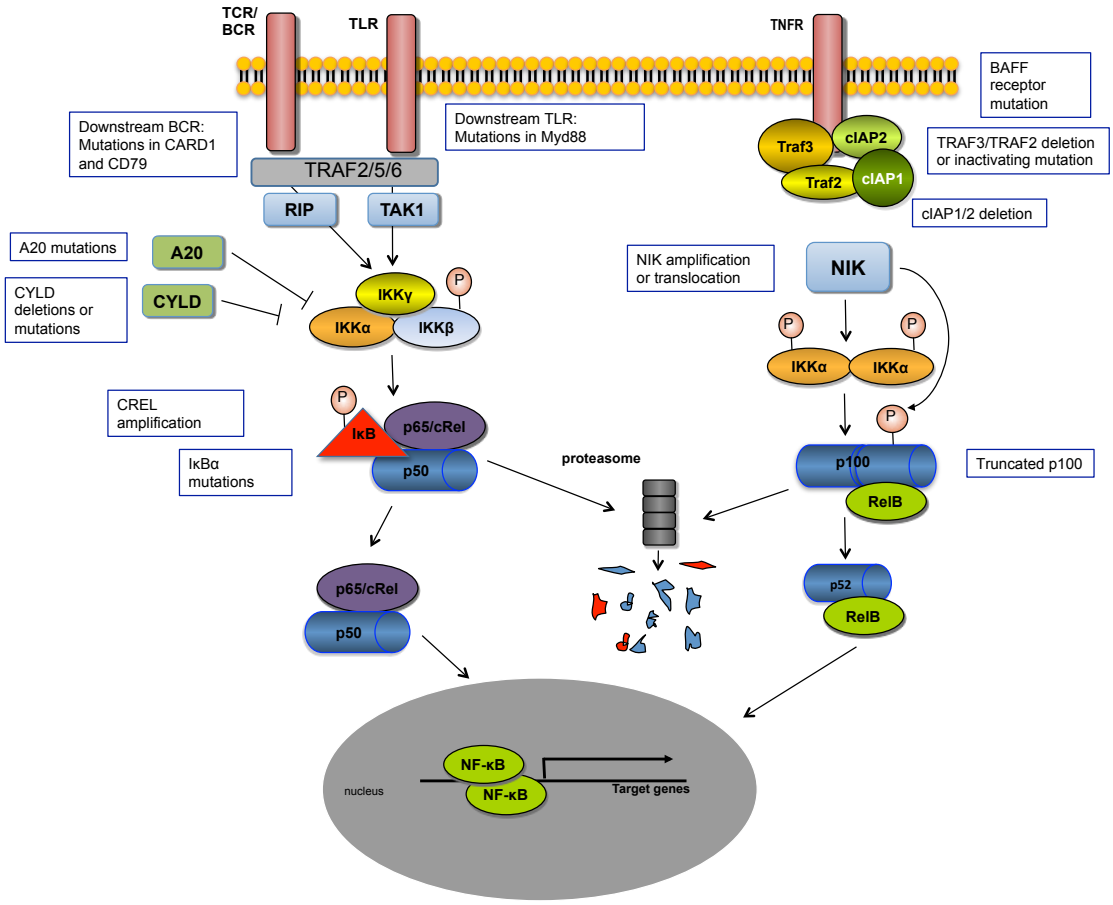

Figure 7. **Genetic alterations affecting NF-κB in human cancer**

Several genetic alterations have been described in human cancers, that give rise to an activated NF-κB pathway. Reported genetic alterations are highlighted in the flowchart.

OBJECTIVES

Deregulated NF-κB activity plays a key role in the development of multiple malignancies and constitutive activation of NF-κB has been suggested to play a key role in several lymphomas. In spite of numerous publications in the last decade concerning the NF-κB pathway, the role of NF-κB signaling in lymphomagenesis and its therapeutic potential is far from being understood.

The first part of the project is focused on the NF-κB pathway in DLBCL, where constitutive NF-κB activation is one of the proposed oncogenic mechanisms in the ABC subtype. However, the actual expression of NF-κB in DLBCL tumors and the presence of both classical and alternative signaling, as well as their clinical correlation, have not been well studied. Consequently, the aims of the first part of this thesis were the following:

a. To characterize the expression pattern of the different NF-κB members in human DLBCL tumor samples and evaluate their impact on patient survival.
b. To analyze the relationship between DLBCL molecular subtypes (GCB and ABC) and NF-κB expression.

PTCL is a group of aggressive lymphomas, presenting dismal clinical outcome with current therapies. The molecular pathology of PTCL is largely unknown and the lack of efficient therapies demands further studies to clarify their molecular background and to identify new therapeutic targets. Previous data indicate that NF-κB could be involved in the pathogenesis of these malignancies. However, the characterization of the pathway in PTCL is vague and there are no specific NF-κB inhibitor drugs in clinical use for PTCL today, indicating a need for more detailed studies and the identification of novel molecular targets able to interfere with NF-κB activation. The aims of this part of the projects were thus the following:

c. To characterize the expression of NF-κB in different PTCL subtypes and its impact on clinical outcome.
d. To investigate the role of NIK in the regulation of the NF-κB signaling pathway and of downstream gene expression in PTCL.
e. To study the role of NIK and other NF-κB components in PTCL cell survival in order to find putative therapeutic targets.

2. MATERIALS AND METHODS

2.1 Patient samples and cell lines

2.1.1 Primary tumor samples

The use of all patient samples in this study was approved by the Clinical Research Ethics Committee of Hospital Universitario Marqués de Valdecilla, HUMV (Santander, Spain). Tumor biopsies were obtained from several hospitals around Spain and administered by the tumor banks of CNIO (Madrid, Spain) and HUMV (Santander, Spain). Samples were obtained before treatment and were diagnosed according to the criteria of the WHO (Swerdlow et al. 2008). For the gene expression data analysis, 37 frozen PTCL cases were used. Paraffin-embedded tissues from 127 PTCL, 260 DLBCL, 30 splenic marginal zone lymphoma (SMZL), 32 mantle cell lymphoma (MCL), 35 Hodgkin lymphoma (HL), and 33 follicular lymphoma (FL) samples, arranged into tissue microarrays were used for immunohistochemistry and *in situ* hybridization. The clinical parameters of the different patient series included in the survival analyses in this study, are summarized in Tables 2.1 – 2.3.

Table 2.1 Clinical characteristics for 88 DLBCL patients.

Characteristics	Number of patients	Percentage
Gender		
Male	42	47.7%
Female	46	52.3%
Age (years)		
Average (63.6 years)		
≤60	36	49.9%
>60	51	58.0%
-	1	0.0%
IPI		
0-2	45	51.1%
3-5	38	43.2%
-	5	5.7%
DLBCL subtype (CHOI)		
GCB	41	46.6%
ABC	46	52.3%
-	1	0.0%
Total	88	100%

Note: DLBCL subclassification was performed using immunohistochemistry and the algorithm of Choi. GCB = Germinal center B-cell-like, ABC = Activated B-cell-like, IPI = International prognostic Index.

Table 2.2 Clinical characteristics for PTCL-NOS and AITL patients.

Characteristics	Number of patients	Percentage
Gender		
Male	46	59.7%
Female	31	40.3%
Age (years)		
Average	63.2	
≤60	32	41.6%
>60	45	58.4%
Ann Arbor Stage		
I-II	17	22.1%
III-IV	60	37.9%
ECOG		
0-1	53	68.8%
2-4	24	31.2%
IPI		
0-2	34	44.2%
3-5	41	53.2%
-	2	2.6%
LDH level		
Normal	34	44.2%
High	42	54.5%
-	1	1.3%
PTCL subtype		
AITL	29	37.7%
PTCL-NOS	48	62.3%
Total	77	100.0%

Abbreviations: ECOG = Eastern Cooperative Oncology Group, IPI = International Prognostic Index, LDH = lactate dehydrogenase.

Table 2.3 Clinical characteristics for ALCL patients

Characteristics	Number of patients	Percentage
Gender		
Male	15	62.5%
Female	9	37.5%
Age (years)		
Average	44.6	
≤60	18	75.0%
>60	6	25.0%
Ann Arbor Stage		
I-II	10	41.7%
III-IV	14	58.3%
ECOG		
0-1	18	75.0%
2-4	6	25.0%

IPI		
0-2	19	79.2%
3-5	5	20.8%
LDH level		
Normal	18	75.0%
High	6	25.0%
ALK status		
ALK positive	8	33.3%
ALK negative	16	66.7%
Total	24	100.0%

Abbreviations: ECOG = Eastern Cooperative Oncology Group, IPI = International Prognostic Index, LDH = lactate dehydrogenase.

2.1.2 Isolation of T cells from peripheral blood

T cells from peripheral blood of healthy donors or Sézary syndrome patients were isolated through negative selection using the RosetteSep Kit (StemCell Technologies, Grenoble, France). The protocol was performed according to the manufacturer's instruction starting with 10 ml of peripheral blood in tubes containing Heparin as an anticoagulant. Briefly, human T cell enrichment cocktail (containing a mixture of monoclonal antibodies for CD16, CD19, CD36, CD56, CD66b and glycophorin A) was added to the blood sample at 50 µl/ml and incubated for 20 min at room temperature to allow for unwanted cells to form complexes with antibodies and red blood cells. Dilution with an equal volume of phosphate buffer saline, PBS (NaCl 137 mM, Na_2HPO_4 10 mM, KCl 2.7 mM, KH_2PO_4 2 mM, pH 7.4) + 2% fetal bovine serum (FBS) and centrifugation in RossetteSep density medium (20 min at 1200 x g in room temperature with the brake off) separated the enriched cells (including T cells) from the unwanted complexes and plasma. The enriched cell layer was collected and washed with PBS. Remaining red blood cells were lysed resuspending the pellet in 2 ml of erythrocyte lysis buffer (Buffer EL, Quiagen, Hilden, Germany) on ice for 10 minutes. The sample was then washed again and resuspended in culture medium. If cells were left for later use, they were frozen slowly in 90% FBS and 10% dimethyl sulfoxide (DMSO) and stored in liquid nitrogen until use. In order to check the purity of the samples, cells were labeled with CD3-fluorescein isothiocyanate (FITC) (BD Biosciences, San José, CA, USA) and CD19-Phycoerythrin (PE) (Miltenyi Biotec, # 130-091-247) antibodies for 15 minutes at RT, washed and resuspended in PBS and analyzed with a FACS Canto II flow cytometer (BD Biosciences). The proportion of T cells (CD3+) in the samples was ensured to be >90%.

2.1.3 Culture and stimulation of isolated T cells

To stimulate proliferation of healthy T cells, the isolated T cells were grown in Roswell Park Memorial Institute (RPMI) medium supplemented with 20% FBS, 1% penicillin/streptomycin and the T stimulatory reagents Concanavalin A (ConA) (10 μg/mL, Sigma-Aldrich Co. St. Louis, MO, USA) and interleukin-2 (IL-2) (1500U/mL, PeproTech, Rocky Hill, NJ, USA). Control cells were grown in medium without ConA and IL-2. Cells were plated in triplicate and the cells were counted manually using a Neubauer chamber at day 0, 2, 4, and 7. Whereas control cells died or proliferated slowly, cells treated with ConA and IL-2 were induced to proliferate. Cells were harvested for RNA extraction and NIK (*MAP3K14*) expression analysis at day 4 when T cells were proliferating.

2.1.4 Cell lines and culture conditions

The human cell lines used in the study are summarized in Table 2.4. The cell lines were purchased from the German Collection of Microorganism and Cell Cultures (DSMZ, Braunschweig, Germany), the American Type Culture Collection (ATCC, Rockville, MD, USA), the European Collection of Cell Cultures (ECACC, Wiltshire, UK), or a supplied as a kind gift from Dr. Martínez-Climent at the Centre of Applied Medical Research (Pamplona, Spain). Cell lines were grown in RPMI 1640 medium (Sigma Chemical, St Louis, MO, USA), Iscove´s modified Dulbecco´s medium (IMDM, Invitrogen, Carlsbad, CA, USA), or Dulbecco´s modified eagle medium (DMEM, Sigma Chemical) supplemented with 10-20% heat-inactivated fetal bovine serum, FBS, (Invitrogen) and 1% penicillin/streptomycin. Interleukin 2 (PeproTech, Rocky Hill, NJ, USA) was added to the culture medium of DERL-7 at a concentration of 20ng/ml. Cells were maintained at 37°C in a humidified 5% CO2 incubator. All cell lines were authenticated (year 2010-2011) by DSMZ. Cells were counted in a Neubauer chamber and Trypan Blue (Sigma Chemical) was used to distinguish dead (blue) and alive (uncolored) cells. For proliferation curves, cells were plated in triplicate at a density of 100 000 cells/ml and viable cells were counted at determined time points.

Table 2.4. Description of the cell lines used in the study

Cell line	Lymphoma type	Growth medium	Growth	Origin
My-La	Mycosis Fungoides	RPMI + 10% FBS	Suspension	ECACC
SR-786	Anaplastic large T cell lymphoma, ALK+	RPMI + 10% FBS	Suspension	DSMZ
DERL-7	Hepatosplenic gamma-delta T cell lymphoma	RPMI + 20% FBS + IL2	Suspension	DSMZ
HuT 78	Sezary Syndrome	RPMI + 10% FBS	Suspension	ATCC
HH	Cutaneous T cell lymphoma	RPMI + 10% FBS	Suspension	ATCC
MJ	Peripheral T cell lymphoma, HTLV+	IMDM + 10% FBS	Suspension	ATCC
FARAGE	Diffuse large B-cell lymphoma, EBV+	RPMI + 20% FBS	Suspension	DSMZ
DOHH-2	Diffuse large B-cell lymphoma, EBV+	RPMI + 20% FBS	Suspension	DSMZ
SUDHL-4	Diffuse large B-cell lymphoma	RPMI + 10% FBS	Suspension	DSMZ
SUDHL-6	Diffuse large B-cell lymphoma	RPMI + 10% FBS	Suspension	DSMZ
HBL-1	Diffuse large B-cell lymphoma	RPMI + 20% FBS	Suspension	Dr. Martínez-Climent
OCILY-3	Diffuse large B-cell lymphoma	RPMI + 20% FBS	Suspension	Dr. Martínez-Climent
KARPAS-422	Diffuse large B-cell lymphoma	RPMI + 10% FBS	Suspension	DSMZ
HEK 293T	Embryonic kidney	DMEM + 10% FBS	Adherent	ATCC

Abbreviations: FBS = Fetal bovine serum, EBV = Epstein-Barr virus, ECACC = European Collection of Cell Cultures, DSMZ = German Collection of Microorganism and Cell Cultures, ATCC = American Type Culture Collection.

2.2. Immunohistochemistry

Tissue microarray contruction and immunohistochemical stainings were performed at the Histology and Immunohistochemistry Unit at the CNIO.

2.2.1. Tissue microarray construction

Tissue microarrays (TMAs) are arrays containing small tissue biopsies (0.6-2 mm) from different tissue blocks organized into one block. This permits the simultaneous staining of many tumor samples on one unique slide. Representative areas from formalin-fixed paraffin-embedded tumors and healthy lymph nodes were selected from hematoxylin and eosin stained sections and two different 1-2 mm tissue cores were extracted from each sample, so that each sample was represented in duplicate on the TMA. A TMA workstation (Beecher Instruments, Silver Spring, MD) was used to arrange the cores into a unique paraffin block, using previously described methods (Kallioniemi et al. 2001).

2.2.2. Immunohistochemical staining

Antibodies and conditions used for immunohistochemistry are summarized in Table 2.5. Briefly, formalin-fixed, paraffin-embedded tissue sections were subjected to deparaffinization and hydration by incubation at 56º overnight, followed by immersion in xylene and a decreasing ethanol gradient. A heat-induced epitope retrieval step was then performed by pressure-cooking the slide at 98º for 20 minutes in the antigen retrieval buffers specified in Table 2.5. The deparaffinization, hydration and antigen retrieval steps were performed in PT Link instrument (DAKO, Glostrup, Denmark). Immunohistochemical staining was then performed in a robotized system using Autostainer Link (DAKO) and EnVision FLEX – horseradish peroxidase (HRP) visualization system (DAKO), applying the following steps. Endogenous peroxidase activity was blocked by incubation of the slides in peroxidase-blocking reagent (0.03% hydrogen peroxidase containing sodium azide) for 5 minutes at room temperature. Slides were then washed in wash buffer (0.05 mol/L Tris Buffered Saline, TBS, with Tween) and incubated with the primary antibodies at room temperature for 30 minutes (see dilutions in Table 2.5). After another wash step, slides were incubated with secondary antibodies conjugated with HRP-labeled polymer for 30 minutes, washed again, and immersed in a buffer containing the substrate and chromogen

diaminobenzidine (DAB) for 10 minutes. Preparations were contra-stained with hematoxylin for one minute, washed and dehydrated through consecutive incubations in increasing concentration of ethanol and xylene, and then mounted automatically in Autostainer Link.

Table 2.5 Antibodies and conditions for immunohistochemistry.

Antibody	Species (clone)	Company	Dilution	Antigen Retrieval
p100/p52	mouse monoclonal	Millipore (Billerica, MA, USA)	1/1000	Citrate pH 6 + Proteinase K
p105/p50	rabbit polyclonal	GeneTex (Irvine, CA, USA)	1/1	Citrate pH 6
RelB	rabbit polyclonal	Santa Cruz biotechnlogy (Santa Cruz, CA, USA)	1/1250	Citrate pH 6
p65 (RelA)	mouse monoclonal (F-6)	Santa Cruz biotechnlogy	1/350	Citrate pH 6
c-REL	rabbit polyclonal	Calbiochem (Darmstadt,Germany)	1/400	Citrate pH 6
LMP1	mouse monoclonal (CS. 1-4)	Novocastra (Newcastle, UK)	1/50	EDTA 1mM pH 9
CD10	mouse monoclonal (56C6)	Novocastra	1/10	Citrate pH 6
BCL6	mouse monoclonal (GI191E/A8)	CNIO (Madrid, Spain)	1/4	Citrate pH 6 + Proteinase K
MUM1/IRF4	goat polyclonal	Santa Cruz biotechnology	1/250	Citrate pH 6
GCET1	mouse monoclonal (RAM)	CNIO	1/4	EDTA 1mM pH 9
FOXP1	mouse monoclonal (JC12)	CNIO	1/100	Citrate pH 6

2.2.3. Scoring

To assess NF-κB activation in human tumors, nuclear expression of p50, p52, p65 (RelA), RelB or c-Rel was evaluated. For PTCL samples, a scoring system including three different levels was followed; negative, positive grade 1 (pos +), and positive grade 2 (pos ++). Cases

presenting nuclear staining in >20% of tumor cells were considered positive, grade 1 (pos +), while cases with strong nuclear staining in >50% of cells were considered positive, grade 2 (pos ++). For DLBCL cases, a threshold of 30% of positive tumoral nuclei was used, based on previous reports in DLBCL (Hans et al. 2004; Compagno et al. 2009). Cases with inconsistent results between the duplicated cores or those showing no reactivity in none of the cells were discarded from the study. The evaluation of the stained tumors was done next to two different pathologists with expertise in hematological malignancies.

2.2.4. Statistical Analysis

To determine the independence of variables analyzed by immunohistochemistry, crosstabs applying a Pearson's $\chi 2$ test was used. SPSS version 15.0 (SPSS Inc., Chicago, IL, USA) was used to carry out these tests. Values of $p<0.05$ were considered statistically significant.

2.2.5. DLBCL subclassification

To classify DLBCL cases into molecular subtypes, immunohistochemistry of a panel of five markers (GCET1, CD10, BCL6, MUM1 and FOXP1) was performed and the classification into GCB or ABC was done according to the algorithm of Choi (Choi et al. 2009). This approach was described to classify DLBCL samples with 93% concordance compared to gene expression profiling (Choi et al. 2009), which is considered as the gold standard for DLBCL classification. Tissues from 60 additional DLBCL samples, kindly provided by Dr. Ken H Young (MD Anderson, TX, USA) were previously classified as GCB or ABC using gene expression profiling (Wright et al. 2003; Hu et al. 2013). In our cases, 91.7% concordance was obtained between immunohistochemistry and gene expression profiling.

2.3 *In Situ* Hybridization of EBER

The presence of EBV in the tumor specimens were analyzed on paraffin-embedded tissues using *In Situ* hybridization of Epstein-Barr Virus encoded RNA (EBER) as in (Chang et al. 1992). A specific probe for EBER (Bond ISH EBER probe, Vision BioSystem, Wetzlar, Germany) was used and Bond–maX autostainer (Vision BioSystem) was used for automatic *In Situ* hybridization at the Histology and Immunohistochemistry Unit at the CNIO.

2.4. Survival Analysis

All statistical analyses were performed using SPSS software version 15.0 (SPSS Inc). As clinical endpoint, overall survival was chosen. Overall survival is defined as the time interval between diagnosis and death due to lymphoma or any other cause. Clinical parameters of the patients included in the survival analyses are summarized in Table 2.1-2.3. The PTCL series included 77 PTCL samples of which 48 were PTCL-NOS and 29 were AITL. These patients were followed between the years 1994 and 2010 and had an average follow-up of 24 months. In the ALCL series, 24 patients were followed between the years 2001 and 2010 and had an average follow-up of 33 months. The 88 DLBCL patients were followed between the years 2002 and 2013 and presented an average follow-up time of 46 months.

2.4.1 Kaplan-Meier Analysis

The Kaplan-Meier method applying the log-rank test was used to estimate the differences in overall survival between NF-κB-positive and negative cases in different patient series. For T-cell lymphomas, samples presenting nuclear staining of NF-κB (either p52, p50, RelB, p65 or c-Rel) in over 50% (pos++) of tumor cells were considered positive for NF-κB. In the DLBCL series, a 30% positivity threshold was used and the individual NF-κB members were analyzed separately.

2.4.2 Multivariate Cox Regression analysis

To adjust for the effect of other covariates on survival in PTCL, a multivariate survival analysis was performed using a Cox proportional hazard regression model. Clinical parameters included in the analysis were age (>60 years), Ann-Arbor stage (>2), ECOG performance status (>1), extranodal sites (>1) and LDH levels. The combined presence or absence of these symptoms is used to calculate the international prognostic index (IPI) in a scale from 1-5 (summing one point for the presence of any of these risk factors). The clinical impact of NF-κB was estimated both adjusting for the covariates age, stage, extranodal sites, ECOG, LDH levels and adjusting for IPI as a prognostic covariate. The *Enter* model was used for entering the covariates into the analysis and p-values <0.05 were considered statistically significant.

2. 5. Protein extraction and Western blotting

2.5.1. Total protein extraction

Cells in culture were collected by centrifugation, washed two times in PBS and pellets were stored at -80^{o}C until use. Protein was extracted using radio immunoprecipitation assay (RIPA) lysis buffer (150mM NaCl, 1.0% IGEPAL® CA-630, 0.5% sodium deoxycholate, 0.1% SDS, and 50mM Tris, pH 8.0; Sigma-Aldrich Inc.) supplemented with protease and phosphatase inhibitors (PhosSTOP and Complete cocktail tablets, Roche Diagnostics, Inidanapolis, IN, USA) and phenylmethylsulfonyl fluoride (PMSF, Roche Diagnostics). Pellets were resuspended in the lysis buffer and incubated on ice for 30 minutes. After a centrifugation step (maximum speed, 4ºC, 30 min), the supernatant was transferred to a clean tube and protein concentrations were measured using the Bio-Rad *DC* Protein Assay (Bio-Rad, Hercules, CA, USA) following the manufacturer's instructions and using bovine serum albumin (BSA) as a standard and 98-well microplates for sample preparation. The Bio-Rad *DC* Protein Assay is a colorimetric assay for protein concentration based on the Lowry assay principles (Lowry et al. 1951). Concentrations were calculated after reading the absorbance at 750 nM in a spectrophotometer plate reader (Bio-Rad).

2.5.2 Nucleus/cytoplasm separation

Pellets were collected by centrifugation (1,200 x g, 5 min at room temperature) and washed in PBS. Pellets were immediately subjected to the extraction protocol and never stored or frozen prior to nuclear separation in order to avoid rupture of cellular membranes. Nuclear fractions were separated from cytosolic fractions using the BioVision nuclear/cytosol fractionation kit (#K266-25, BioVision, Mountain View, CA, USA) according to the manufacturer's instructions. Briefly, cells were first resuspended in a cytosolic extraction buffer and incubated on ice for 10 minutes. After the addition of a second cytosolic extraction buffer and a short incubation on ice, cells were centrifuged and the supernatant (the cytoplasmic fraction) is collected. The pellet was then resuspended in a nuclear extraction buffer and incubated on ice for 40 minutes with repeated vortexing every 10 minutes. After centrifugation, the supernatant, which contains the nuclear extract, was collected. Proteins were quantified using the Bio-Rad *DC* Protein Assay as mentioned

previously and stored at -80ºC. To verify a proper separation of the two compartments, the expression of Lamin B1 (nuclear) and α-tubulin (cytoplasmic) was analyzed by Western blot.

2.5.3. Western blot

After protein extraction and quantification, Laemmli sample buffer (4X composition: 62.5mM TrisHCl pH 6.8, glycerol 20%, SDS 2%, 2-mercaptoethanol 5%, bromophenol blue 0.025%) was added to the extract and heated for 5 minutes at 99^{o}C. Samples were then immediately put on ice and subjected to western blot or stored at -80^{o}C until later use. Western blot was performed following standard protocols. For NIK detection, cell lines were treated for 3 hours with 20 μM proteasome inhibitor MG132 (C2211, Sigma, Missouri, USA) prior harvesting. MG132 was exclusively added to cells only for NIK detection and separate untreated cells were collected for detection of other proteins. Twenty to 40 μg of protein were loaded and separated by electrophoresis on 6-12% sodium dodecyl sulfate polyacrylamide (SDS-PAGE) gels in electrophoresis buffer (5X composition: TrisHCl 0.13M, glycine 0.95M, SDS 0.5%). Following electrophoresis, the proteins were wet-transferred onto nitrocellulose membranes (Whatman, Dassel, DE) using Mini Trans-Blot Cell equipment (BioRad). Transference was performed in transfer buffer (TrisHCl 0.025M, glycine 0.2M, 20% of methanol) at 40 mA overnight or 400 mA during 1.5 hour at 4ºC. Membranes were then blocked in 5% milk in PBS-T (phosphate-buffered saline with 0.1% Tween-20) for 1 hour with continuous shaking and incubated with the primary antibody diluted in 5% BSA PBS-T. Primary antibodies and their conditions are summarized in Table 2.6. Membranes were then washed in PBS-T (3 x 5 minutes on a shaker) and incubated for 1 hour (in darkness on a shaker) with a fluorescent-labeled secondary antibody (Alexa 680 and Alexa800, Rockland, Gilbertsville, PA, USA) diluted in 5% BSA PBS-T. The membranes were then again washed in PBS-T (3 x 5 min) and the signal was read in an Odyssey Infrared System Scanner (LI-COR Biosciences, Lincoln, NE, USA). Band intensities were quantified using the ImageJ 1.34S software (National Institute of Health, Bethesda, MD, USA) and normalized against the loading control (α-tubulin or GAPDH).

Table 2.6. Characteristics of primary antibodies used in western blot.

Antibody	Species (clone)	Dilution	Incubation time	Manufacturer
NIK	Rabbit polyclonal	1/250	overnight	Cell Signaling, Beverly, Massachusetts, USA
p100/p52	Mouse monoclonal	1/1000	1h	Upstate Biotechnology, NY, USA
p105/p50	Rabbit polyclonal	1/1000	1h	Novus Biologicals
α-tubulin	Mouse monoclonal (DM1A)	1/10 000	30 min	Sigma-Aldrich Inc., St. Louis, MO, USA
α-tubulin	Rabbit polyclonal (B-5-1-2)	1/10 000	30 min	Abcam plc, Cambridge, UK
Caspase-3	Rabbit polyclonal	1/1000	overnight	Cell Signaling
IKK alpha	Rabbit polyclonal	1/1000	2h	Cell Signaling
IKK beta	Rabbit polyclonal	1/500	overnight	Cell Signaling
pStat-3 (Tyr705)	Rabbit polyclonal	1/1000	overnight	Cell Signaling
Lamin B1	Rabbit polyclonal	1/1000	2h	Abcam
Stat3	Mouse monoclonal (124H6)	1/1000	overnight	Cell Signaling
PARP	Rabbit polyclonal	1/1000	overnight	Cell Signaling
C-Rel	Rabbit polyclonal	1/1000	overnight	Cell Signaling
RelB	Mouse monoclonal	1/1000	overnight	Active Motif
pStat-5	Mouse monoclonal (Y694)	1/1000	overnight	BD Biosciences
Traf-3	Rabbit polyclonal	1/1000	1h	Santa Cruz
phospho-IKKalpha/beta (S176/S177)	Rabbit monoclonal (C84E11)	1/500	overnight	Cell Signaling
GAPDH	Rabbit monoclonal (14C10)	1/1000	1h	Cell Signaling
LMP1	Mouse monoclonal (CS. 1-4)	1/1	2h	DAKO

2.6. RNA extraction

2.6.1 RNA extraction from cell lines and isolated T cells

Total mRNA was extracted from cell lines or isolated primary T cells using the RNeasy Mini Kit (Qiagen, Hilden, Germany) according to the guidelines described by the manufacturer. Briefly, approximately 10^6 cells were harvested and washed in PBS. Then, 350μL RLT lysis buffer (supplemented with 10% β-mercaptoethanol) were added to the pellet and the suspension was passed several times through a 23G syringe needle to allow homogenization. The same volume of 70% ethanol was then added and the suspension was transferred to an RNeasy mini column (containing a silica-gel membrane that selectively binds RNA). The contaminant DNA was digested by adding DNAse I (RNase-free DNase I Set; Qiagen) to the membrane and incubating for 15 minutes. After a few wash steps, the RNA was eluted in RNase-free water. RNA integrity and concentration were checked by gel electrophoresis and analysis by NanoDrop ND-100 (NanoDrop, Wilmington, DE).

2.6.2. RNA extraction from tissues

Total RNA extraction from whole frozen tissue was carried out using the TRIzol reagent (Invitrogen, Carlsbad, CA, USA) as follows: Frozen tissues were cut with a cryostat and the sections were then homogenized using a Polytron homogenizer (Capitol scientific, Inc; Austin, TX). The homogenized samples were lysed by addition of 1 mL of TRIzol (a monophasic solution of phenol and guanidine isothiocyanate that maintains the integrity of the RNA while disrupting cellular components). Then, 200 μL of chloroform were added, mixed and the sample was centrifuged at 12,000 rpm for 15 minutes at 4°C. The aqueous phase, containing the RNA, was transferred to a clean tube and the RNA was recovered by isopropanol precipitation. The pellet was washed with 70% ethanol and resuspended in RNAse-free water. The resulting RNA was further purified using the RNeasy kit (Qiagen Inc., Valencia, CA) and digested with RNase-free DNase I following the manufacturer's instructions and procedures described in section 2.6.1. The integrity and concentration of RNA was verified by electrophoresis and measured by NanoDrop ND-100 (NanoDrop, Wilmington, DE) or by the 2100 Bioanalyzer (Agilent Technologies, Inc., Santa Clara, CA, USA).

2.7. Gene expression microarrays

Gene expression microarrays are high-throughput techniques that allow the analysis of the expression of thousands of genes simultaneously. In this study we used the 4x44K Whole Human Genome Microarray (Agilent Technologies), a microarray containing 60-mer oligonucleotides representing 19,596 Entrez gene RNAs covering the whole human genome. For the gene expression analysis in primary samples, 38 frozen PTCL cases were used, including 20 PTCL-NOS, 15 AITL and 3 ALCL (1 ALCL ALK+ and 2 ALCL ALK-). RNA extraction was performed from frozen sections as described in 2.6.2. For analysis of gene expression after NIK knockdown in T cell lymphoma cell lines, pellets were collected 48 hours after siRNA transfection and RNA was extracted using the RNeasy Mini Kit as described above. Three independent experiments were performed and each sample was hybridized onto a separate microarray. Purification, amplification, labeling and hybridization onto 4x44K Whole Human Genome Oligo Microarray was done according to the manufacturer´s instructions (Agilent Technologies) as follows.

2.7.1. cDNA synthesis from total RNA

Two µg of total RNA was mixed with 2 µl of a 5,000-fold dilution of Agilent's Two-Color Spike-in RNA control and amplified using Agilent Low RNA Input Fluorescent Amplification Kit (Agilent Technologies). The mixture in a final volume of 6.5 µl (total concentration at least 5ng/µl) was mixed with 5 µl of T7 promoter primer. The primer and the template were denatured by incubating the reaction at 65^{O}C for 10min and placing on ice for 5min. Following, 8.5 µl of cDNA Master Mix was added and the samples were incubated first at 40^{O}C in a circulating water bath for 2h and then at 65^{O}C in a heating block for 15 min to inactivate Moloney murine leukemia virus reverse transcriptase (MMLV-RT). Following that time, the samples were incubated on ice for 5 min.

cDNA Master Mix composition: 4µl of 5X First strand buffer, 0.1M DTT 2 µl, 10mM dNTP mix 1 µl, 1 µl of MMLV-RT and 0.5 µl of RNaseOUT.

2.7.2. Fluorescent cRNA synthesis: In vitro trasnscription and incorporation of fluorochromes

To each sample tube, either 2.4 µl of 10mM cyanine 3-CTP (sample) or 2.4 µl of 10 mM cyanine 5-CTP (Stratagene Universal Human Reference RNA) was added and mixed. Following, to each sample, 57.6 µl of Transcription Master Mix was added an incubated in a circulated water bath at 40^{O}C for 2h. Following amplification and labeling, each sample was assessed on the Nanodrop ND-1000 to measure yield and specific activity.

Transcription Master Mix composition: 15.3 µl of Nuclease-free water, 20µl of 4X Transcription buffer, 6µl 0.1M DTT, 8µl of NTP mix, 6.4µl 50% PEG, 0.5µl of RNase OUT, 0.6µl of inorganic pyrophosphatase and 0.8µl T7 RNA Polymerase.

2.7.3. Hybridization

cRNA target was prepared as follows: 0.75 µg cyanine 3-labeled, linearly amplified sample cRNA was mixed with 0.75 µg cyanine 5-labeled, linearly amplified reference pool cRNA, 50µl of 10X control targets and nuclease-free water to final volume of 240 µl. The hybridization solution was prepared by adding 240 µl of 2X target solution to 10 µl of 25X fragmentation buffer. The mixture was incubated at 60^{O}C in the heating block for 30 min. Following, 250 µl of 2X hybridization buffer (from In situ Hybridization kit) to the final volume of 500 µl, mixed, spinned and 490 µl of the hybridization solution was applied to 60-mer Agilent 44K (or 4X 44K) Human Whole Genome oligonucleotide microarrays and assembled in microarray hybridization chamber (G2534A). Once fully assembled, the chambers were loaded into the hybridization rotator rack and set to rotate at 4 rpm. The hybridization was performed in a rotating oven at 60^{O}C for 17h.

All the washing steps were performed at room temperature. First the sandwiched slides were submerged in Wash Solution 1 to remove oligo microarray slide. The slides were washed for 1min in the Wash Solution 1 with the magnetic stir. The slides were then transferred to the staining dish containing Wash Solution 2 and washed for 1 min. Following, the slides were transferred to the staining dish containing the Wash Solution 3 and washed

for 30 sec. All steps were performed in the dark. The dried slides were scanned with a G2565BA Microarray Scanner System (Agilent Technologies).

Wash solution 1 composition: 6X SSPE, 0.005% N-Lauroylsarcosine, deionized nuclease free water.

Wash solution 2 composition: 0.06X SSPE, 0.005% N-Lauroylsarcosine, deionized nuclease free water.

The buffers 1 and 2 are passed through a 0.2µm sterile filtration unit before use.

Wash solution 3 composition: The Agilent Stabilization and Drying Solution contain an ozone scavenging compound dissolved in acetonitrile.

2.7.4. Data analysis

Feature extraction software (Agilent Technologies, version 10.7.3.1) was used to read and process the microarray images. Lowess intraarray and quantiles interarray normalization was applied and subsequent statistical analyses were performed.

2.7.4.1. Gene Set Enrichment Analysis

The Gene Set Enrichment Analysis tool (http://www.broad.mit.edu/gsea/) (Subramanian et al. 2005) was used to classify gene expression profiles into functional pathways. Gene sets were selected using the Molecular Signature Database (http://www.broadinstitute.org/gsea/msigdb/), including those relevant to either lymphoid cell biology or cancer. The gene set for the NF-κB target genes was manually added and described in (Compagno et al. 2009). A minimum of 15 and a maximum of 500 genes in a gene set were required to qualify for further analysis. The gene sets co regulated with NIK expression in primary samples were identified using Pearson correlation comparing the expression of NIK with the expression of the rest of the genes in the genome in the 37 primary PTCL samples. To identify pathways up- or downregulated in NIK knockdown cells, a limma t-test was performed between NIK silenced and control cells. Gene sets with a false discovery rate (FDR) below 0.15 were considered statistically significant.

2.7.4.2. Differential gene expression analysis

Genes differentially expressed between control cells and NIK knockdown cells were identified using a paired t-test using the Pomelo tool for class comparisons (http://pomelo2.bioinfo.cnio.es) and visualized using Gene Cluster and Treeview softwares (http://rana.lbl.gov/EisenSoftware.htm). Genes presenting an FDR<0.05 and a foldchange >±1.6 were considered significant. Venn diagrams were created using the free online tool VENNY (http://bioinfogp.cnb.csic.es/tools/venny/index.html).

2.8. Reverse transcription quantitative PCR (RT-qPCR)

2.8.1 Retrotranscription

RNA was isolated from cell lines and primary samples using the RNeasy Mini Kit as described in 2.6.1. cDNA was synthesized from 500 ng DNaseI-treated RNA with SuperScript II Reverse Transcriptase (Invitrogen) and random primers following the recommendations of the manufacturer. Briefly, 500 ng of RNA were mixed with 50 ng of random primers, 1 1 µL of 10 mM dNTPs mix and water was added to a final volume of 12 µL. The RNA was then denaturated by a heating step at 65º C for 5 minutes. The following components were added: 4 µl of 5X first strand buffer, 2 µL of 0.1 M DTT and 1 µL of ribonuclease inhibitor (RNAsin) at 40 U/µL and the mixture was incubated for 2 minutes at 25^{o}C prior to adding 1 µL of 200 U/µL SuperScript. The samples were then put in a thermocycler where they were first hold for 10 minutes at 25^{o}C, then for 50 minutes at 42^{o}C, and finally an inactivation step at 70^{o}C for 15 minutes.

2.8.2. Quantitative PCR

Primers used for quantitative PCR (qPCR) are listed in table 2.7. For NIK *(MAP3K14)* and BCL2-like 1 (*BCL2L1)* detection, TaqMan assays (Applied Biosystems) were performed. For the rest of the genes analyzed in this study, quantification of RNA expression was done by labeling the RNA with SYBR Green (Applied Biosystems). Human glucuronidase beta (GUSB) and 18S FAM primers or probes were used as endogenous controls in samples and cell lines. All samples were analyzed in a 7900HT Fast Real-Time PCR System (Applied Biosystems).

Table 2.7 Primer sequences for quantitative PCR

Gene	Forward primer (5´--> 3´)	Reverse primer (5´--> 3´)
*MAP3K14**	GGCCTGGGAAAGTCCTTG	CTGCTCCAGACATCCACCTT
IL6	GAAAGGAGACATGTAACAAGAGT	GATTTTCACCAGGCAAGTCT
IL21	AGCTGAAGAGGAAACCACCTTC	GAATCACATGAAGGGCATGTTAG
KLF2	CAAGAGTTCGCATCTGAAGGC-3	TGTGCTTTCGGTAGTGGCG
NFKBIA	CAACTACAATGGCCACACGTG	GCAGTCCGGCCATTACAG
YAP1	GACATCTTCTGGTCAGAGATACT	ACTGATTCTCTGGTTCATGG
CFLAR	CTGATGGCAGAGATTGGTGAG	GGCAACCAGATTTAGTTTCTCCA
CCND2	AGCTGCTGGAGTGGGAACTGGT	CTTAAAGTCGGTGGCACACAGAGC
GUSB	GGCTCCGAATCACTATCGC	CCTTGGGATACTTGGAGGTG

* Primers for MAP3K14 are used together with probe 17 (Roche Diagnostics) for TaqMan analysis

2.8.2.1 TaqMan assays

Two µL of cDNA were mixed with 7.5 µL of 2X Universal Master Mix (Applied Biosystems), 0.75 µL of the specific TaqMan Assay and water up to a final volume of 15 µL. Samples were added in triplicate on a 384-well MicroAmp optical reaction plate (Applied Biosystems). The PCR cycling conditions were standard: 95^{o}C for 10 minutes (one step), 95^{o}C for 15 seconds, and 60^{o}C for 1 minute (40 cycles). The relative changes in gene expression were calculated by the ΔΔCt method using the Sequence Detection System (SDS) 2.1 software (Applied Biosystems). The ΔΔCt method gives the amount of target normalized to an endogenous reference and relative to calibrator. The level of each transcript was quantified by the cycle at which the PCR amplification was in log phase where there was significant fluorescent signal (Ct) with glucuronidase beta (*GUSB)* or human 18S ribosomal RNA (*18S*), as endogenous controls.

2.8.2.2 SYBR Green assays

Two µL of cDNA were mixed with 5 µL SYBR Green PCR Master Mix (Applied Biosystems), 0.3 µL of specific forward and reverse primers (Table X) and 2.4 µL of water. As in the TaqMan assays, samples were added in triplicate on a 384-well plate. The PCR cycles were as follow: 50^{o}C for 2 minutes (one step), 95^{o}C for 10 minutes (one step), 95^{o}C for 15 seconds, 60^{o}C for 30 seconds and 72º C for 30 seconds (40 cycles) and then a dissociation step involving 95^{o}C for 15 seconds and then a slow increase of the temperature from 60^{o}C to 95^{o}C. The relative changes in gene expression were calculated by the ΔΔCt method using the Sequence Detection System (SDS) 2.1 software (Applied Biosystems), as in the TaqMan assays.

2.9 NF-κB binding activity assay

Nuclear fractions were separated from cytosolic fractions using the BioVision Nuclear/Cytosol Fractionation Kit (see section 2.5.2) and 5 µg of nuclear extract were used to quantify the NF-κB transcription activation using the ELISA-based TransAM NF-κB Family Transcription Factor Assay Kit (Active Motif, Carlsbad, CA, USA). The protocol was carried out following the manufacturer´s instructions. In brief, nuclear extracts were added to a 96-well plate containing immobilized NF-κB consensus oligonucleotide sequences. The active form of NF-κB then binds to the immobilized sequence and the addition of specific NF-κB subunit antibodies and secondary HRP-conjugated antibodies provide a colorimetric readout for the amount of DNA-bound transcription factor. Nuclear extracts were plated in triplicate. The specificity of the assay was confirmed performing a competition assay with wild-type and mutated consensus oligonucleotides.

2.10 Flow cytometry techniques

All analyses were performed in a FACS Canto II flow cytometer (BD Biosciences) using the BD FACS Diva software 6.0 (BD Biosciences). Ten thousand events were acquired in each sample. Acquired data were then analyzed and quantified with the FlowJo software (FlowJo version 7.6.1, TreeStar Inc., Ashland, OR, USA).

2.10.1 Analysis of apoptosis by AnnexinV staining

In order to meassure cell viability in cell lines after transfection, double staining with Annexin V and 4',6-diamidino-2-phenylindole (DAPI) was carried out. Annexin V is a 35-36 kDa Ca2+ dependent phospholipid-binding protein that has a high affinity for phosphatidylserine, and binds to cells with exposed phosphatidylserine. Loss of plasma membrane asymmetry, that includes flipping of phosphatidylserine from the inner to the outer leaflet of the plasma membrane, is an early event in apoptosis. Thus annexin V stains cells that are undergoing apoptosis. DAPI is a DNA intercalating molecule that stains nucleic acids. It is used to stain dead cells that have lost their membrane integrity. Since DAPI is a cell membrane impermeable compound, it is excluded from alive and early apoptotic cells while staining late apoptotic and necrotic cells. Double staining with these two compounds allows the discrimination between alive (double negative), early apoptotic (annexin V

positive, DAPI negative) and late apoptotic/necrotic cells (double positive). Small interference RNA (siRNA)-transfected cells were harvested 48, 72 and 96 hours after microporation, washed with PBS and resuspended in 200 µl Annexin V binding buffer (BD Biosciences) (10 mM HEPES, pH 7.4; 140 mM NaCl; 2.5 mM CaCl2). Two µL allophycocyanin (APC)-Annexin V (BD Biosciences) were added to each tube and cells were incubated in the dark for 15-20 minutes. Before acquisition in the cytometer, DAPI (final concentration 10 µg/ml) was added and the viable cell population (DAPI/AnnexinV negative) was quantified using FlowJo software (FlowJo version 7.6.1, TreeStar Inc., Ashland, OR, USA). Thus, the proportion of non-viable cells plotted in the cell viability graphs considers all cells positive for either DAPI or Annexin V.

2.10.2 Cell cycle analysis

To analyze the distribution of cells in the different stages of the cell cycle, cells were stained with propidium iodide (PI) and analyzed by flow cytometry. PI is able to indicate the amount of DNA in permeabilized cells. PI fluorescence signal is directly proportional to the amount of DNA inside the cell and can thus distinguish between different cell cycle stages by the DNA amount. Cells were collected 24, 48 and 72 hours after siRNA transfection, washed with PBS and fixed with chilled 70% ethanol. Before acquisition in the cytometer, cells were washed in PBS and 200 ng/ul RNase A (Qiagen) was added. After 30 minutes of incubation, 10 µL of PI (P4864, Sigma Aldrich) was added and cells were acquired in the cytometer.

2.11 RNA interference

RNA interference is a powerful technology for loss-of-function studies. RNA interference takes advantage of the cell´s natural machinery to knock down a gene of interest. Short/small interfering RNAs (siRNAs) are synthetic 20-25 base pair (usually 21 base pair) RNA duplexes. Once introduced into a cell by transfection, the antisense strand of the siRNA duplex becomes part of a multiprotein complex (RNA-induced silencing complex, RISC), which identifies the corresponding mRNA sequence from the gene of interest. RISC is then able to cleave the mRNA molecule, targeting its degradation and subsequent loss of protein expression (Elbashir et al. 2001). All the siRNAs used for gene knock down in this thesis, were purchased from Invitrogen (*Stealth* type siRNAs). SiRNA sequences are presented in table 2.8. A non-template control (NTC) (*Stealth* siRNA negative control LO GC, Invitrogen),

which is not homologous to any mRNA in the vertebrate transcriptome, was used as a control in all experiments. The concentration of siRNA in the final culture medium after transfection was 100 nM in all experiments. If several siRNAs were used in the same transfection, a total concentration of 100 nM was used. SiRNAs were efficiently introduced into the cell lines by microporation (see below). Twenty-four, 48, 72 and 96 hours after transfection, cells were harvested for measurement of cell viability, protein extraction and RNA extraction. Experiments were conducted as independent triplicates.

2.11.1 Microporation

Microporation is a transfection method based on electroporation technology that permits the transfection of cells with high efficiency and survival rate. All microporation experiments were done using the MicroPorator MP100 (NanoEnTek Inc. Seoul, Korea) with Neon tranfection system kit (100 µL tips, Invitrogen) using a gold capillary tip, which permits a less harmfull electroporation compared to a cuvette. One day prior to microporation, cells were seeded in fresh medium without antibiotics. The next day, cells were washed in PBS, counted, and $2x10^6$ cells were resuspended in 110 µL buffer R in a 2 mL eppendorf tube. The siRNA was added (so that a final concentration of 100nM siRNA would be achieved in the culture medium) and 100 µL of cell suspension was then taken with the gold tip and the pipette was inserted into the MicroPorator. After the electroporation cells were seeded in 3 mL of culture medium and incubated at 37^oC until analysis. To optimize the transfection efficiency and minimize cell death, microporation conditions were set for each individual cell line. Briefly, $3x10^5$ cells were resuspended in 10 µL buffer R and 50 nM of SiGLO (Thermo Fisher Scientific Inc., Waltham, MA, USA), a fluorescent oligonucleotide for assessment of uptake into cells, was added. Ten µL of cell suspension were microporated using different conditions, varying pulse voltage (900 to 1600 V), pulse width (from 10 to 40 ms) and number of pulses (1-3), and then incubated in 0,5 mL of culture medium for 24h. Cells were then analyzed by flow cytometry and the porcentage of positive (Cy3 positive for SiGLO uptake) and viable cells (Annexin V and DAPI negative) were assessed. The condition presenting the highest efficiency with the lowest effect on cell viability was chosen for the siRNA experiments. Table 2.9 shows the microporation conditions for the cells used in this thesis. For all gene silencing experiments, a transfection efficiency greater than 95% was achieved, as estimated in a parallel microporation using siGLO.

Table 2.8. SiRNA sequences used for gene knockdown.

siRNA name	Gene	Sequence	Reference name
siNIK 1	*MAP3K14*	AUCUGAUCAAGACUCUCGGACUGGC	MAP3K14VHS40827
siNIK 2	*MAP3K14*	CCCAAGCUAUUUCAAUGGUGUGAA	MAP3K14HSS113310
siIKKα 1	*CHUK*	GGGCCAUUUGCUUCCAGAAGUUUAU	CHUKHSS101936
siIKKα 2	*CHUK*	CAGCAAUGUUAAGUCUUCUUAGAUA	CHUKHSS174353
siIKKβ 1	*IKBKB*	CCGCCAUGAUGAAUCUCCUCCGAAA	IKBKBHSS105292
siIKKβ 2	*IKBKB*	GCGAAGACUUGAAUGGAACGGUGAA	IKBKBHSS105294
siNFKB1 1	*NFKB1*	CCAUCCUGGAACUACUAAAUCUAAU	NFKB1HSS107143
siNFKB1 2	*NFKB1*	GCCAGAGUUUACAUCUGAUGAUUUA	NFKB1HSS107145
siNFKB2 3	*NFKB1*	GGGAGGAAAUUUAUCUUCUUUGUGA	NFKB1HSS181512
siNFKB2 1	*NFKB1*	CCCAGGUCUGGAUGGUAUUAUUGAA	NFKB2HSS107146
siNFKB2 2	*NFKB1*	GAUUUCAAAUUGAACUCCUCCAUUG	NFKB2HSS107147
siNFKB2 3	*NFKB1*	GGGUGGAGAUGAAGUUUAUCUGCUU	NFKB2HSS107148
siRELB 1	*RELB*	GAGGACAUAUCAGUGGUGUUCAGCA	RELBHSS109162
siRELB 2	*RELB*	GCGAGGAGCUCUACUUGCUCUGCGA	RELBHSS184267
siRELB 3	*RELB*	CCCUACAACGCUGGGUCCCUGAAGA	RELBHSS184268
siCREL 1	*CREL*	CCUCCGGUGCGUAUAACCCGUAUAU	RELHSS109157
siCREL 2	*CREL*	ACAUGGUAAUUUGACGACUGCUCUU	RELHSS109158
siCREL 3	*CREL*	CAGAAUUAAGGAUUUGUCGUGUAAA	RELHSS184261
siKLF2 1	*KLF2*	GCUGGAAGUUUGCGCGCUCAGACGA	KLF2HSS145585
siKLF2 2	*KLF2*	GGCCAUUCCAGUGCCAUCUGUGCGA	KLF2HSS145586
siKLF2 3	*KLF2*	CCUACACCAAGAGUUCGCAUCUGAA	KLF2HSS173585
siSTAT3 1	*STAT3*	GCAGUUUCUUCAGAGCAGGUAUCUU	STAT3VHS40491
siSTAT3 2	*STAT3*	CCUGCAAGAGUCGAAUGUUCUCUAU	STAT3VHS40497
siLMP1 A	*LMP1*	GAGCCCUUUGUAUACUCCUACUGAU	Custum design
siLMP1 B	*LMP1*	UCGCUCUCUGGAAUUUGCACGGACA	Custum design

Table 2.9. Microporation conditions for lymphoma cell lines

Cell line	Pulse Voltage	Pulse Width	Pulse Number
My-La	1300 V	20 ms	2
SR-786	900 V	30 ms	2
DERL-7	1100 V	20 ms	2
HuT78	1150 V	20 ms	2
FARAGE	1100 V	20 ms	2

2.12 Cloning of human MAP3K14 into pCDNA3.1 vector

MAP3K14 cDNA (encoding full length human NIK) inserted into pENTR/D-TOPO (Invitrogen) was kindly provided by the CNIO Proteomics Unit. The *MAP3K14* cDNA was amplified by polymerase chain reaction (PCR) from pENTR/D-TOPO-MAP3K14 and subcloned into the pCDNA3.1 vector (Invitrogen) using the EcoRI and XhoI restriction sites in the multiple cloning site. The sequence of the forward primer including an EcoRI site and Kozak sequence (for enhanced expression in mammalian cells) was 5´-CCTAGAATTCGCCACCATGGCAGTGATGGAAATGGC – 3´, and the sequence of the reverse primer including XhoI restriction site was 5´-CTAGCTCGAGCTAGGGCCTGTTCTCCAGC – 3´. Shortly, KOD proofreading DNA polymerase (Toyobo Co., Osaka, Japan) was used to amplify *MAP3K14* cDNA by PCR from 60 ng of pENTR/D-TOPO-MAP3K14 by standard PCR following the manufacturer´s instructions for KOD Polymerase. PCR reactions took place in a GeneAmp® PCR System 9700 (Applied Biosystems). The PCR product was cleaned by QIAquick PCR Purification Kit (Qiagen) and then digested at 37^{o}C overnight with EcoRI and XhoI (New England Biolabs Inc., Ipswich, MA, USA) as was the destination vector, pCDNA3.1 (Invitrogen). The digested DNA was then loaded onto a 1% agarose gel and the bands were excised and purified using QIAquick Gel Extraction Kit (Qiagen). The ligation of *MAP3K14* with pCDNA3.1 was performed with a vector:insert ratio of 1:3 with T4 DNA ligase (New England Biolabs Inc.) at 16ºC overnight. The ligation was then used to Heat-Shock transform One Shot® TOP10 Chemically Competent E. coli (Invitrogen) and the transformed bacteria culture was plated on an agar plate with ampicillin (the resistance cassette of pCDNA3.1) at 37^{o}C overnight. Colonies were picked, grown in 3 mL Luria-Bertani (LB) broth (supplemented with 100 ug/mL ampicillin) at 37^{o}C in continuous shaking (225 rpm) for approximately 16 hours. To isolate the plasmid from the bacterias, the PureYield Plasmid Miniprep System (Promega) was used following the protocol of the manufacturer. Colonies presenting DNA with a correct restriction enzyme pattern (after digestion with EcoRI and XhoI) were then

sequenced (conventional Sanger sequencing) to confirm a proper cloning process. In order to obtain high quality plasmids for further use in cell culture, the convenient colony was expanded and the plasmid isolated by PureYield Plasmid Maxiprep System (Promega) following the provided instructions.

2.13 Transfection of HEK 293T cells using FUGENE HD transfection reagent

For the overexpression of NIK, HEK293T cells were transfected with pCDNA3.1-MAP3K14 using FuGene® HD Transfection Reagent (Roche, Basel, Switzerland). FuGene® HD is a reagent containing lipids and other components that form complexes with DNA that are transported into the cells. The HD formulation allows transfection of cells cultured at high density (80-90% confluence). The transfection was done following the manufacturer's recommendations. The day before the tranfection, 4.5 million cells were seeded in a 10 cm plate. The next day the medium was replaced by 10 mL of fresh medium and the cells were put back into the incubator. 9 µg of plasmid (pCDNA3.1-MAP3K14 or pCDNA3.1 empty control vector) were mixed in 500 µL of prewarmed OPTIMEM® medium (Invitrogen) with 27 µL of FuGene® HD. The mixture was incubated for 30 minutes with gentle shaking every 5-10 minutes at room temperature. The mixture was then added dropwise to the cells and the cells were cultured normally. Fourty-eight hours after tranfection, cells were trypsinized and washed and the pellet was stored at -80ºC for later protein extraction and analysis by western blot. A control vector expressing green fluorescent protein (GFP) (pCDNA3.1-GFP) was transfected in parallel to estimate the transfection efficiency which was around 80%.

2.14 Dominant negative NIK

NIK (KK/AA) is a dominant negative form of NIK containing two amino acid substitutions in the kinase domain (KK429-430AA), forming a kinase-dead protein (Malinin et al. 1997). The expression vector pCDNA3.1-NIK(KK/AA) was a kind gift from the Experimental Therapeutics Programme at the CNIO. My-La and SR-786 cells were transfected with pCDNA3.1–NIK(KK/AA) using microporation (see section 2.11.1). Ten µg DNA and $2x10^6$ cells were used for each transfection and the microporation conditions are represented in table 2.9. pCDNA3.1 empty vector was used as a control and pCDNA3.1-GFP was used to estimate the

transfection efficiency, which ranged between 40 and 60% in the different experiments. After 24 and 48 hours, cells were harvested for cell viablility assay and protein extraction.

2.15 Immunofluorescence

Immunofluorescence staining of c-Rel was made 48 hours after transfecting the cells with siNIK or a non-template control. To attach cells to a coverslip, Poly-L-Lysine (10% diluted in water) was first added to the coverslip and incubated at 37^{o}C for 1 hour. The coverslip was washed once in PBX 1X, put into a well of a 24-well plate, and approximately 400 000 cells in its growth medium were added to the well. Cells were incubated at 37^{o}C until the cells had attached to the coverslip (approximately 1-2 hours). Cells were then washed in PBS 1X and fixed with 4% paraformaldehyde for 10 minutes at room temperature. After two wash steps (2 x 3 minutes) in PBS 1X, 0.5% Triton was added and cells were incubated for 5 minutes at room temperature. Cells were washed twice and then blocked with 5% FBS (diluted in PBS) for 30 minutes at 37^{o}C. Coverslips were placed in a humid chamber and the c-Rel antibody was added (1/100 in 1% PBS, Cell Signaling 4727) and incubated for 1 hour at room temperature. Coverslips were then washed 2 x 3 minutes in PBS and the secondary antibody was added (Alexa 488 Donkey anti-Rabbit, Invitrogen A21206) and incubated in darkness for 1 hour at room temperature. Coverslips were washed in PBS 1X once and were then incubated in DAPI solution (100ng/mL) for 10 minutes. After another wash step coverslips were rapidly dipped in water and then mounted on slides using Prolong Gold reagent (Invitrogen). Slides were left to dry horizontally in darkness overnight. Images were obtained by a Leica SP5 MP confocal microscope (Leica Microsystems, Germany) with LAS AF v.3.x software (Leica Microsystems).

3. RESULTS – PART I

Characterization of classical and alternative NF-κB activation in diffuse large B cell lymphoma

3.1 NF-κB expression in different human lymphomas

Aberrant NF-κB signaling has been reported in several types of lymphomas and NF-κB has been suggested to play a role in the underlying pathogenesis of some of these neoplasms (Jost et al. 2007). However, there is a lack of studies including patient samples and there are only few studies involving the alternative pathway. We therefore decided to analyze the expression of both classical and alternative NF-κB factors in patient tumor samples from a variety of different lymphoma types; splenic marginal zone lymphoma (SMZL), mantle cell lymphoma (MCL), Hodgkin lymphoma (HL), follicular lymphoma (FL), diffuse large B-cell lymphoma (DLBCL) and peripheral T cell lymphoma (PTCL). As the activation of the NF-κB pathway results in translocation of the transcription factor dimers to the nucleus, we evaluated the nuclear expression of NF-κB as a measure of an activated NF-κB signaling, using immunohistochemistry on paraffin-embedded tissues. As readout for the alternative NF-κB pathway, we used nuclear p52, and for the classical pathway, nuclear p50 was assessed (Figure 3.1 A). From here on, if not otherwise specified, when we talk about NF-κB expression or NF-κB-positive tumors, we refer to nuclear expression of these proteins. If more than 30% of the tumoral cells presented nuclear staining by immunohistochemistry, the tumor was considered positive for NF-κB. In six B cell lymphoma cell lines, we performed both immunohistochemistry and an ELISA assay, which assessed the DNA-binding activity of the NF-κB factors (Figure 3.1 B). This comparison showed that cell lines that presented nuclear staining of p50 or p52, also had an increased DNA-binding activity of these proteins, suggesting that nuclear expression of NF-κB corresponds to active NF-κB.

The frequencies of nuclear p52 and p50 expression in various tumors are shown in Figure 3.1 C. While classical NF-κB signaling (p50) was present in a significant proportion of cases of most types of lymphomas, alternative NF-κB signaling was practically absent in some lymphoma types, such as FL and SMZL. The highest frequencies of nuclear p52 and p50 expression were observed in PTCL and Hodgkin lymphoma, where the vast majority of tumors were positive for both markers. Both pathways were also activated in approximately a third of DLBCL tumors. In this work, the pathway has been further studied in PTCL and DLBCL, given its frequent activation and relevance to the pathogenesis of these diseases.

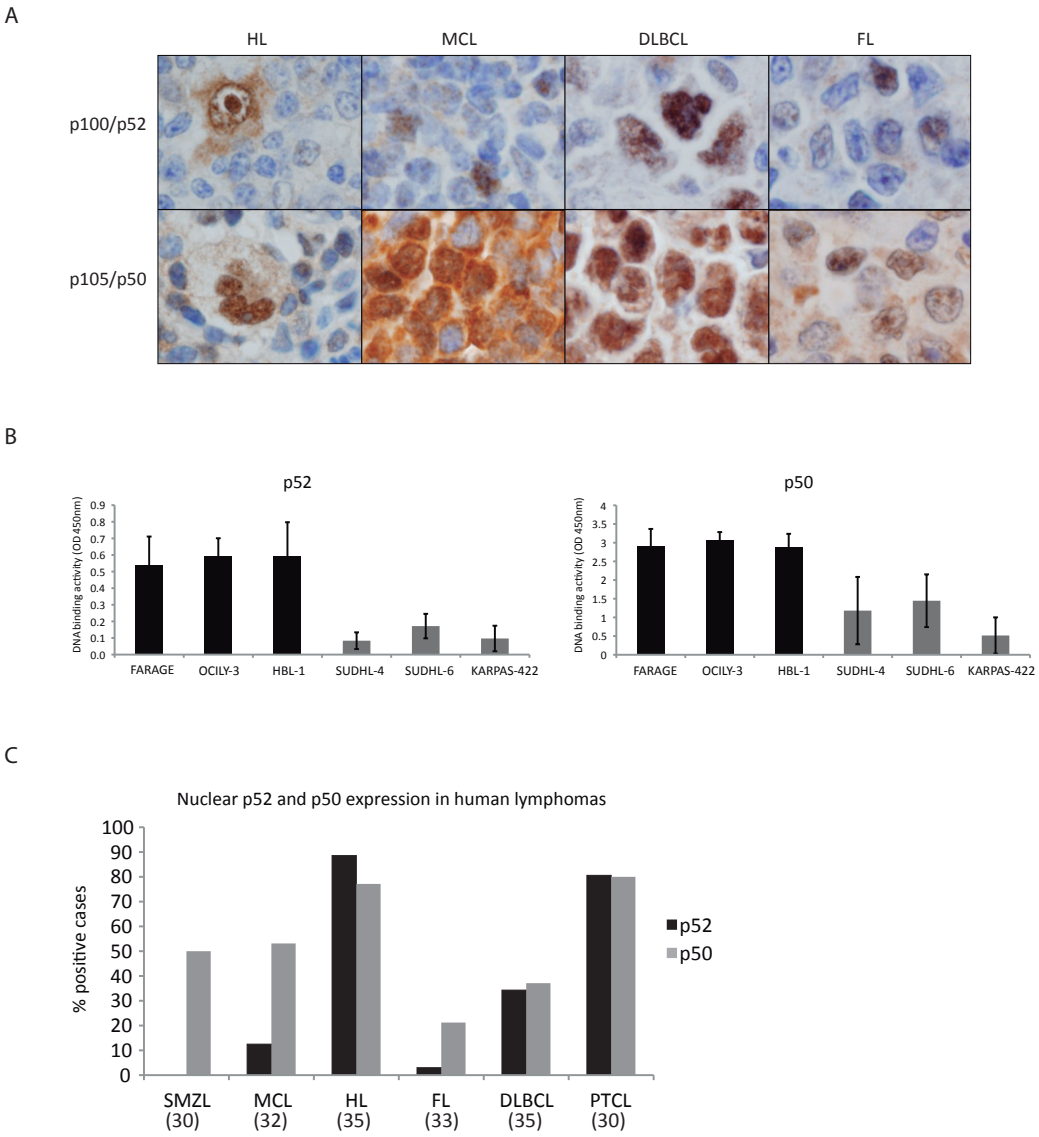

Figure 3.1 Expression of p100/p52 and p105/p50 in human lymphoma tissue.

A) Immunohistochemistry showing nuclear staining of p52 and p50 in different lymphoma types. B) Comparison between immunohistochemistry and DNA-binding activity in lymphoma cell lines. Graphs represent the DNA-binding activity of p52 and p50 measured by an ELISA TransAM assay. Black bars represent cell lines with nuclear expression of p52 and p50 and grey bars indicate cell lines that lack nuclear p52 or p50, as assessed by immunohistochemistry. C) Percentages of cases positive for nuclear p52 (black bars) or p50 (grey bars) among different lymphoma types. The numbers below the graph indicate the number of tumors analyzed in each category. SMZL = splenic marginal zone lymphoma , MCL = mantle cell lymphoma, HL = Hodgkin lymphoma, FL = follicular lymphoma, DLBCL = diffuse large b-cell lymphoma, PTCL = peripheral T cell lymphoma.

3.2 NF-κB activation in DLBCL

Even though constitutive NF-κB activation is one of the proposed oncogenic mechanisms underlying the molecular pathology of DLBCL, particularly the ABC subtype, the actual expression of NF-κB in DLBCL tumor specimens and the presence of both classical and alternative signaling component as well as their clinical correlation, has not been well studied. Bearing in mind that the NF-κB pathway was found to be activated in a significant group of DLBCL samples (as shown in Figure 1), and its proven importance in this kind of malignancy (Davis et al. 2001), we decided to study this pathway further in an extended series of DLBCL samples.

3.2.1 Correlation between EBV, LMP1 and NF-κB in DLBCL

EBV-positive DLBCL of the elderly has been recognized as a provisional separate lymphoma entity in the latest WHO classification (Swerdlow et al. 2008), due to its distinct molecular and clinical profile. EBV-positive DLBCL has a more aggressive clinical course than EBV-negative DLBCL (Montes-Moreno et al. 2012). Experimental studies have demonstrated that EBV can induce NF-κB activation (Devergne et al. 1996; Keller et al. 2006; de Oliveira et al. 2010). The extent and features of this phenomenon in lymphoma primary samples has not yet been elucidated, however. For that reason, we examined whether there was any connection between EBV status and the expression of nuclear p52 or p50 in human DLBCL samples. In a large series of 260 DLBCL tumor samples, 8.1% of the tumors were EBV positive, as established by EBV-encoded RNA (EBER) in situ hybridization. Additionally, we evaluated the expression of the EBV-derived antigen latent membrane protein 1 (LMP1) in our samples, because it has been suggested as one of the triggers of EBV-induced NF-κB activation (Eliopoulos et al. 2001). Only 5.4% of all cases in our series expressed LMP1. Overall, in the cohort of 260 tumors, 34.2% were positive for p52 and 38.8% were positive for p50. In the EBV-positive cases (EBER-positive), this number was raised to 71.4% and 61.9%, respectively (Figure 3.2 A). Hence, there was a positive and highly significant correlation between EBV status and nuclear p52 and p50 in our series (Chi-square test, $p=0.0002$ for p52 and $p=0.02$ for p50). Interestingly, this correlation was even stronger when evaluating the expression of LMP1, where 92.8% and 85.7% of the LMP1-positive cases were positive for nuclear p52 and p50, respectively (Figure 3.2 A, $p=0.000002$ for p52 and $p=0.0002$ for p50).

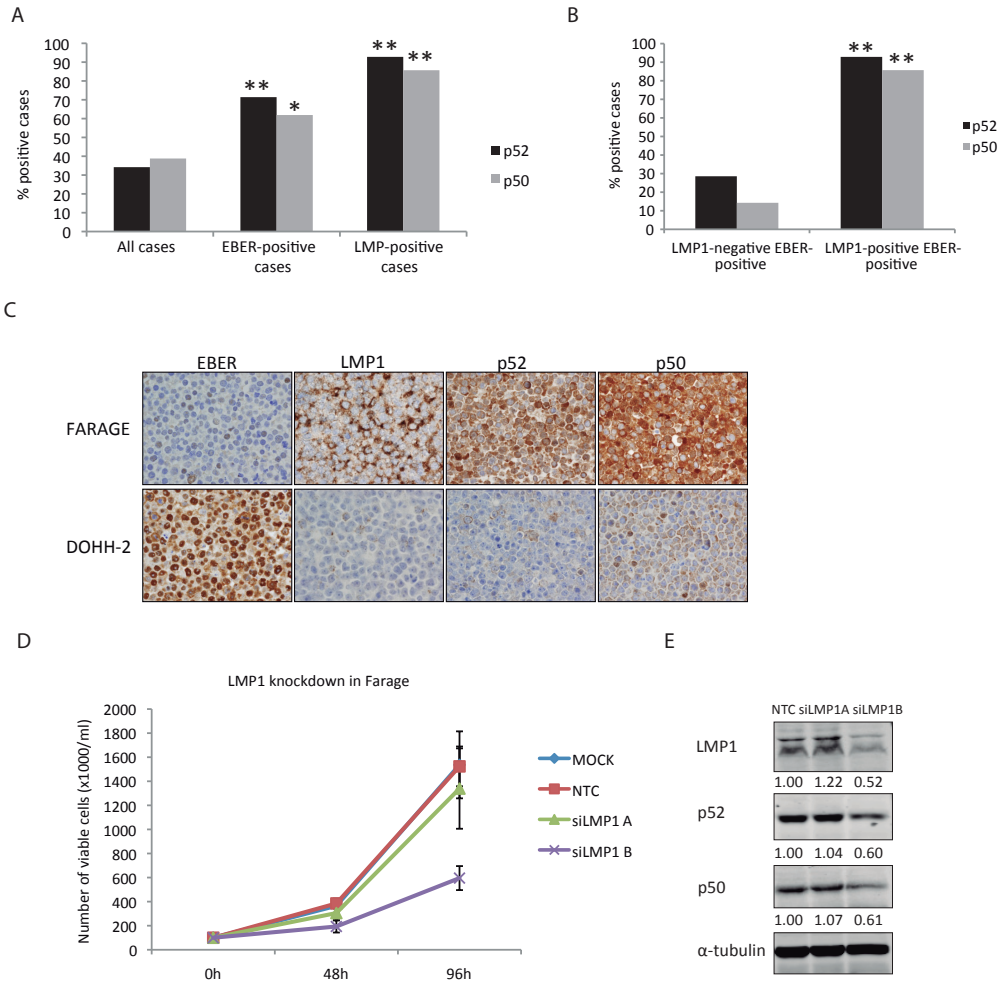

Figure 3.2 Correlation between EBV, LMP1 and NF-κB in DLBCL.

A) Percentages of primary DLBCL cases expressing nuclear p52 or p50 depending on EBV and LMP1 status. One asterisk means $p<0.05$ and two asterisks stand for $p<0.01$, estimated with a Student´s t-test. B) Comparison of nuclear NF-kB expression in EBV-positive DLBCL, taking into account the status of LMP1. C) Images of the expression of EBER (in situ hybridization), LMP1, p50 and p52 (immunohistochemistry) in two EBV-positive DLBCL cell lines, FARAGE and DOHH-2. D) Proliferation assay after LMP1 knockdown in FARAGE cell line. The graph represents number of viable cells after 0, 48 and 96 hours after LMP1 knockdown. E) Western blot showing the levels of LMP1, p52 and p50 after LMP1 silencing. The quantification of p50 and p52, normalized to the levels of α-tubulin and represented as a ratio to NTC, is shown below each panel. EBV = Epsten-Barr virus, EBER = EBV-encoded RNA, LMP1 = Latent membrane protein 1.

Notably, in cases positive for EBER but negative for LMP1, only 28.6% expressed nucear p52 and 14.3% expressed nuclear p50, suggesting an essential role for LMP1 in EBV-induced NF-

κB activation (Figure 3.2 B). Moreover, in two EBV-positive DLBCL cell lines (FARAGE and DOHH-2), only the one expressing high levels of LMP1 (FARAGE) showed nuclear NF-κB localization (Figure 3.2 C).

Knockdown of LMP1 with two siRNAs (siLMP1A and siLMP1B, with only siLMP1B producing an effective knockdown) in FARAGE cell line led to reduced cell growth (Figure 3.2 D) compared to untransfected cells (MOCK) or non-template control (NTC)-transfected cells, confirming the role of LMP1 for cell growth and survival of infected lymphocytes (de Oliveira et al. 2010) Analyzing the effect of LMP1 knockdown on downstream NF-κB expression, we observed a reduction of both p50 and p52 expression (Figure 3.2 E), suggesting a role of LMP1 in the regulation of the alternative and classical pathways in DLBCL. Taken together, these results indicate that EBV-positive DLBCL is characterized by frequent NF-κB activation and suggest that one of the possible triggers for both alternative and classical NF-κB activation in DLBCL is LMP1. Even though the relationship between EBV, LMP1 and NF-κB has previously been shown in experimental models, our results provide animportant verification that this correlation also exists in primary tumors from patients with DLBCL and identify NF-κB expression as a cardinal feature of LMP1-positive DLBCL tumors.

3.2.2 Expression pattern of different NF-κB members in EBV-negative DLBCL

Since the family of NF-κB consists of 5 different transcription factors, we decided to evaluate the expression of all of them in order to get a complete picture of the expression pattern in these tumors. In a series of 113 consecutive EBV-negative human DLBCL biopsies, taken at the time of diagnosis, the nuclear expression of p50, p52, RelB, p65 and c-Rel was assessed (Figure 3.3 A). If more than 30% of the tumoral cells presented nuclear staining, the tumor was considered positive. This threshold was chosen because it has previously been used for NF-κB expression in DLBCL (Compagno et al. 2009; Pham et al. 2011) and is also a threshold commonly used for standard immunohistochemistry markers in DLBCL (Hans et al. 2004; Choi et al. 2009). In addition to the association observed between nuclear NF-κB staining and DNA-binding activity (Figure 3.1 B), Compagno and coworkers (Compagno et al. 2009) showed that nuclear expression of p50 or p52 in DLBCL, evaluated by immunohistochemistry, was associated with enhanced transcription of NF-κB target genes, suggesting that immunohistochemical analysis of nuclear NF-κB could be a valid approach for assessing active NF-κB signaling.

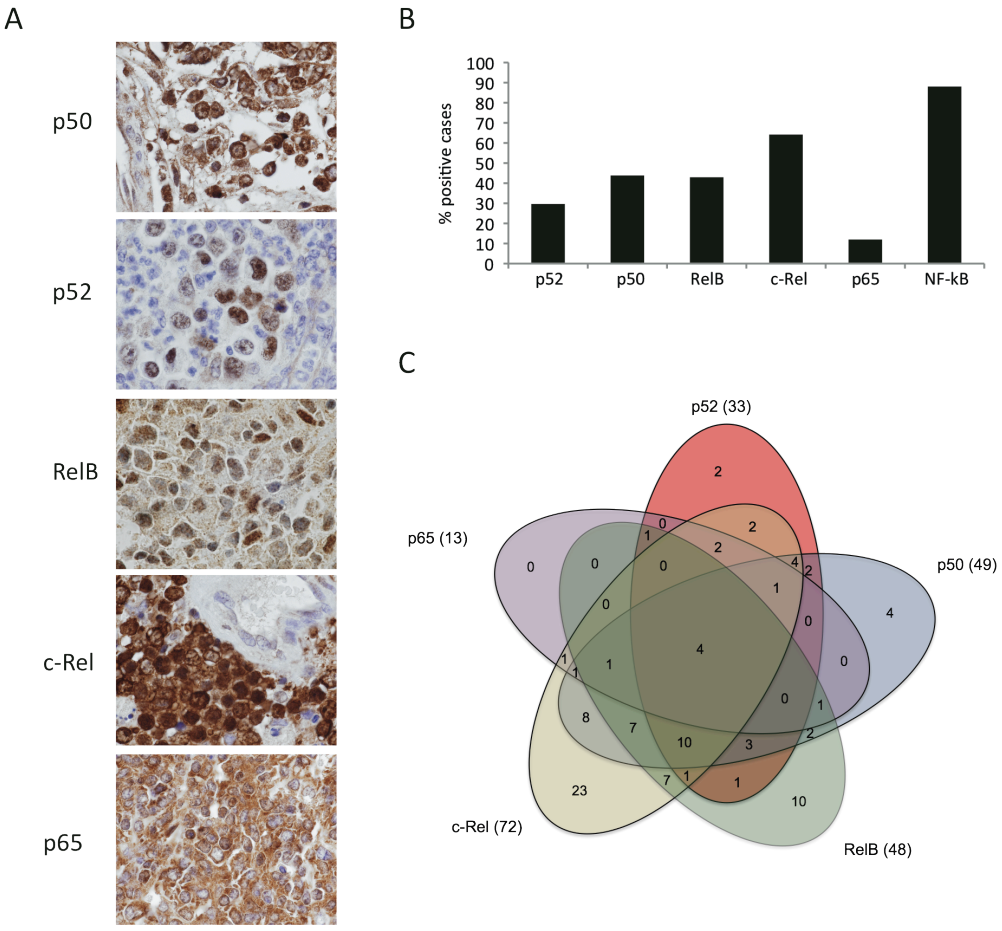

Figure 3.3 Expression of different NF-κB proteins in EBV-negative DLBCL

A) Immunohistochemical staining shows nuclear staining of p50, p52, RelB, c-Rel and p65 in representative DLBCL samples. B) Porcentages of DLBCL cases staining positive for NF-κB subunits (nuclear staining in >30% of the tumoral cells) in a series of 113 tumors. NF-κB in the last column represents the porcentage of cases staining positive for any NF-κB subunit. C) Venn diagram showing the overlap in number of positive cases, between the different NF-κB factors.

The percentages of positive cases for each of the NF-κB proteins are respresented in Figure 3.B. Interestingly, only 12.4% of cases lacked the expression of all NF-κB subunits. Of the five proteins, c-Rel was the most commonly expressed (63.7%), followed by RelB (42.5%), p50 (43.4%) and p52 (29.2%). Surprisingly, nuclear p65 was only detected in 11.5% of the samples. The relationship between the expression of the different subunits is represented in the Venn diagram in figure 3.3 C..3

Notably, the expression pattern of the different factors is complex, and doesn't follow the classical outline of the NF-κB pathway. There is a significant correlation between the

expression of factors of the classical and alternative pathway, such as between p50 and p52 (p=0.000052), p52 and p65 (p=0.006), and between p50 and RelB (p=0.006) (Table 3.1), indicating an overlap between classical and alternative factors and suggesting that no precise line exists distinguishing these two pathways. It is also remarkable that 23 c-Rel-positive cases do not express any other NF-κB factor.

3.2.3 Correlation between NF-κB expression and DLBCL subclassification

Based on gene expression profiling, two different molecular subtypes of DLBCL were recognized according to the putative cell of origin: the more aggressive activated B-cell-like (ABC) subtype and the germinal center B-cell-like (GCB) subtype (Alizadeh et al. 2000; Wright et al. 2003). Due to practical reasons, algorithms to classify these subtypes using immunohistochemistry of a few markers instead of gene expression profiling have been developed and extensively used (Hans et al. 2004; Choi et al. 2009). These subtypes also differ in their oncogenic programs and several subtype-specific genetic alterations have been described (Lenz et al. 2010; Pasqualucci et al. 2011; Zhang et al. 2013). A hallmark of ABC-DLBCL is constitutive NF-κB activation, and a disruption of this activation induces apoptosis in ABC-DLBCL cell lines (Davis et al. 2001). The overall survival of patients of the ABC subtype is significantly inferior than that of patients with GCB subtype (Rosenwald et al. 2002). Since ABC-DLBCL is characterized by prominent NF-κB activation, we wanted to explore how the expression of the five transcription factors was distributed between the GCB and ABC subtypes. In our series of 113 tumors, DLBCL subclassification was done using immunohistochemistry according to the algorithm of Choi (Choi et al. 2009). Surprisingly, we see a fairly even distribution of NF-κB-positive staining of all subunits between the subtypes, with only a slight but not significant increase of positive cases in ABC-DLBCL (Figure 3.4 A and Table 3.1).

To validate this finding, we performed the study in a second series of 60 DLBCL samples, where subclassification had been done using gene expression profiling (described and published in (Hu et al. 2013). Still, the expression of NF-κB showed no correlation with DLBCL subtype (Figure 3.4 B). Moreover, only 5 out of 60 cases were misclassified using immunohistochemistry for subclassification in this series (concordance of 91.7%), suggesting that this is a valid approach for GCB/ABC stratification in our cohorts.

Table 3.1. Distribution and correlation between the expression of different NF-κB factors

		p52		p50		RelB		c-Rel		p65		GCB/ABC	
		neg	*pos*	*neg*	*pos*	*neg*	*pos*	*neg*	*pos*	*neg*	*pos*	*GCB*	*ABC*
p52	*neg*			55	25	52	28	32	48	75	5	34	46
	pos			9	24	13	20	9	24	25	8	12	21
p50	*neg*	0.000052				44	20	28	36	60	4	31	33
	pos					21	28	13	36	40	9	15	34
RelB	*neg*	0.012		0.006				23	42	59	6	26	39
	pos							18	30	41	7	20	28
c-Rel	*neg*	0.201		0.059		0.817				38	3	20	21
	pos									62	10	26	46
p65	*neg*	0.006		0.045		0.378		0.292				41	59
	pos											5	8
GCB/ABC	*GCB*	0.546		0.056		0.859		0.187		0.861			
	ABC												

Note: The upper part of the table (white section above the diagonal) represent contingency tables of the number of negative and positive tumors in each category. The lower part of the table (light grey) represents the p-value for a Chi square correlation test between the different categories.

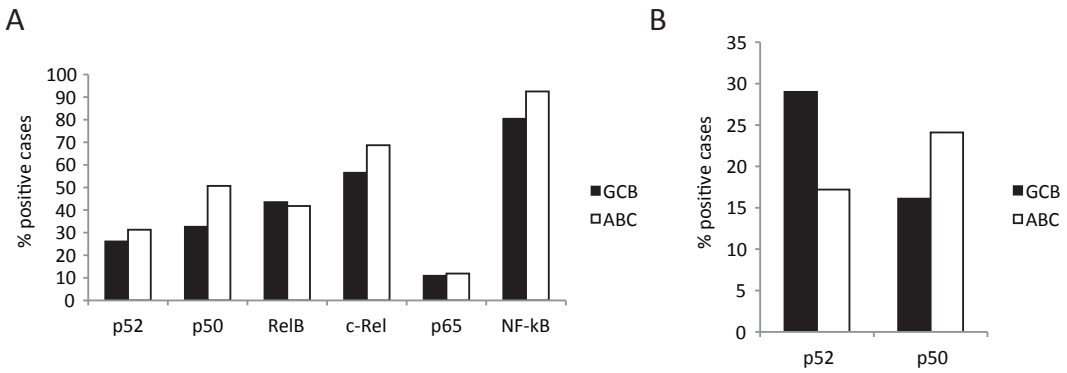

Figure 3.4 Analysis of the expression of NF-κB family members and their distribution between DLBCL molecular subtypes.

A) 113 primary DLBCL tumors were analyzed. The graph shows the percentage of positive cases in each DLBCL subtype (black columns represent ABC-DLBCL, and white columns represent GCB-DLBCL). DLBCL classification was performed using immunohistochemistry. B) Comparison of percentage of positive cases for p50 and p52 in different DLBCL subtypes when classification was performed using gene expression profiling.

3.2.4 Clinical correlation of NF-κB in DLBCL

Samples from a cohort of 88 DLBCL patients treated with R-CHOP immunochemotherapy (Rituximab combined with cyclophosphamide, doxorubicin, vincristine, and prednisone) were used to estimate if NF-κB expression had any impact on the clinical course of the malignancy (See Table 2.1 in the materials and methods section for patient characteristics). Of all the five NF-κB subunits, only c-Rel had a significant impact on the clinical outcome. Patients having c-Rel-positive tumors had a significantly superior overall survival than patients with c-Rel-negative tumors (with estimated 5-year overall survival rates of 73.7% versus 59.7%, Figure 3.5, p=0.041). The expression of p52 was also associated with enhanced overall survival, although this difference was not statistically significant.

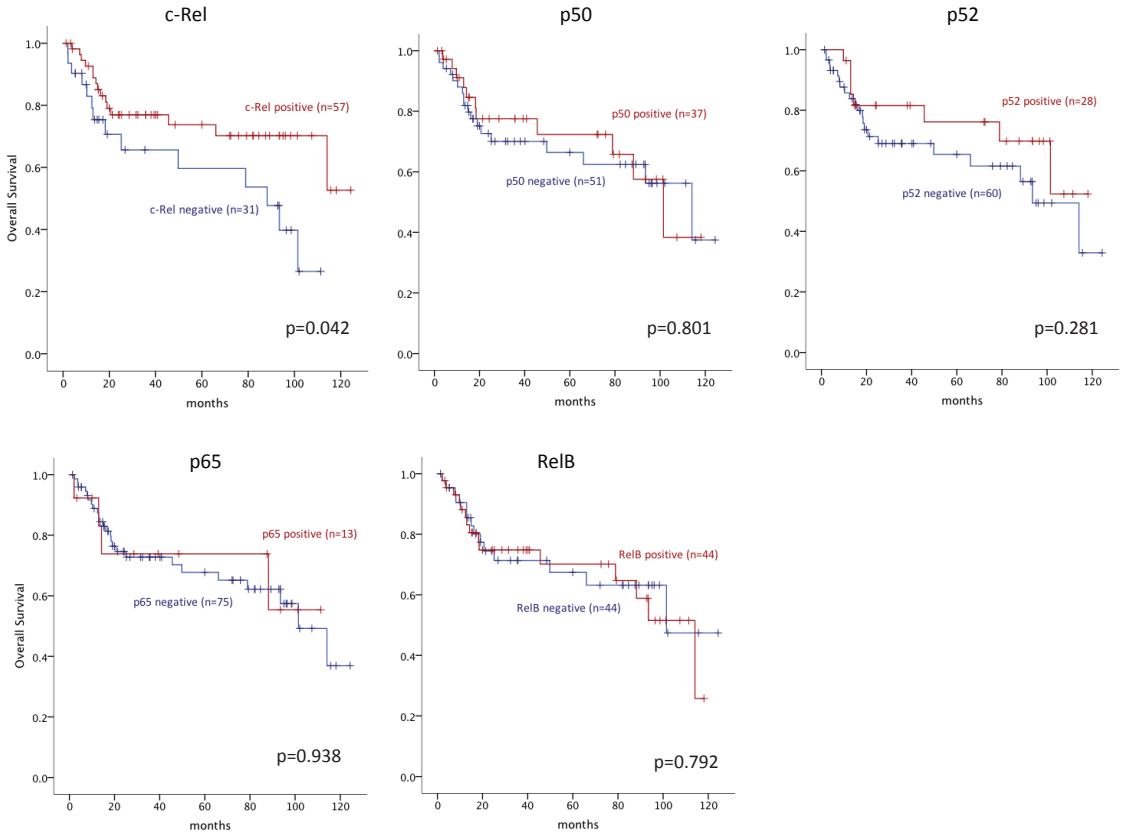

Figure 3.5. Clinical impact of NF-κB expression in DLBCL.

Kaplan-Meier plots estimating the overall survival in patients with positive (red line) or negative tumors (blue line) for the five different NF-κB subunits. Tumors positive for c-Rel are significantly associated with a superior overall survival (p=0.042, Log-Rank test).

In order to take into account other important prognostic features in DLBCL, a multivariate analysis, including DLBCL subclassification and the international prognostic index (IPI), was performed (Table 3.3). Interestingly, c-Rel was proven to be a favorable prognostic factor, independently of both GCB/ABC classification and IPI.

Table 3.3 Results from c-Rel multivariate survival analysis

Variable	p-value	Hazard ratio (CI 95%)
c-Rel	0.038	0.442 (0.205-0.953)
IPI (≥3)	0.025	2,454 (1.122-5.368)
GCB/ABC	0.165	1.793 (0.787-4.086)

Abbreviations: IPI = International Prognostic Index, GCB = Germinal center B-cell-like, ABC = Activated B-cell-like

4. RESULTS – PART II

The NF-κB pathway in T cell lymphomas: NIK as a regulator of classical and alternative signaling and cell survival

4.1 NF-κB expression in human PTCL samples

NF-κB activation has been reported in PTCL, but there are few studies including patient material and the expression pattern of the various NF-κB members has not been described in detail. In order to characterize the expression of NF-κB in PTCL, we performed immunohistochemistry on paraffin-embedded tissues from patients with the most common types of PTCL: angioimmunoblastic T-cell lymphoma (AITL), PTCL-not otherwise specified (PTCL-NOS), and anaplastic large T-cell lymphoma (ALCL) (Figure 4.1 A). All samples were taken at diagnosis. The nuclear expression of the five NF-κB proteins was evaluated. To represent different levels of NF-κB expression among the tumors, two positivity thresholds were used based on the number of tumor cells with nuclear staining; 20% (pos +) and 50% (pos ++) (Figure 4.1 B).

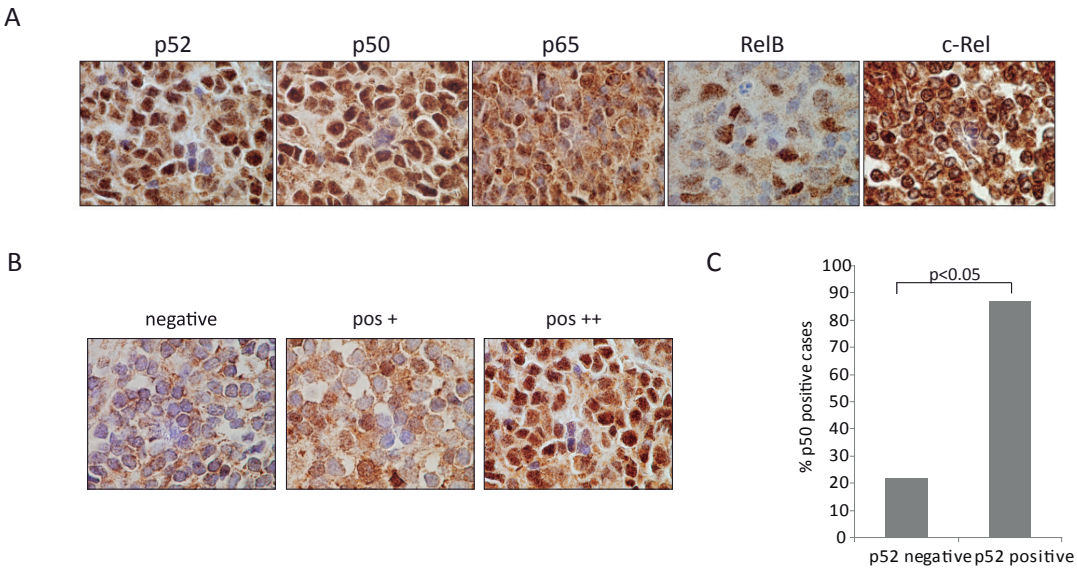

Figure 4.1: **Immunohistochemistry staining of NF-κB in PTCL tumors**

A) Protein expression of the different NF-κB factors in representative paraffin-embedded PTCL tumors. B) Cases were categorized into three different levels according to their nuclear staining of NF-κB: negative, pos +, or pos ++. Tumors with over 20% positive nuclei are grouped into category pos +, while tumors with more than 50% positive nuclei are grouped under category pos ++. C) A significant and positive correlation was observed between p50 and p52 expression ($p<0.05$)

The frequencies of NF-κB expression among the different PTCL subtypes are summarized in Table 4.1. Nuclear expression of components defining both the classical (p50 and c-Rel) and

alternative (p52 and RelB) pathways was detected in the majority of PTCLs. Surprisingly, the commonly used marker for NF-κB activation, p65, showed only cytoplasmic expression in most cases, suggesting that other factors of the family are more frequently involved in NF-κB signaling in PTCL. Moreover, as we observed in B cell lymphomas, a significant positive correlation ($p<0.05$) was established between nuclear p50 and p52 expression (Figure 4.1 C), indicating frequent activation of both pathways in the same sample.

Table 4.1: NF-κB expression in human PTCL tumors

PTCL subtype	Antigen	Evaluable cores	neg	pos +	pos ++
ALCL	p52	28	4 (14.3)	9 (32.1)	15 (53.6)
	p50	28	3 (10.7)	8 (28.6)	17 (60.7)
	RelB	28	7 (25.0)	12 (42.9)	9 (32.1)
	c-Rel	28	7 (25.0)	16 (57.1)	5 (17.9)
	p65	13	11 (84.6)	2 (15.4)	0 (0.0)
PTCL-NOS	p52	57	17 (29.8)	35 (61.4)	5 (8.8)
	p50	57	11 (19.3)	34 (59.6)	12 (21.1)
	RelB	57	14 (24.6)	38 (66.7)	5 (8.8)
	c-Rel	57	17 (29.8)	35 (61.4)	5 (8.8)
	p65	35	34 (97.1)	1 (2.9)	0 (0.0)
AITL	p52	42	4 (9.5)	35 (83.3)	3 (7.1)
	p50	42	1 (2.4)	27 (64.3)	14 (33.3)
	RelB	42	4 (9.5)	35 (83.3)	3 (7.1)
	c-Rel	42	7 (16.7)	33 (78.6)	2 (4.8)
	p65	35	34 (97.1)	1 (2.9)	0 (0.0)

Note: *The number and percentages (in parenthesis) of PTCL tumors that are negative or positive for NF-κB among different PTCL subtypes are represented in the table. Abbreviations: ALCL = Anaplastic large T-cell lymphoma, PTCL-NOS* = Peripheral T-cell lymphoma - not otherwise specified, AITL = Angioimmunoblastic T-cell lymphoma

4.2 Impact of NF-κB on T cell lymphoma patient survival

The biological and prognostic importance of NF-κB activation is still unknown and contradictory results have been reported for the clinical correlation of NF-κB in different tumors. Apart from ALK-expression, there is a lack of prognostic markers as well as markers for treatment prediction in PTCL. PTCL patients still present a highly aggressive clinical course with poor management options. To estimate the impact of nuclear NF-κB expression on the clinical outcome of patients with PTCL, we performed a Kaplan-Meier analysis to compare the overall survival between NF-κB-positive and negative tumors. Tumors with

>50% positive nuclei (tumors included in category pos ++) for any NF-κB factor were considered positive. Similar thresholds have previously been used for immunohistochemistry of NF-κB in other studies in the lymphoma field (Piccaluga et al. 2007; Espinosa et al. 2008; Compagno et al. 2009). In our series of 77 PTCL-NOS and AITL cases (see patient characteristics in Table 2.2), 31.2% of the cases were positive for NF-κB. The PTCL-NOS and AITL subtypes were included in the same survival analysis, since these patients did not present any significant difference in basal OS due to PTCL subtype in our series (Figure 4.2 A) or in studies published by others (Vose et al. 2008). When NF-κB was taken into account, however, patients with NF-κB-positive tumors had a significantly inferior overall survival compared with the negative group (Figure 4.2 B, log rank test, p=0.003). The 2-year overall survival in the NF-κB-positive group was only 41.7% compared with 67.9% in the negative group. NF-κB activation in PTCL was still significantly associated with inferior overall survival when the impact of other clinical covariates was taken into account (age, extranodal sites, LDH levels, ECOG performance status and Ann Arbor stage). The IPI, which is a combination of these clinical variables, was though still a more accurate estimate of prognosis in our series (Table 4.2 and 4.3).

ALCL tumors were studied in a separate analysis due to their distinct clinical behavior and biology. In a series of 24 ALCL cases (see table 2.3 in the material and methods section for patient characteristics), NF-κB was positive in 75.0% of the tumors. As seen in PTCL-NOS and AITL, NF-κB expression was once again correlated with inferior overall survival, although the number of patients was too low to reach statistical significance (Figure 4.2 C, log rank test, p=0.153). ALCLs are usually subcategorized into ALK-negative or ALK-positive tumors, where ALK-positivity is associated with a favorable outcome and recently, ALK inhibitors are emerging which might improve their outcome even more. Interestingly, NF-κB was more frequently activated in the ALK-negative tumors (Figure 4.2 D, p= 0.007) which are characterized by an aggressive clinical course (Figure 4.2 E) and where novel treatment strategies are needed.

The observation that NF-κB signaling is activated in a subset of T-cell lymphomas with very poor clinical outcome, merit the evaluation of NF-κB inhibition strategies in these tumors.

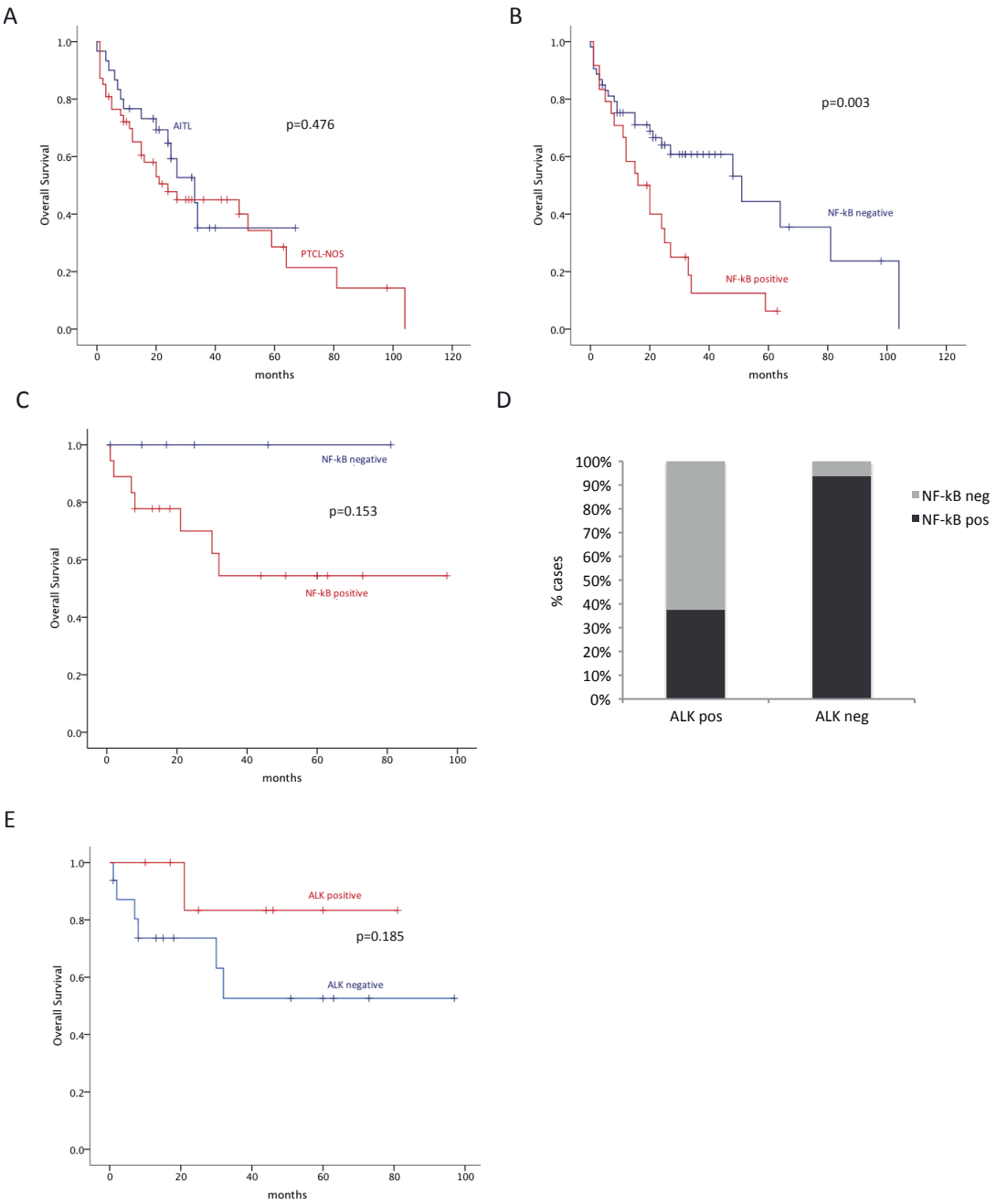

Figure 4.2. Impact of NF-κB on overall survival in PTCL

A) Kaplan-Meir analysis comparing the OS curves of 48 PTCL-NOS and 29 AITL cases. No significant difference in OS was observed between these subtypes (p=0.476). B) Kaplan-Meir analysis in a series of 77 PTCL cases comparing NF-κB positive and negative tumors. NF-κB was associated with a significantly worse OS (p=0.003). C) Kaplan-Meir analysis of 24 ALCL cases comparing NF-κB positive and negative tumors. NF-κB positive cases presented a poorer OS, although statistical significance was not archieved (p=0.153). D) NF-κB expression in ALK positive and ALK negative ALCL tumors. NF-κB expression was more frequent in ALK negative tumors (p=0.007). AITL = Angioimmunoblastic T-cell lymphoma, PTCL-NOS = Peripheral T-cell lymphoma – Not otherwise specified, ALK = anaplastic lymphoma kinase.

Table 4.2. Results from NF-κB multivariate analysis

Variable	p-value	Hazard ratio (CI 95%)
NF-κB	0.047	2.145 (1.009-4.560)
Age	0.17	1.860 (0.767-4.511)
Extranodal sites	0.97	1.018 (0.401-2.585)
LDH	0.012	2.890 (1.268-6.591)
ECOG	0.451	1.329 (0.635-2.783)
Stage	0.993	0.996 (0.383-2.587)

Abbreviations: ECOG = Eastern Cooperative Oncology Group, IPI = International Prognostic Index, LDH = lactate dehydrogenase.

Table 4.3. Results from multivariate analysis, including NF-κB and IPI

Variable	p-value	Hazard ratio (CI 95%)
NF-κB	0.065	1.820 (0.964-3.438)
IPI	0.016	1.378 (1.061-1.790)

Abbreviations: IPI = International Prognostic Index

4.3 NIK expression in PTCL

The NF-κB inducing kinase, NIK, is involved in the activation of NF-κB signaling in some cells and settings and has been described as a molecular target for therapy in malignancies. Given our observation that NF-κB signaling is activated in a subset of T cell lymphomas and associated with an aggressive phenotype, we wanted to examine whether NIK was involved in NF-κB activation in these tumors. Analyzing the expression levels of NIK by qPCR, we observed a remarkable overexpression of NIK mRNA in several PTCL cell lines and primary Sézary Syndrome samples (Figure 4.3 A and B). Sézary Syndrome is a leukemic subtype of PTCL and was here used as a model since its neoplastic T cells easily can be purified and extracted from the peripheral blood of the patient, in contrast to other PTCL subtypes. The expression levels were compared with the expression of NIK in T lymphocytes from healthy donors (Figure 4.3 A and B). To rule out the possibility that NIK expression is higher in tumor cells due to an increased proliferation and hence transcriptional activity, healthy T cells were induced to proliferate by the addition of interleukin 2 (IL2) and Concanavalin A (ConA). Proliferating healthy T cells did not present any increase in NIK expression (Figure 4.3 C), confirming that NIK overexpression is associated with malignant T cells. The cell lines expressing high levels of NIK mRNA, also expressed elevated protein levels of NIK (Figure 4.3 D). To obtain detectable levels of NIK proteins in cell lines, cells were treated with the proteasome inhibitor MF-132 3 hours prior to harvesting. It's important to note, that this was exclusively done in cells pelleted for NIK detection; the detection of all other proteins in

this work is done in untreated cells. Immunohistochemistry on paraffin-embedded cells was used to assess the nuclear expression of the different NF-κB factors in this panel of T cell lymphoma cell lines (Table 4.4). As NIK has been described as a regulator of mainly the alternative pathway through the induction of p100 processing and nuclear translocation of p52, a clear correlation between NIK expression and p52 was expected. Indeed, cells expressing NIK also expressed nuclear p52 and to less extent, RelB. Classical NF-κB factors were expressed both in NIK-negative and NIK-positive cell lines.

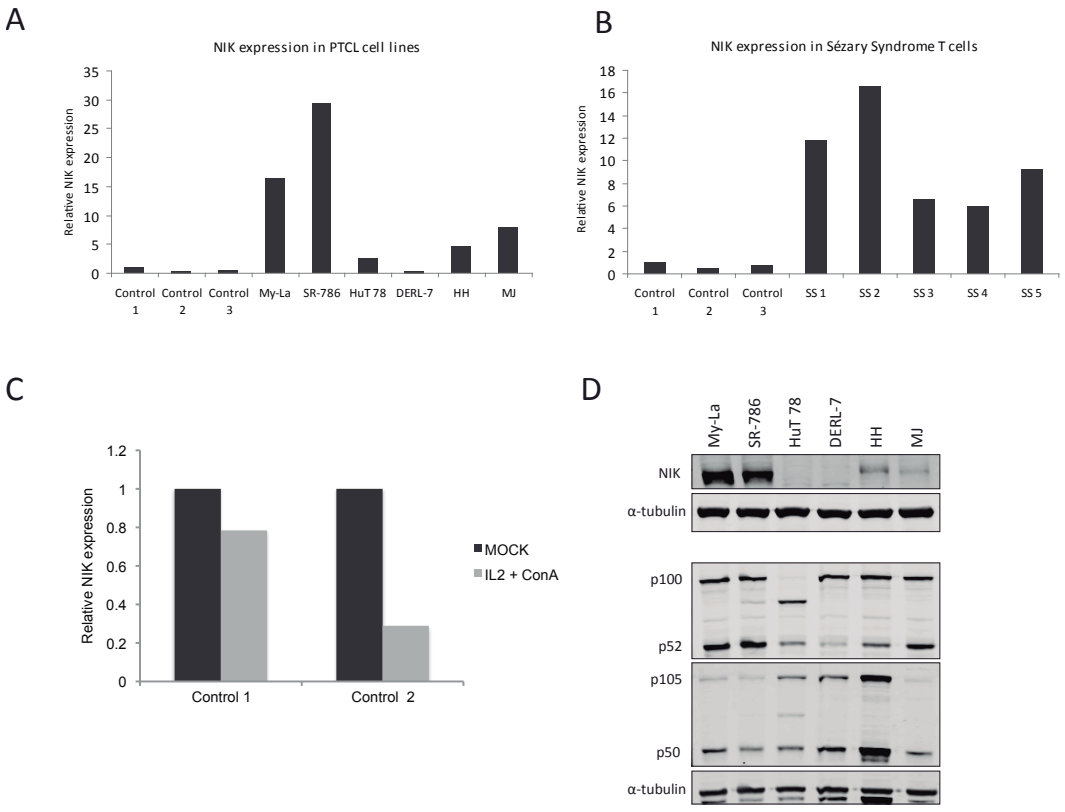

Figure 4.3. NIK expression in T cell lymphoma cell lines and samples.

A) RT-qPCR analysis of NIK expression in PTCL cell lines showed variable expression of NIK as well as a marked overexpression in some of the cell lines, compared with healthy T cells (Control 1-3). B) RT-qPCR analysis of NIK expression in isolated T cells from Sézary Syndrome patients (SS1-SS5). C) RT-qPCR analysis of NIK expression in resting and proliferating healthy T cells. The T cells were induced to proliferate by the addition of Interleukin-2 (IL-2) and Concanavalin A (ConA). D) Western blot showing NIK, p100 and p105 expression in T cell lymphoma cell lines.

While one of the NIK-negative cell lines, DERL-7, lacked nuclear expression of alternative NF-κB factors (p52 and RelB), the other cell line with low NIK levels, HuT 78, expressed both

nuclear p52 and RelB (Table 4.4) To explain this finding, HuT 78 expresses a truncated form of p100 (Figure 4.3 D) which has previously been described to activate the alternative pathway in a NIK-independent manner (Thakur et al. 1994).

Table 4.4 Nuclear expression of NF-κB in PTCL cell lines measured by immunohistochemistry

	p52	RelB	p50	c-Rel	p65
My-La	+++	+	+++	++	+
SR-786	+++	+	+++	++	+
HuT 78	++	++	+++	+	+
DERL-7	-	-	+++	+++	+++
HH	+++	+	+++	+++	++
MJ	+++	++	+++	+++	++

Note: The nucear expression of NF-κB was categorized into strong (+++), medium (++), weak (+) or negative (-).

4.4 TRAF3 expression in PTCL cell lines

A common mechanism for NIK protein accumulation and activation is the lack of one or several of the components in the protein complex responsible for NIK degradation. The most frequently reported alteration is loss of TRAF3 by genetic deletions or mutations. For that reason, we analyzed the expression of TRAF3 in our panel of PTCL cell lines, by western blot (Figure 4.4). Curiously, the levels of TRAF3 are inversely correlated to the levels of NIK, and My-La and SR-786 cells lack expression of TRAF3 or present very low TRAF3 levels compared to DERL-7 and HuT 78. These results support, although do not confirm, a role for TRAF3 as a player in regulating NIK levels in PTCL as well, as described in other cells (Zarnegar et al. 2008).

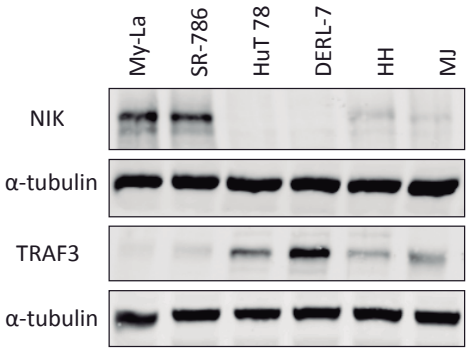

Figure 4.4 Expression of TRAF3 in T cell lymphoma cell lines.
Western blot analysis of basal levels of TRAF3 protein. Cell lines expressing high levels of NIK (My-La and SR-786) present strongly reduced levels of TRAF3.

4.5 Pathways correlated with NIK expression in PTCL tumors

In order to detect NIK protein levels in primary PTCL samples, we tested a handful of different NIK antibodies in paraffin-embedded tissues, but none of these provided consistent results. For that reason we used gene expression microarray data to compare the expression of NIK (MAP3K14) with the expression of NF-κB target genes (Compagno et al. 2009) and other biological pathways. Gene expression data from 37 PTCL samples (including the subtypes PTCL-NOS, AITL and ALCL) were used and to determine the gene sets that are statistically correlated to NIK expression we performed a Gene Set Enrichment Analysis (GSEA). This analysis revealed a significant and positive correlation between the expression of NIK and NF-κB target genes (Figure 4.5), suggesting that NIK possibly is involved in NF-κB signaling in these tumors.

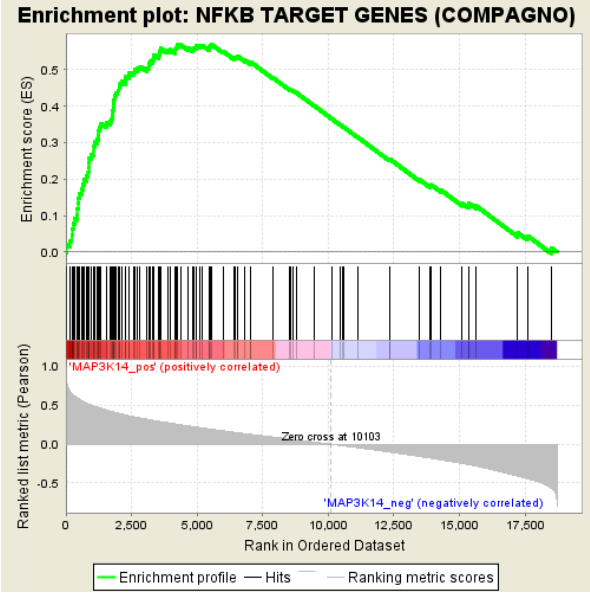

Figure 4.5 GSEA enrichment plot.

The graph represents NF-κB target genes positively correlated with NIK expression in 37 human PTCL tumors. Pearson correlation analysis gives a FDR of 0.093. FDR< 0.15 is considered statistically significant

Other gene sets significantly correlated with the expression of NIK are listed in Table 4.5, and include CD40 signaling, interleukin signaling, PI3K/AKT pathway, TCR signaling, MAPK pathway and JAK/STAT signaling, among others (FDR<0.15). No gene set had a significant

negative correlation with NIK expression. The NF-κB target genes that were correlated with NIK expression, are also involved in many other signaling pathways, such as tumor necrosis factor receptor 2 (TNFR2), interleukin 2 (IL-2), interleukin 1 (IL-1) and TNF- and APOL-related leukocyte expressed ligand 1 (TALL1) pathway. These pathways also result in an activation of NF-κB, which might be the reason why these pathways appeared significant in our study.

Table 4.5 Pathways positively correlated with NIK expression in PTCL

NAME	NES	FDR q-val	SIZE
CD40 SIGNALING DURING GC DEVELOPMENT	1.688	0.090	159
IL1R PATHWAY	1.677	0.091	31
NFKB TARGET GENES	1.642	0.093	111
EXTRINSIC APOPTOSIS	1.690	0.097	78
IL2 PATHWAY	1.644	0.098	23
TALL1PATHWAY	1.651	0.101	15
TNFR2 PATHWAY	1.934	0.102	18
T CELL CYTOKINE SIGNALING	1.690	0.106	158
BLIMP-1 TARGETS	1.601	0.108	153
APOPTOSIS SIGNALING	1.614	0.109	109
B-CELL ANERGY	1.605	0.111	22
DEATH PATHWAY	1.693	0.112	31
TCR PATHWAY	1.737	0.118	43
PI3K/AKT SIGNALING	1.575	0.120	34
NKT PATHWAY	1.564	0.121	27
MAPK PATHWAY	1.697	0.123	86
JAK-STAT SIGNALING PATHWAY	1.847	0.133	82
IL2RB PATHWAY	1.698	0.139	35
BCELL-TCELLCELL CALCIUM SIGNALING	1.738	0.140	140

Note: Gene sets correlated with NIK expression in a series of 37 PTCL samples, analyzed by Gene Set Enrichment Analysis, are presented (FDR<0.15). NES = Normalized Enrichment Score, FDR = False Discovery Rate, SIZE = number of genes included in the gene sets.

4.6 The role of NIK in NF-κB signaling in T cell lymphomas

NIK has been described to regulate the alternative axis of the NF-κB pathway, through phosphorylation of IKKα and subsequent p100 processing, but its role in classical signaling has been debated and seems to be signal- and cell-type specific. As expected, transient overexpression of NIK in HEK-293T cells led to increased levels of p52, indicating an activation of the alternative axis (Figure 4.6 A). On the other hand, the levels of p50 remained unchanged.

For the functional assays aiming to study the role of NIK in T cell lymphoma cells, two cell lines presenting high NIK mRNA and protein levels (My-La and SR-786) and two cell lines with low NIK mRNA levels and absent protein expression (DERL-7 and HuT 78), were used throughout the study. To knock down NIK and other genes in these cells, we used siRNA transfection by microporation, which gave us reproducible and effective gene knockdown, which lasted for approximately 4-5 days. Stable knockdown using a handful of different lentiviral and retroviral constructs and techniques was also performed but all with an insufficient knockdown efficiency in these lymphoid cell lines, which are difficult to transfect or infect.

We knocked down NIK in two PTCL cell lines, My-La and SR-786, and analyzed the expression of downstream targets. We used two different siRNA sequences (siNIK1 and siNIK2) that induced different levels of knockdown efficiencies (siNIK2 always having a higher knockdown efficieny than siNIK1, Figure 4.6 B), allowing us to study the effect of a dose-dependent decrease in NIK. As expected, the levels of p52 were reduced and the levels of p100 were initially (at 24 hours) increased after NIK knockdown compared with cells transfected with a non-templated control (siNTC), indicating an attenuation of p100 processing. We also observed a similar but somewhat delayed decrease of p50 levels and an increase of the levels of p105, linking NIK to the regulation of classical NF-κB activation as well (Figure 4.6 B and C). To ensure that the levels of NF-κB did not remain unchanged in the nucleus, we analyzed the nuclear cell fraction for these proteins and observed that indeed, nuclear levels of both p50 and p52 were also decreased after NIK knockdown (Figure 4.7 A). To confirm that the reduction of NF-κB observed corresponded to a reduction of active NF-κB, and to analyze the effect of the rest of NF-κB members as well (c-Rel, p65 and RelB), we analyzed the NF-κB DNA-binding activity after NIK knockdown, measured by TransAM ELISA assay. Interestingly, we could observe a decrease in the activity of all five transcription factors (Figure 4.7 B) upon NIK depletion. These results confirm the role of NIK as an alternative NF-κB regulator, but also support a role for NIK in the regulation of classical NF-κB activation in PTCL.

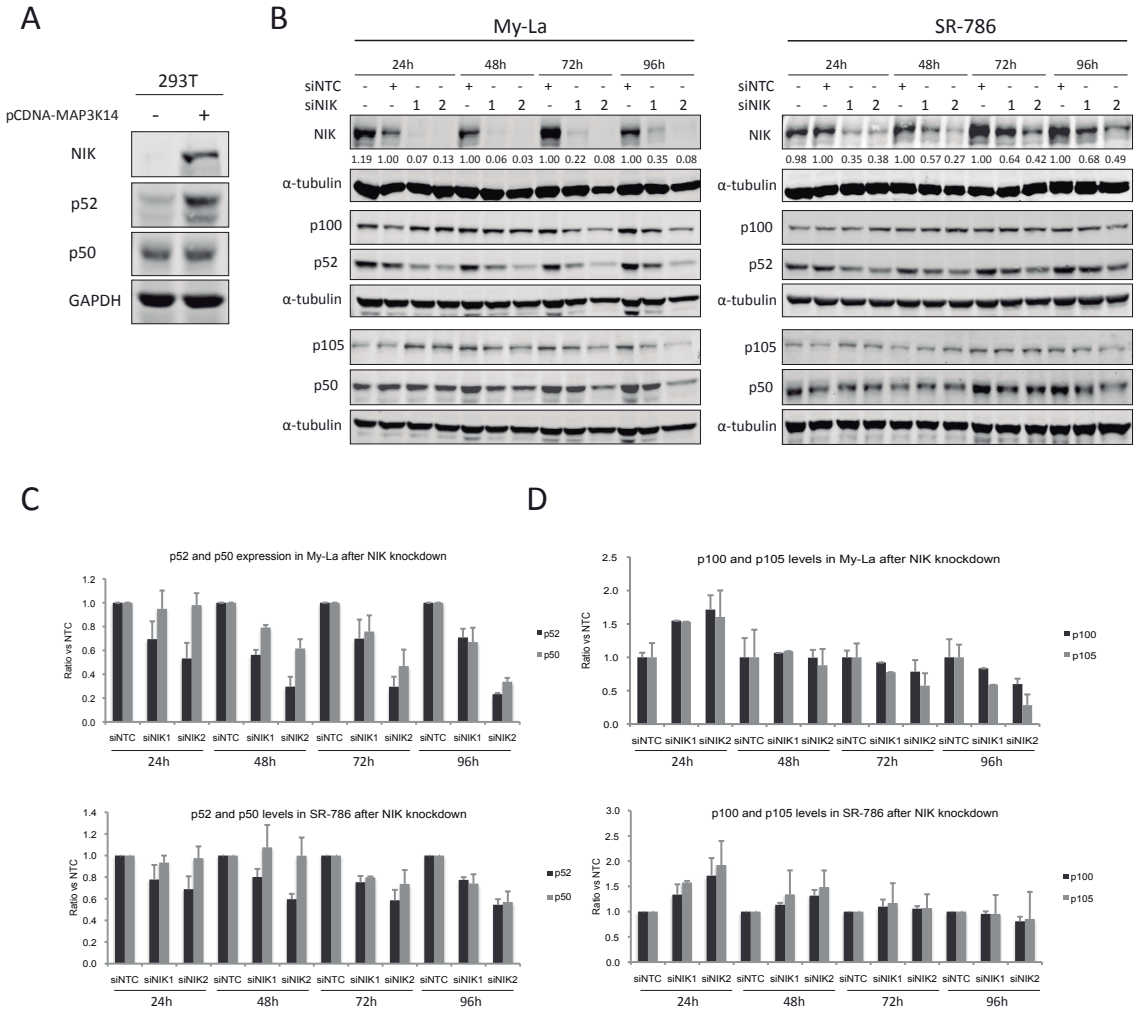

Figure 4.6 The role of NIK in NF-κB signaling.

A) NIK (MAP3K14) was overexpressed in 293T cells and downstream p52 and p50 levels were observed by western blot. B) NIK was knocked down using 2 siRNAs (siNIK1 and siNIK2) or a NTC (siNTC) in My-La and SR-786. After NIK knockdown, the expression of NIK, p100/p52, and p105/p50 was analyzed by Western blot analysis. C and D) Quantification of the immunoblots confirms a decrease in the levels of both p50 and p52 after NIK knockdown. The data are represented as the mean and standard derivation (SD) of 3 independent experiments.

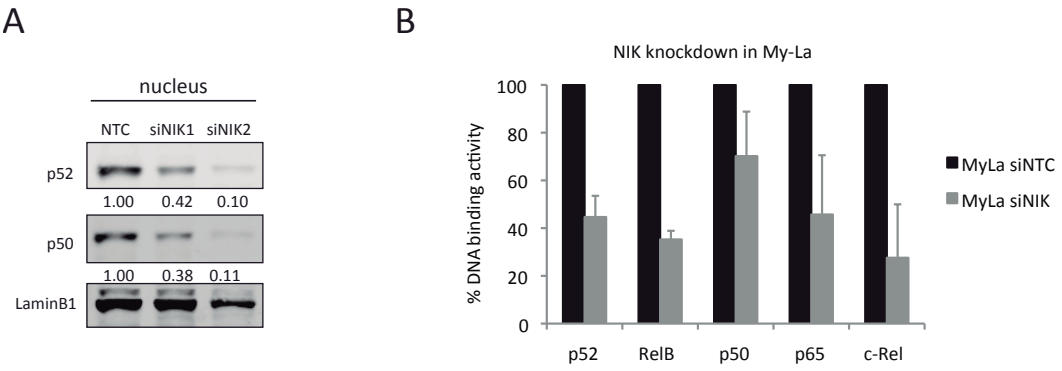

Figure 4.7 Effect of NIK knockdown on NF-κB activity. A) Nuclear levels of p52 and p50 after NIK knockdown. Numbers indicate quantification of the band intensity, normalized to the loading control and as a ratio to the non-template control (NTC). B) DNA-binding activity of p52, RelB, p50, p65, and c-Rel 48 hours after NIK knockdown was measured (in triplicate) using the ELISA-based TransAM assay and reveals a reduction of classical and alternative NF-κB activation. The graph represent the mean +/- SD of two independent experiment meassured each one in triplicates.

4.7 The effect of NIK on PTCL cell survival

Since we have shown that NF-κB and NIK are overexpressed in a subset of T cell lymphomas and that NIK acts as a central regulator of NF-κB activation in these cells, we asked whether NIK had any effect on cell viability. To assess how NIK knockdown affected PTCL cell viability, we measured Annexin V and DAPI by flow cytometry and estimated the cell death induced at different time points after NIK knockdown. Interestingly, in My-La and SR-786 T cell lymphoma cells, NIK knockdown led to a dramatic increase in cell death compared with non-template control (NTC) transfected cells (Figure 4.8 A). The cell death observed after NIK knockdown increased as knockdown became more efficient with siNIK2. The appearance of cleaved caspase 3 and cleaved poly (ADP-ribose) polymerase 1 (PARP) after NIK knockdown in both My-La and SR-786, indicates an induction of a caspase-dependent apoptotic pathway as a result of NIK depletion (Figure 4.8 B). To study the effect of NIK knockdown over a longer period, we repeated the siRNA transfection 4 days after the first microporation. Strikingly, after 1 week of NIK depletion, nearly all cells (98.8 %)had undergone apoptosis, demonstrating the essential role of NIK in the viability of these tumor cells (Figure 4.9 A). Importantly, NIK silencing in DERL-7 or HuT 78 cell lines, presenting low NIK levels, had no effect on cell survival (Figure 4.9 B).

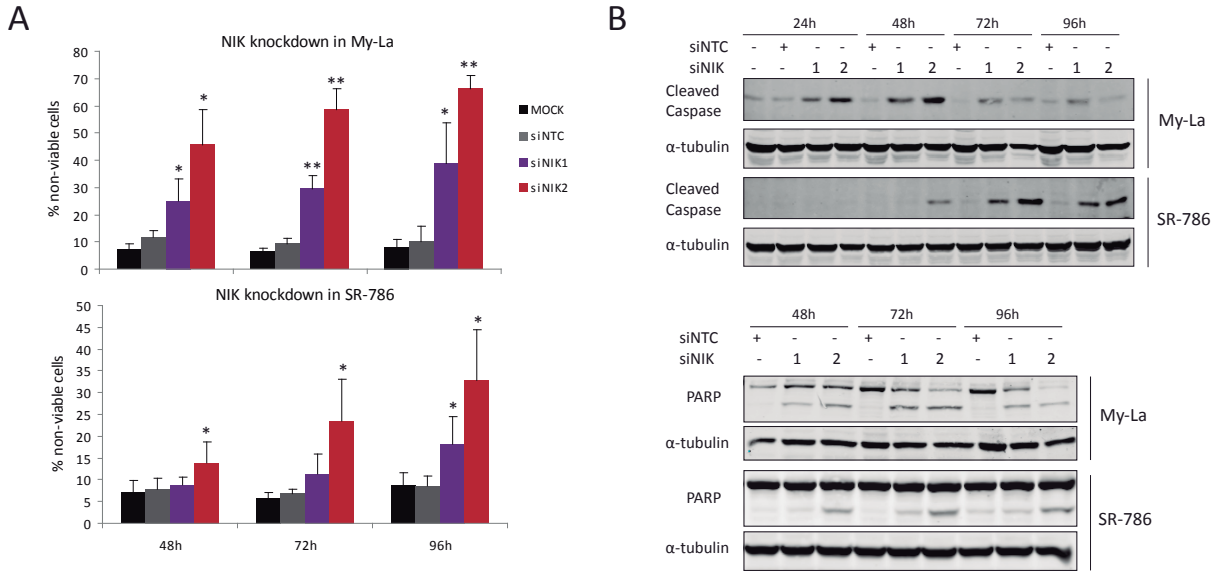

Figure 4.8. The effect of NIK knockdown on PTCL cell survival.

A) NIK knockdown (siNIK) induces cell death in My-La and SR-786 cells compared with untransfected (MOCK) or non-template-transfected (siNTC) cells, as measured by flowcytometry using DAPI and AnnexinV staining 96 hours after transfection. The data are represented as the mean + SD of 3 independent knockdown experiments. B) Detection of cleaved Caspase-3 and PARP after NIK depletion in both MyLa and SR-786 cells. * indicates $p < 0.05$ and ** means $p <$

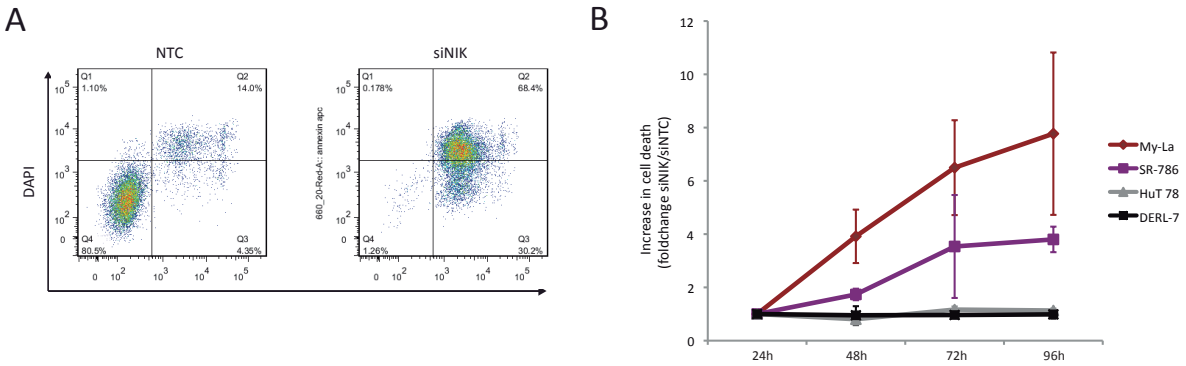

Figure 4.9. Cell viability after NIK knockdown in PTCL cells.

A) Only 1.26% of cells remain viable 7 days after NIK knockdown in My-La (DAPI/AnnexinV–negative). B) Increase in cell death in cell lines with high (My-La andSR-786) or low (HuT 78 andDERL-7) NIK expression, represented as the ratio between the values of cell death in NIK

To confirm the cell killing effect of NIK depletion using another approach, we transfected My-La cells with a dominant negative form of NIK, NIK (KK/AA) (Malinin et al. 1997), presenting two point mutations in the kinase domain, that abolish its kinase activity. The expression of NIK (KK/AA) in My-La cells also resulted in a significant increase in cell death compared with cells transfected with a control vector (Figure 6.10).

These results indicate that NIK is necessary for cell survival of NIK-overexpressing PTCL cells and suggest that NIK targeting has a selective effect only on the cells presenting elevated NIK levels.

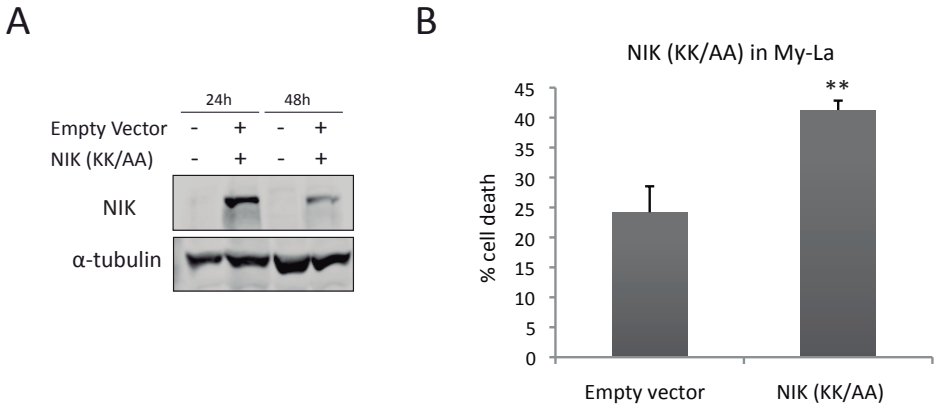

Figure 4.10 NIK dominant negative expression in My-La.

A) Expression of NIK dominant negative, NIK (KK/AA) after transfection in My-La cells. B) Cell death induced in My-La 48 hours after NIK (KK/AA) transfection. Cell viability was measured by DAPI/AnnexinV-staining by flow cytometry. ** indicates $p<0.01$ as a result of a Student´s t-test.

To investigate whether NIK apart from affecting cell survival, also gave rise to any cell cycle perturbations, we analyzed the fraction of cells in each phase of the cell cycle in control and NIK-knockdown My-La cells by propidium iodide staining and flow cytometry. Figure 4.11 shows that no major changes in cell cycle distribution were induced by NIK silencing, apart from an increase of cells in the sub-G1 fraction, corresponding to the apoptotic cell population.

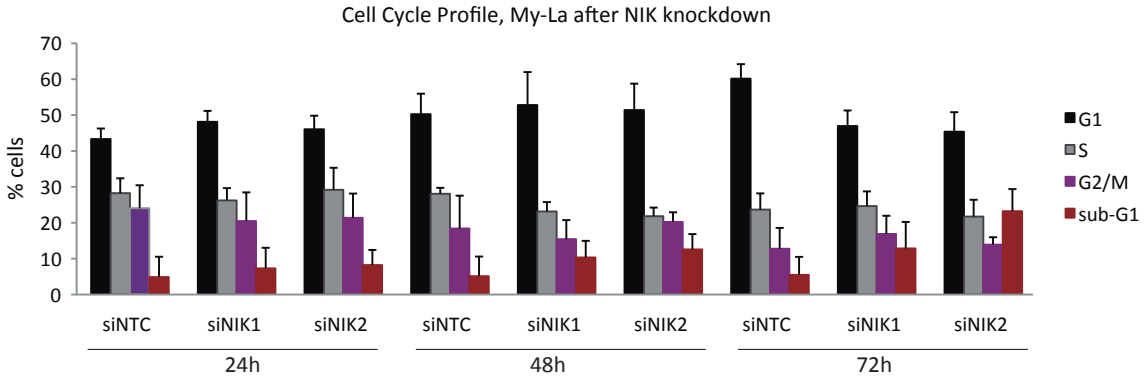

Figure 4.11 Cell cycle analysis after NIK knockdown.

The fraction of cells in each phase of the cell cycle 24, 48 and 72h after NIK knockdown in My-La cells.

4.8 Knockdown of other members of the NF-κB pathway in PTCL

4.8.1 IKKβ and IKKα knockdown

The IKKs are upsteam kinases in the NF-κB cascade and are central regulators of its activation. The IKK complex phosphorylates the IκB proteins, leading to the liberation of sequestered NF-κB dimers and thus permitting their nuclear translocation. IKKα is the subunit of the IKK complex that is responsible and required for the activation of the alternative pathway, while IKKβ is needed for activation of the classical pathway. Inhibition of either IKKβ or IKKα has frequently been employed to selectively block the classical or alternative NF-κB axis. Furthermore, pharmacological inhibition of IKKβ with small molecule inhibitors has been widely used in pre-clinical models as a therapeutic option in a range of different tumors, but its use in the clinic has not been proven (Lam et al. 2005; Sors et al. 2008; Liu et al. 2012).

NIK can phosphorylate and activate IKKα, but IKKβ might also be a target for NIK mediated phosphorylation under some circumstances (Woronicz et al. 1997). In fact, measuring the levels of phosphorylated IKK after NIK knockdown in My-La cells, a reduction in both phosphorylated IKKα and IKKβ was observed (Figure 4.12 A).

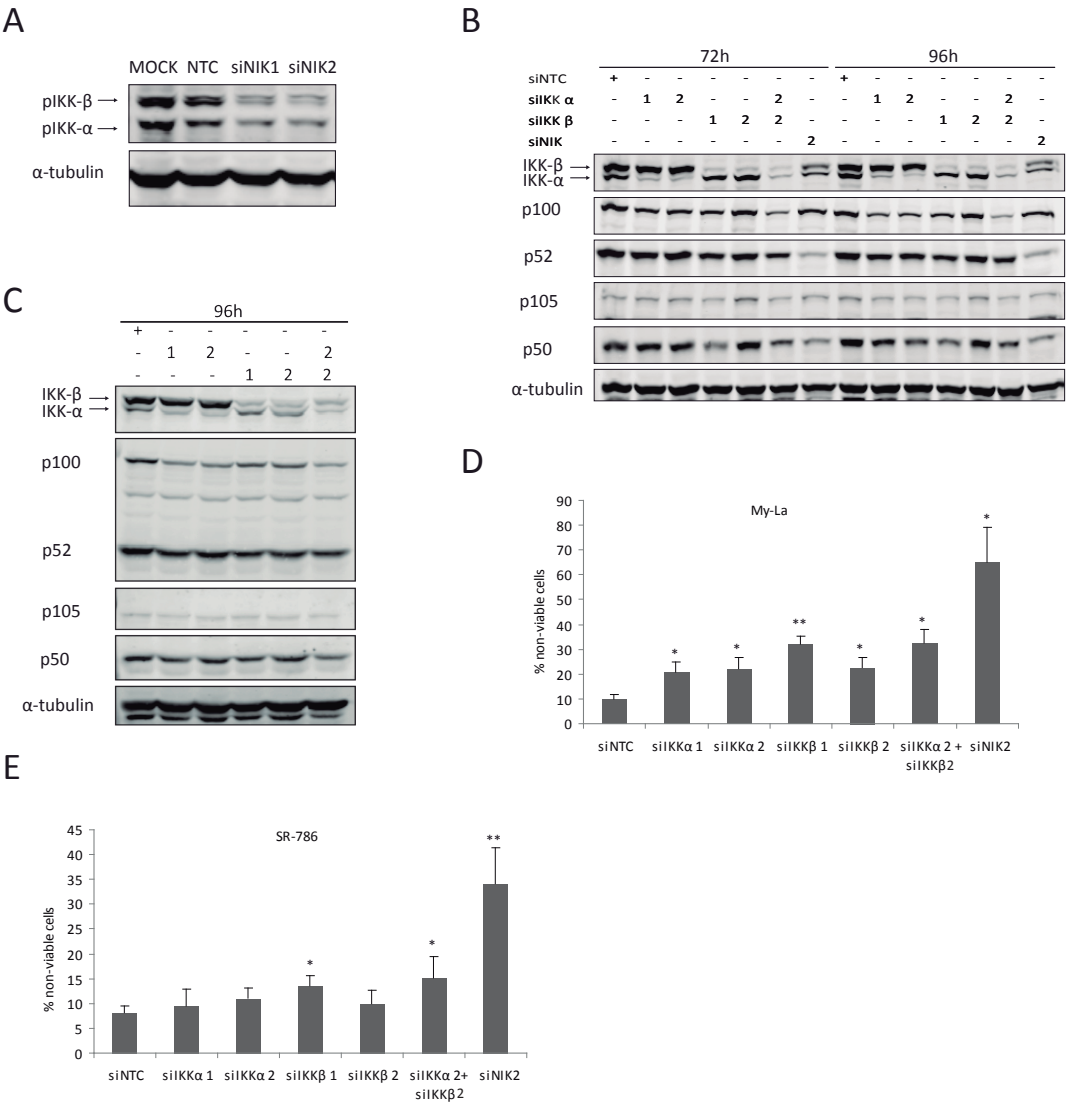

Figure 4.12. Knockdown of IKKα and IKKβ in T cell lymphomas.

A) Expression of phosphorylated IKKα and IKKβ after NIK knockdown in My-La cells. B) Knockdown of IKKα, IKKβ or NIK in My-La cells and analysis of downstream signaling 72 and 96 hours after transfection. C) IKKα and IKKβ knockdown in SR-786 cells 96 hours after transfection. D) Estimation of cell death in My-La cells 96 hours after transfection. E) Cell death in SR- 786 cells 96 hours after transfection. Graphs represent means +SD from three independent experiments. *p<0.05, **p<0.01.

To rule out whether the toxicity of NIK knockdown was due to a blockade of the classical or alternative NF-κB pathway, we knocked down either IKKα, IKKβ, or both, in T cell lymphoma cell lines (Figure 4.12 B and C). As can be observed in Figure 4.12 D and E, both IKKα and IKKβ knockdown led to an increase in apoptosis. However, the effect on apoptosis was mild, compared to NIK knockdown that gave rise to a considerably more potent cell killing effect. The effect on cell death of silencing both IKKα and IKKβ was increased compared to the

knockdown of only one of the kinases, suggesting that blocking both kinases simultaneously might be an advantage (Figure 4.12 D and E, using the combination of siIKKα 2 and siIKKβ 2). However, even the combined knockdown of both IKKα and IKKβ still had a much milder effect on cell survival than had NIK knockdown. Reduced levels of both IKKα and IKKβ can be seen after NIK knockdown (Figure 4.12 B), but interestingly, only the knockdown of NIK, but not the knockdown of IKK, was able to strongly reduce the levels of p52 and p50 (Figure 4.12 B). These results suggest that NIK-induced survival signaling as well as NIK-regulated NF-κB activation, at least in part, might be IKK-independent mechanisms in these cells. Thus, targeting NIK would be a more effective way to shut off NF-κB activity and to induce apoptosis than IKK inhibition in these tumor cells.

4.8.2 Knockdown of individual NF-κB transcription factors

To explore whether any particular NF-κB transcription factor was responsible for providing survival signals in T cell lymphoma cells, we used siRNAs to knock down the NF-κB transcription factors that were seen highly expressed in human T cell lymphoma samples: p52, p50, RelB and c-Rel. All of these four transcription factors were silenced in the two NIK overexpressing cell lines (My-La and SR-786, Figure 4.13 A) using three different siRNAs for each gene. Measuring cell viability by AnnexinV and DAPI staining by flow cytometry (Figure 4.13 B) 96 hours after tranfection, we observed that the apoptotic effect of silencing an individual NF-κB factor was minimal. Of the four transcription factors, only the knockdown of c-Rel gave rise to a significant increase in apoptosis (t-test between NTC and siCREL, $p<0.05$). Neither the knockdown of p52 or RelB, or the combined depletion of both p52 and RelB, were able to reduce cell viability (Figure 4.13 C), suggesting that the reduction of alternative NF-κB activity alone is not sufficient to induce apoptosis in these cells. Combined knockdown of p50 and p52 was not able to reduce tumor cell viability either (Figure 4.13 C). Interestingly, the activity of c-Rel transcription factor seems to be important for T cell lymphoma survival. In My-La cells, the reduction of c-Rel levels led to a 3- to 5-fold increase in cell death (Figure 4.13 B). The effect in SR-786 cells was milder (2-fold increase in cell death), probably due to the lower knockdown efficiency of c-Rel in this cell line, where significant levels of protein are still present after the knockdown (Figure 4.13 A). We have already shown that NIK knockdown led to a reduced activity of c-Rel (Figure 4.7 B). Immunoflourescence staining of c-Rel in My-La cells confirms a reduction of nuclear c-Rel expression after NIK knockdown (Figure 4.13 C).

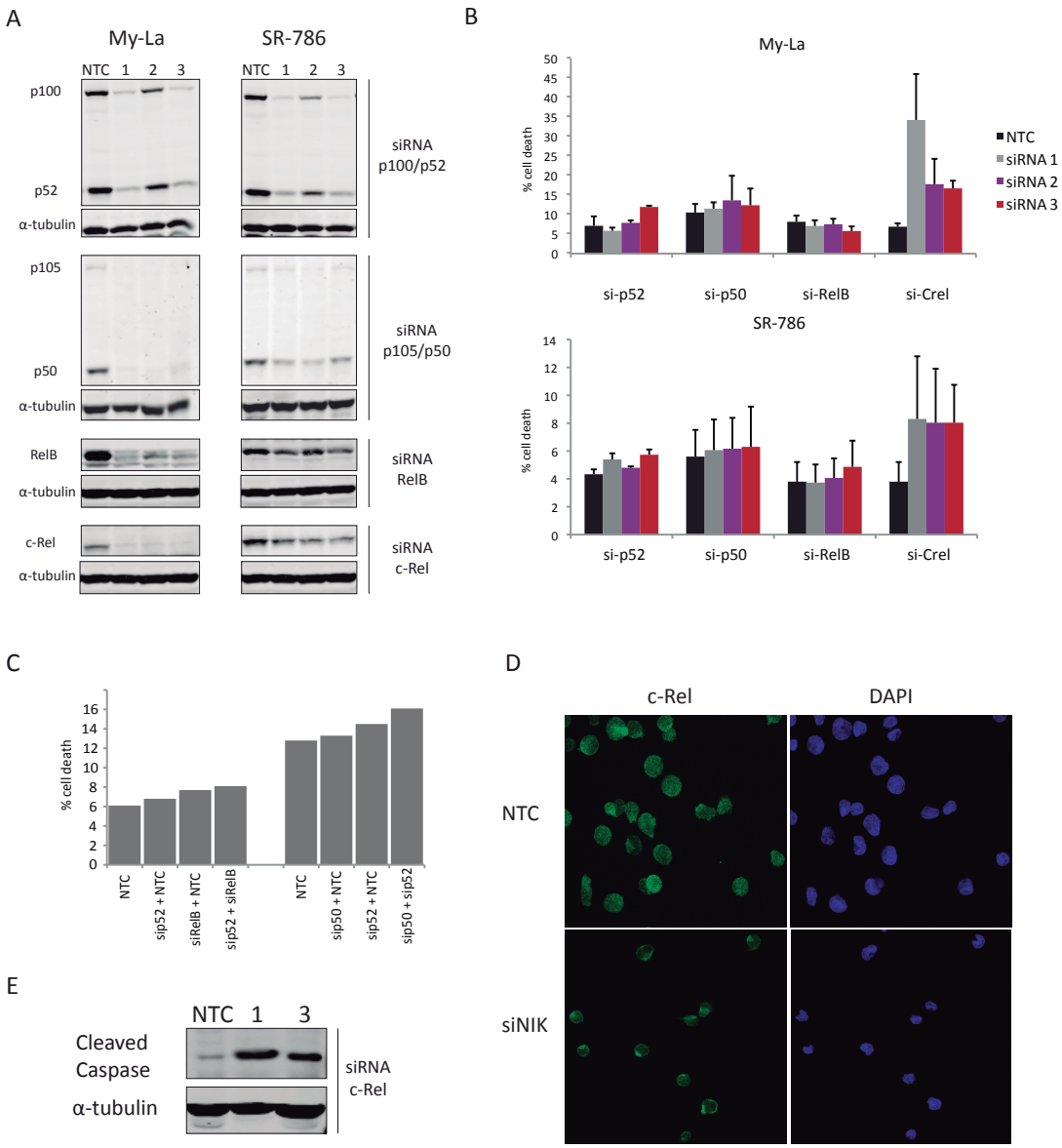

Figure 4.13 Knockdown of different NF-κB members in PTCL cells.

A) siRNA knockdown of p52/p100, p50/p105, RelB and c-Rel in My-La and SR-786 cells 96 hours after transfection. B) Cell viability assay 96 hours after siRNA transfection. C) Estimation of cell death after the combined knockdown of p52 and RelB, or p52 and p50 in My-La cells 96 hours after transfection. D) Immunoflourescence staining of c-Rel 48 hours after NIK knockdown in My-La cells shows decreased nuclear staining in siNIK cells compared to NTC.

Cleaved caspase 3 is expressed after c-Rel knockdown in T cell lymphoma cells, confirming the induction of apoptosis (Figure 4.13 D). DERL-7 and HuT 78 are NIK-negative cell lines that express nuclear c-Rel. We asked whether c-Rel was required for survival in these cells as well. However, knockdown of c-Rel in these cell lines did not affect cell viability, indicating that c-

Rel regulate different processes in different contexts and is not always necessary for T cell survival (Figure 4.14). Surprisingly, knocking down p100/p52 in HuT 78, the cell line expressing an oncogenic truncated p100 protein, did not induce cell death either (Figure 4.14 B).

Taken together, these results suggest that c-Rel is important for survival of T cell lymphoma cells and the reduction of c-Rel could be responsible for part of the cell killing effect observed after NIK silencing. However, NIK depletion still has a more drastic and profound effect on T cell lymphoma cell viability and cannot solely be confined to the effect of a specific NF-κB transcription factor.

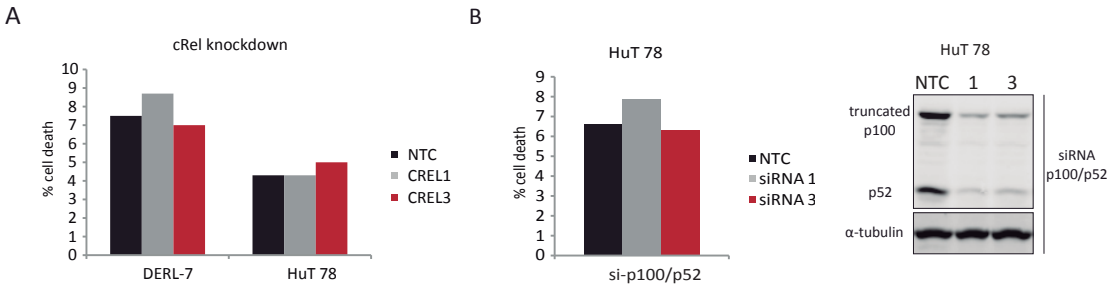

Figure 4.14 Knockdown of c-Rel and p100/p52 in DERL-7 and HuT 78.

A) Percentages of dead DERL-7 and HuT 78 cells 96 hours after c-Rel silencing. B) Cell viability and expression of truncated p100 protein 96 hours after p100/p52 knockdown in HuT 78 cells.

4.9 Changes in gene expression after NIK knockdown

To gain a better insight into the mechanisms involved in NIK-dependent survival, we analyzed the gene expression profile induced by NIK silencing in T cell lymphoma cells. Using whole genome microarray analysis, we explored the impact of NIK silencing on the expression of genes and pathways in My-La and SR-786 cells 48 hours after transfection. Three independent experimental replicates were performed for each cell line and siRNA, and knockdown efficiencies from each experiment are shown in Supplementary figure 1 (in Appendix I). For pathway analysis, Gene Set Enrichment Analysis applying a t-test comparing siNIK1 and siNIK2 with control cells was performed. The gene sets significantly lost

(FDR<0.15) in the siNIK cells, and thus enriched in the control cells, are described in Table 4.6. No gene set was significantly upregulated after NIK knockdown. The NF-κB target genes were significantly underrepresented after NIK knockdown in both cell lines, indicating again a pivotal role for NIK in NF-κB activation (Figure 4.15 A). Other gene sets that were underrepresented after NIK depletion, were X-box binding protein 1 (XBP1) target genes, interleukin pathways, JAK-STAT signaling and BCL6 target genes.

Table 4.6 Gene sets enriched in control cells after NIK knockdown

	Gene Set	NES	FDR	Size	Genes in core enrichment
MYLA	XBP1 TARGETS	-2.133	0.001	58	SSR3, RPN1, FTSJ1, ITGAM, SSR1, PDIA4, SPCS3, GLRX, SLC33A1, DNAJC10, SYVN1, LMAN1, TMED10, HM13, PDIA5, ARF3, SEC24C,SPOP, SLC3A2, SEC23B, FKBP14, DDOST, PDIA3, COX15, COPE, PPIB, HERPUD1
	NFKB TARGET GENES (COMPAGNO)	-1.977	0.004	106	ICAM1, BCL2L1, EMR1, SDC4, NFKBIA, HLA-F, IL6, TNFAIP3, CD44, PLEK, STAT5A, VIM, LTA, CFLAR, STX4, SMAD7, CD40LG, BUB1B, PRKCD, CEP110, BIRC3, STAT1, CCL3, IRF1, FNDC3A, CD83, GADD45B, CCND2, REL, FAS, RRAS2, LSP1, ELL2, IER2, MAP3K1, RFTN1, NFKB2, IL10, NFKB1, NCF2, CXCL9
	G2M CHECKPOINT REGULATION	-1.757	0.053	75	AURKA, KIF2C, SKP2, TOP2A, MDC1, BUB1, CCNH, BUB1B, CUL1, BRSK1, CCNB3, MDM2, CENPA, GADD45B, UBD, BUB3, IRF5, CDC20, PRC1, TTK, ZC3HC1, HMMR, STIL, CDC16, CENPF, CCNF, PRKDC, PLK1, BRCA1, CDC6, CDKN2D, CHEK2, CCNB1, SFN, BIRC5, CDC34, KIF11
	IL3PATHWAY	-1.664	0.094	15	MAP2K1, IL3RA, STAT5A, STAT5B, MAPK3, CSF2RB, IL3
	Gene Set	NES	FDR	Size	Genes in core enrichment
SR786	XBP1 TARGETS	-2.098	0.001	58	SSR3, ISG20, GLRX, DNAJC10, FKBP14, SLC33A1, SRP54, PDIA4, LMAN1, SPCS3, PDIA3, PDIA5, SPOP, PPIB, SLC3A2, ARF3, DAD1, HSP90B1, RPN1, RHOQ, SEC23B, SEC24C, ITGAM, DNAJB9
	JAK-STAT SIGNALING PATHWAY	-1.806	0.042	72	IL7, STAT3, IL6, IL26, MAP2K1, IL12RB2, STAT5A, STAT6, IL4, IL15, SOCS3, STAT1, IL23R, STAT5B
	NFKB TARGET GENES (COMPAGNO)	-1.738	0.056	106	CD44, ID2, IL6, ICAM1, EMR1, SPI1, STAT5A, BIRC2, TNFAIP3, GADD45B, IER2, CCL3, STX4, STAT1, LTA, RFTN1, NFKBIA, CFLAR, VIM, PLEK, CD40LG, CSF2, BCL2A1, HLA-F, RET, BANK1, IL10, SDC4, JUNB, TNF, BIRC3, NFKB2, PRKCD, NFKB1, SMAD7, FNDC3A, SLAMF7
	BCL6 TARGETS	-1.592	0.148	17	CD44, ID2, CCL3, STAT1, CD80, NFKB1, CDKN1B, CCND2, IFITM3, CDKN1A
	IL7 PATHWAY	-1.564	0.146	15	IL7, STAT5A, STAT5B

Abbreviations: NES = Normalized Enrichment Score, FDR = False Discovery Rate, Size = number of gene in the gene set.

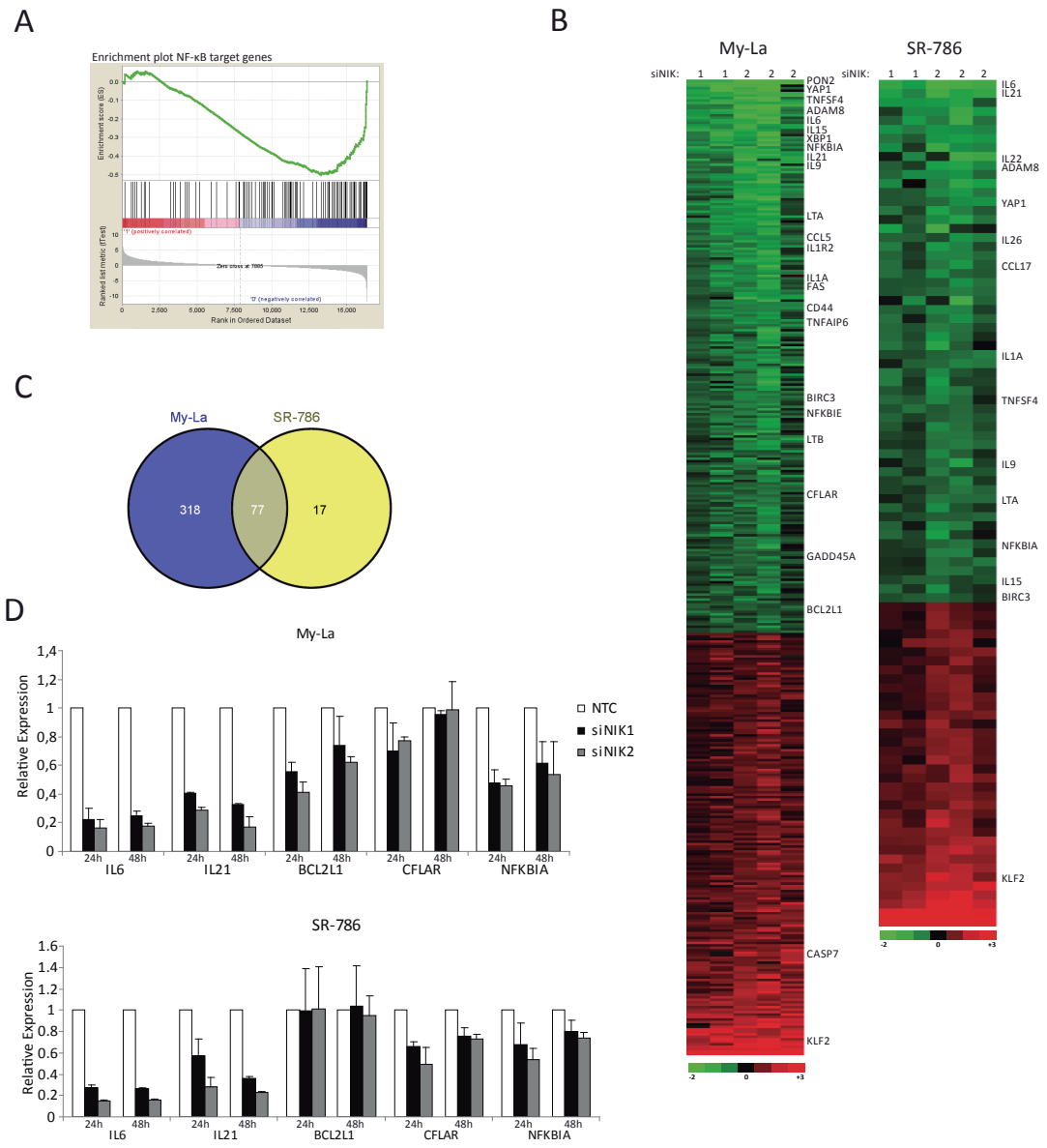

Figure 4.15 Gene expression profile after NIK knockdown.

Whole genome microarray analysis was conducted 48 hours after NIK knockdown in My-La and SR-786. A) GSEA enrichment plot of the NF-κB target genes. The NF-κB target genes were significantly underrepresented in the NIK knockdown cells. B) Heatmaps of differentially expressed genes (FDR < 0.05 and log2 fold change > 0.6) between control and NIK knockdown cells. The numbers on top of the heatmap represent the sequence of siNIK used (1 or 2) in a particular experiment. Negative log2 foldchanges (ratio siNIK/control) are represented in green (downregulation in siNIK cells) and positive fold changes are represented in red (upregulation in siNIK cells). C) Venn diagram showing the overlap of differentially expressed genes in My-La and SR-786 cells. D) Relative gene expression in siNIK cells compared with the NTC measured by RT-qPCR.

Analyzing the altered gene expression induced by NIK at the individual gene level, a paired t-test revealed 395 genes in My-La, and 94 genes in SR-786, that were significantly and differentially expressed (FDR<0.05 and $\log_2$ foldchange >0.6 in either direction) between NIK knockdown and control cells (Figure 4.15 B, see Supplementary Table 1 (Appendix I) for the complete list of genes). Of these genes, 77 were common between My-La and SR-786 (Figure 4.15 C). This number might seem low, but having in mind that SR-786 only presented 94 significantly differentially expressed genes, this means that 82% of the differentially expressed genes in SR-786 were shared by My-La. RT-qPCR was performed on selected genes to validate the gene expression data (Figure 4.15 C and D). Several NF-κB target genes involved in cancer cell survival were downregulated upon NIK silencing, such as the antiapoptotic *BCL2L1* (Bcl-x(L)) and *CFLAR* (c-FLIP) as well as several interleukins. Interleukin 6 (IL-6) and interleukin 21 (IL-21) are cytokines with known functions in cell proliferation and survival of cancer cells and were strongly downregulated after NIK depletion in both cell lines. Apart from known NF-κB target genes, NIK depletion also modulated the expression of other genes involved in tumorigenesis, such as Yes-associated protein 1 (YAP1), paraoxonase 2 (PON2) and Kruppel-like factor 2 (KLF2). In summary, NIK knockdown leads to a decrease in the expression of NF-κB target genes and modulates the expression of many genes involved in tumor growth and survival.

4.10 NIK and the JAK/STAT pathway

The JAK/STAT pathway is activated by cytokines and growth factors and mediates a range of different cellular responses such as proliferation, differentiation, apoptosis, migration and cell survival (Vainchenker et al. 2013). Briefly, activation of cytokine or growth factor receptors, leads to the phosphorylation of STATs by the JAKs, which then results in activation and nuclear translocation of the STAT transcription factors. There are several STATs, but the involvement of STAT3 and STAT5 has been reported in lymphoid malignancies, where they have been described to be persistently phosphorylated and active (Eriksen et al. 2001; Meier et al. 2009; Vainchenker et al. 2013).

One of the affected pathways in T cell lymphoma cells after NIK knockdown apart from the NF-κB pathway, was the JAK/STAT pathway (table 4.6). Furthermore, this pathway was also positively correlated with NIK expression in our series of primary PTCL samples (table 4.5). To explore the suggested relationship between NIK and the JAK/STAT signaling pathway, we

analyzed the expression of phosphorylated STAT3 and STAT5 in our T cell lymphoma cell lines by Western blot. Curiously, only the NIK-expressing cell lines (My-La and SR-786) expressed the phosphorylated form of STAT3 (p-STAT3) (Figure 4.16 A). This was confirmed by immunohistochemical staining of p-STAT3 in the nucleus of these cells (Figure 4.16 B), proposing that this transcription factor is active in NIK-expressing cells. They also expressed higher levels of phospho-STAT5 than did the NIK-negative cell lines (Figure 4.16 A). We then analyzed the expression of phosphorylated STAT after NIK knockdown. Interestingly, the levels of p-STAT3 decreased markedly upon NIK depletion (Figure 4.16 C). Decreased p-STAT5 levels were also observed, although the effect on p-STAT5 was not as prominent as the effect on p-STAT3. This was also accompanied by a decrease in total STAT3 levels. STAT3, as well as STAT5 are NF-κB target genes, which may explain the decrease in total protein expression levels observed upon NIK silencing.

IL-6 is a known trigger of activation of the JAK/STAT signaling pathway and can induce the phosphorylation of STAT3 (Sansone et al. 2012). Additionally, in T cell lymphoma, IL-21 has been reported as a trigger for STAT3 activation (Dien Bard et al. 2009; van der Fits et al. 2012). In Figure 4.15 we observed a consistent and profound decrease of IL-6 and IL-21 levels as a result of decreased NIK protein. Strikingly, following the same expression pattern as p-STAT3, IL-6 and IL-21 are strongly expressed only in the NIK expressing cell lines My-La and SR-786 compared to HuT 78 and DERL7 (Figure 4.17 A). This is independent of the presence of NF-κB activation, since HuT 78 and DERL-7 also present an activated NF-κB pathway. We asked whether the decrease of these cytokines could be responsible for the reduced phosphorylation of STAT3 and STAT5 seen after NIK depletion. After adding IL-6 or IL-21 to the culture medium of My-La and SR-786 cells, we observed that the addition of IL-21, but not IL-6, was able to restore p-STAT3 levels (and to a lesser extent, p-STAT5) after NIK knockdown (Figure 4.17 B). This can suggest that IL21 is involved in the crosstalk between NIK and the JAK/STAT pathway. However, the addition of IL21 24 hours after NIK knockdown, was not able to rescue the apoptotic effect induced by NIK knockdown (Figure 4.17 C). Consistent with this, knockdown of STAT3 alone in My-La, was not able to induce cell death, suggesting that STAT3 is not by itself sufficient to induce cell survival in these cells (Figure 4.17 D).

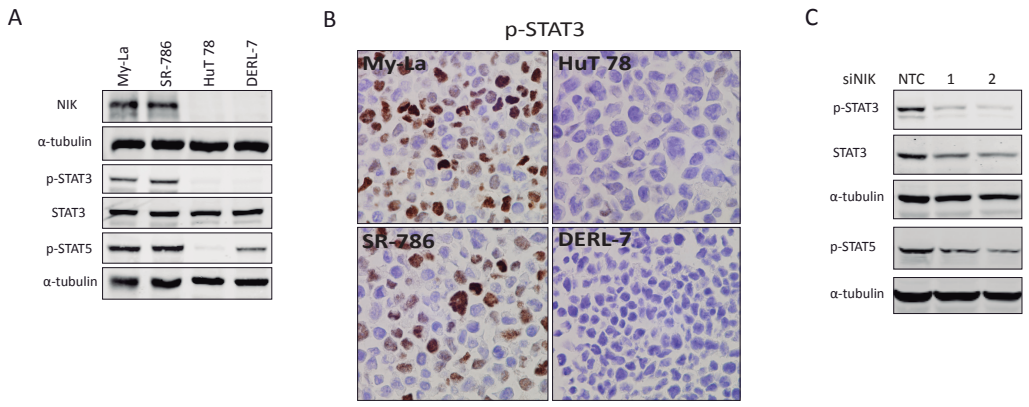

Figure 4.16 Association between NIK, p-STAT3 and p-STAT5.

A) Basal levels of p-STAT3 and p-STAT5 in PTCL cell lines. B) Nuclear expression of p-STAT3 in PTCL cell lines analyzed by immunohistochemistry. C) Reduction of p-STAT3 and p-STAT5 protein levels 48 hours after NIK knockdown in My-La cells. The numbers under the p-STAT3 and p-STAT5 panels represent the quantification of the band intensities normalized to the loading control and as a ratio to the NTC.

4.11 NIK and KLF-2

KLF-2 is a transcription factor to which tumor suppressive roles such as growth-inhibition, apoptosis induction and inhibition of angiogenesis, have been assigned (Wu et al. 2004; Bhattacharya et al. 2005; Wang et al. 2005). KLF2 expression is diminished in several malignancies, such as prostate, ovarian and breast cancer and the reintroduction of KLF-2 into tumor cells shows antitumor effects (Taniguchi et al. 2012). A dramatic upregulation of KLF-2 was seen by gene expression microarray after NIK depletion in T cell lymphoma cells (Figure 4.15). Here, we confirm by RT-qPCR the strong overexpression of KLF-2 after NIK knockdown in My-La and SR-786 (Figure 4.18 A). Considering the tumor suppressive functions of KLF2, it was tempting to knock down KLF-2 in our cells and see if this had any effect on the NIK-induced apoptosis. Using siRNAs for KLF-2, we knocked down the expression of KLF-2 in My-La. KLF-2 knockdown was not toxic by itself (Figure 4.18 B). When combined with siNIK, cells were first transfected with siKLF2, and the next day, with siNIK. At day 4, cells were collected for RT-qPCR and apoptosis assays. As can be seen in Figure 4.18 C and D, restoring the levels of KLF2 close to initial levels, did not have any effect on the cell death induced by siNIK in My-La. In SR-786, we were unable to revert the strong upregulation of KLF-2 induced by NIK knockdown, by the use of KLF2 siRNA. Moreover, we

were not able to confirm the knockdown efficiency of KLF2 at the protein levels, due to the lack of a reliable antibody. Taken together, these results indicate that NIK depletion permits the upregulated expression of KLF2 in T cell lymphoma cells. Even though KLF-2 was described to have tumor-suppressor functions in T cells, KLF2 knockdown alone was not able to rescue the apoptotic phenotype of siNIK cells.

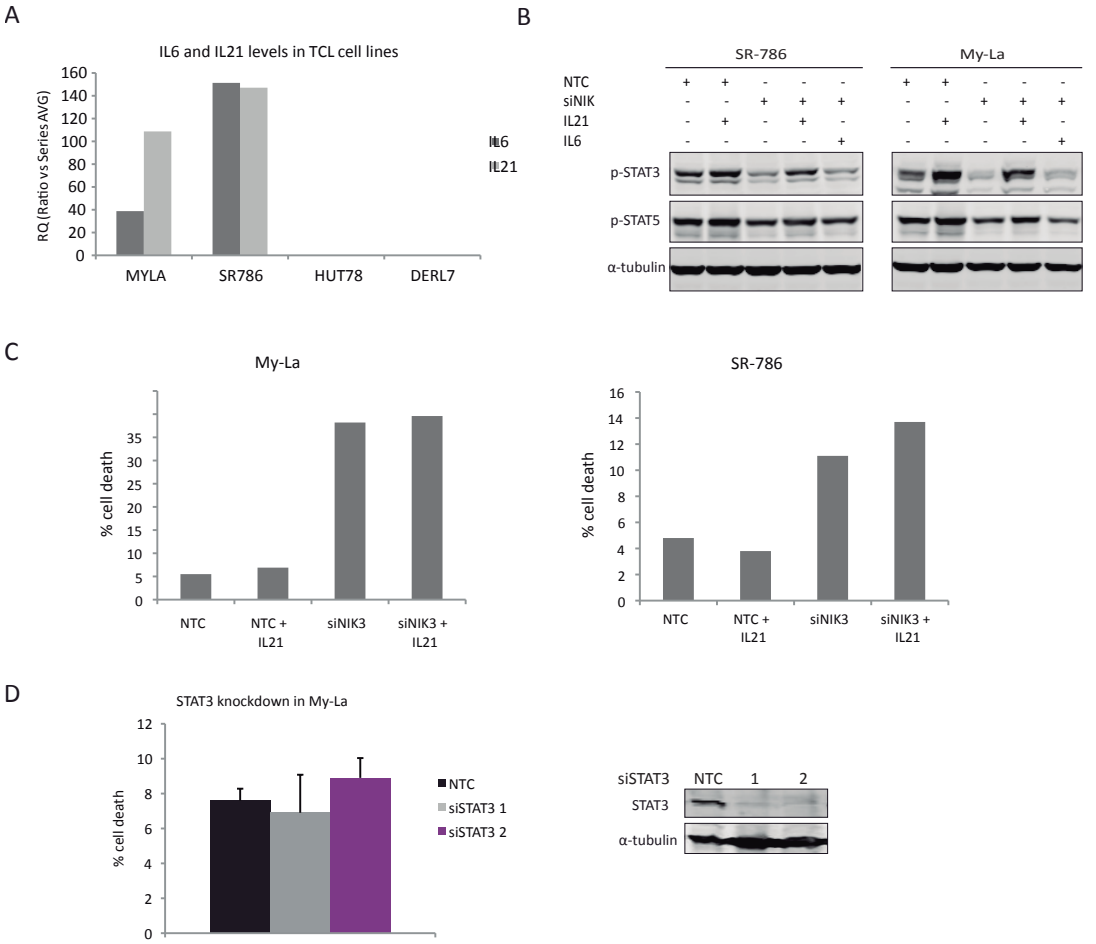

4.17. Role of IL-6 and IL-21 in NIK-induced STAT phosphorylation.

A) Basal mRNA expression levels of IL6 and IL21 in PTCL cell lines. B) Recombinant IL-6 or IL21 was added to the culture medium after NIK knockdown and the levels of p-STAT3 and p-STAT5 were analyzed. The addition of IL-21 restored the levels of p-STAT3 and p-STAT5 in both SR-786 and My-La cell lines. C) Cell viability assay 96 hours after NIK knockdown with or without addition of IL-21. D) Knockdown of STAT3 in My-La cells with siRNA shows effective knockdown levels but no effect on cell viability, 96 hours after transfection.

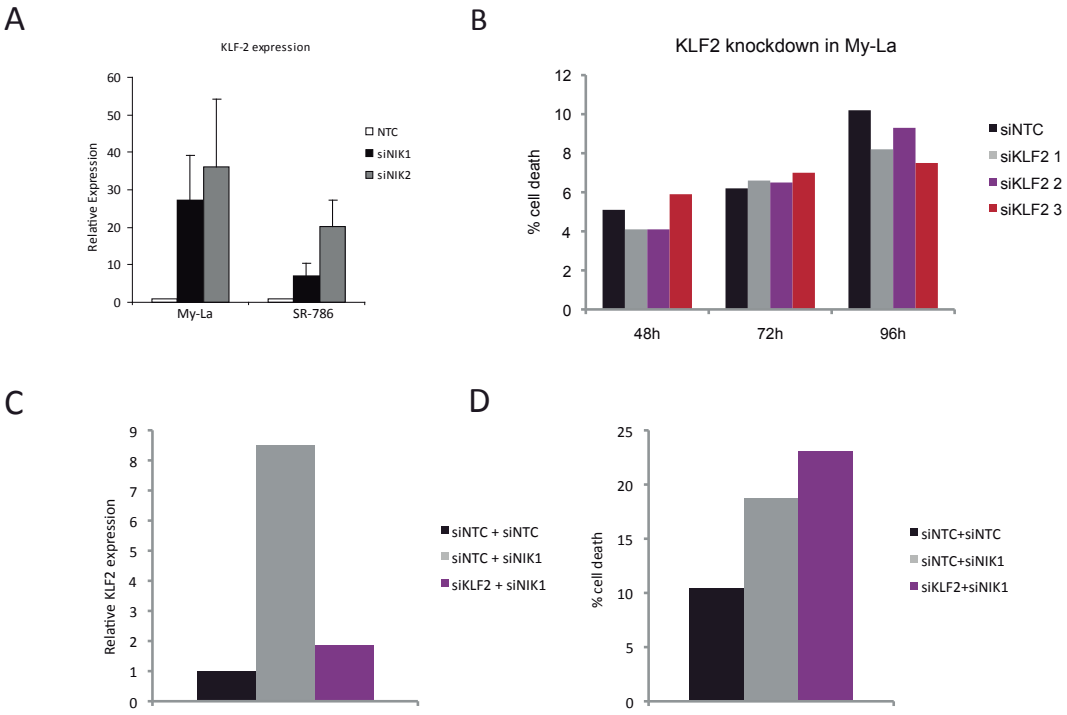

Figure 4.18 Effect of NIK knockdown on KLF-2.

A) Expression of KLF-2 mRNA 48 hours after NIK knockdown. Means of three independent experiments +/- SD are represented. B) Knockdown of KLF-2 in My-La cells. The relative levels of KLF-2 mRNA, obtained by RT-qPCR, are shown in the graph. C) Levels (mRNA) of KLF-2 after NIK and KLF-2 knockdown in My-La. D) Analysis of cell death in cells silenced with siKLF2 and siNIK, measured 4 days after NIK knockdown.

5. DISCUSSION

Cancer is characterized by an accumulation of genetic or epigenetic alterations affecting regulatory circuits that manage normal cell proliferation and homeostasis. Cancer biology is extremely complex, and it is important to bear in mind that cancer is not one but many different diseases, each with distinct characteristics and therapeutic requirements. One of the signaling pathways frequently associated with a range of different cancer types, is the NF-κB pathway. The numerous target genes regulated by NF-κB transcription factors, are in fact involved in the majority of the well-known "Hallmarks of Cancer"(Hanahan et al. 2000; Hanahan et al. 2011), necessary for tumor formation and propagation. Constitutive NF-κB activation has been reported in several hematological tumors and suggested as a key feature in the pathogenesis of some lymphomas (Davis et al. 2001; Jost et al. 2007). However, the complexity of the signaling network and the multiple biological functions of NF-κB have made its investigation and therapeutic targeting a challenge. In order to develop NF-κB–based cancer therapies efficiently and safely, it is necessary to identify molecular targets as well as biomarkers with which to stratify patients who are likely to benefit from the therapy. In the present work, we evaluated the expression of NF-κB transcription factors in human tumor biopsies, and analyzed their expression pattern, subtype-specificity and clinical impact. Furthermore, we aimed to identify novel molecular targets able to interfere with NF-κB activation and lymphoma cell survival.

5.1 Characterization of classical and alternative NF-κB activation in diffuse large B cell lymphoma

5.1.1 NF-κB expression in lymphoma tumor samples

There are few reports assessing the protein expression of NF-κB in lymphoma tumor samples, and to our knowledge, this is the first work reporting the expression of the entire family. Since most studies regarding the NF-κB pathway have been conducted in animal models or in cell lines, the use of patient material in our study offers important translational relevance to current and future studies. We showed by immunohistochemistry, that markers of both classical and alternative NF-κB activation are present in a range of lymphoma types, and were especially frequent in Hodgkin Lymphoma, PTCL and DLBCL. We then performed more detailed studies in PTCL and DLBCL, due to the observed extent of pathway activation and its relevance in the pathobiology of these neoplasms. Both classical and alternative NF-

κB factors were often co-expressed in the same sample, both in PTCL and DLBCL, suggesting the simultaneous engagement of the two pathways. This is not surprising though, since several NF-κB activating signals featured in lymphocytes (such as CD40 or BAFF) are capable of inducing both signaling pathways (Coope et al. 2002; Pham et al. 2011). However, looking closer at the expression of the different transcription factors in a large series of DLBCL cases, we observed an intricate expression pattern. Even though the expression of the different NF-κB proteins was heterogeneous in DLBCL, the vast majority of tumors (87.6%) expressed nuclear NF-κB. Correlated expression between specific pairs of NF-κB subunits, such as p50 and p52, p52 and RelB, p52 and p65, p50 and RelB, and between p50 and p65, was observed, although simultaneous expression of other combinations also was present. This remark suggests that the actual NF-κB expression in tumors is far from being represented by the prototypic NF-κB model and that there is no precise line distinguishing the classical and alternative pathways. However, apart from the most representative and frequent dimerization complexes (p52/RelB, p50/p65 and p50/c-Rel), both homo-dimers and dimers including a variety of NF-κB members as well as atypical partners, have already been described (Hoffmann et al. 2006). Interestingly, c-Rel presented a distinct expression pattern and even though an association between p50 and c-Rel could be perceived (not statistically significant), around a third of the c-Rel-positive tumors did not express any other NF-κB member. Yet, nuclear dimers of CD40 and c-Rel have been described to activate transcription of NF-κB target genes in DLBCL (Zhou et al. 2007). To determine the different dimerization partners was though beyond the scope of this report. The complicated expression pattern of the different subunits is also an indicator of that looking specifically at only a single NF-κB factor as an estimate of NF-κB activation will probably lead to a significant underestimation of the actual NF-κB signaling. Another surprising remark from our studies in DLBCL was that the NF-κB member p65 was only expressed in the nuclei of a minority of cases (11.5%). In agreement with this observation, three previous publications evaluating p65 expression by immunohistochemistry in DLBCL, also report low nuclear p65 expression (Talwalkar et al. 2006; Espinosa et al. 2008; Bavi et al. 2011). The conformity between immunohistochemistry and DNA binding activity (as measured by TransAM ELISA) in our study, and the fact that other studies have obtained similar results using distinct p65-antibodies, suggest that the low expression of p65 observed in our series, is not an issue of antibody specificity. The rare expression of p65 is something that should been taken into account when evaluating the role of p65 in experimental models, or when using only p65 as a measure of NF-κB activation. In the present work, only nuclear expression of NF-κB has

been considered, and even if nuclear p65 expression is rare, p65 was detected in the cytoplasmic compartment in the majority of cases. Thus, the possibility that cytoplasmic expression of NF-κB might accomplish other functions in lymphomagenesis, can't be excluded. One could argue that analyzing the gene expression of NF-κB target genes would be a better approach to estimate NF-κB activation. Indeed, with this approach you would better deduct whether nuclear NF-κB is transcriptionally active or not. On the other hand, gene expression profiling does not give any information about which transcription factors are involved and where they are expressed (tumoral cells or stromal cells). Moreover, NF-κB target gene regulation presents high complexity with context-dependency and crosstalk between non-NF-κB signaling pathways (Oeckinghaus et al. 2009). These techniques thus both provide valuable information about NF-κB signaling and are complementary to each other.

Furthermore, we observed that the expression of nuclear p50 and p52 was a widespread feature in EBV-positive DLBCL. More concisely, NF-κB was only associated with the subpopulation of EBV-positive cases expressing LMP1, where 92.8% and 85.7% expressed nuclear p52 or p50, respectively. Since only a small population of DLBCL patients is EBV-positive (8.1% in our study population), our studies are based on a relatively small number of EBV-positive cases. Even though an increased number of samples would be desirable, our results are clear and highly significant. Previous studies establishing a link between EBV and NF-κB are mainly based on observations in cell lines or murine models (Sylla et al. 1998; Eliopoulos et al. 2001; Atkinson et al. 2003; Thornburg et al. 2006). Here, we confirm that LMP1 is associated with both classical and alternative NF-κB pathway activation in primary DLBCL tumors. EBV-associated DLBCL, which is typically present in elderly people, has worse overall survival and poorer chemotherapy response than EBV-negative DLBCL (Park et al. 2007; Morales et al. 2010; Montes-Moreno et al. 2012), emphasizing the need for new and effective treatments for these patients. Previous knowledge that NF-κB is required for survival of EBV-transformed cells (Cahir-McFarland et al. 2000; He et al. 2000) together with our observation that LMP1-expressing tumors from EBV-positive DLBCL patients are highly associated with NF-κB activation, suggest the exploration of NF-κB interfering therapies in LMP1-positive DLBCL. Due to the different clinical and biological profile of EBV-related DLBCL, EBV-positive and negative DLBCL have been analyzed separately in the present work.

Several factors are known to trigger NF-κB activation in lymphomas. Some of these are provided by the microenvironment (Herreros et al. 2008) and others are intrinsic mutations leading to constitutive activation of the pathway (Staudt 2010). In DLBCL, apart from EBV, several oncogenic mutations in the NF-κB pathway have been reported which could explain the activated pathway observed in a part of the cases (for more details, see section 1.2 of the Introduction). However, the high frequency of nuclear NF-κB expression can probably not be explained solely by the previously reported oncogenic events, especially in GCB-DLBCL, where few NF-κB-activating mechanisms have been described.

5.1.2 NF-κB in ABC/GCB DLBCL

DLBCL is a clinically and molecularly heterogeneous disease with a cure rate of only 40-50% (Coiffier et al. 2010). The division of DLBCL into the molecular subtypes ABC and GCB, has facilitated the molecular understanding of lymphoma pathogenesis and has permitted to stratify the patients into a clinically favorable (GCB) and unfavorable (ABC) group (Rosenwald et al. 2002). This classification has been widely applied by researchers (Swerdlow et al. 2008; Lenz et al. 2010) and is now also used for stratification in clinical trials (Hernandez-Ilizaliturri et al. 2011; Yang et al. 2012). A hallmark of ABC-DLBCL is constitutive NF-κB activation, and a disruption of this activation induces apoptosis in ABC-DLBCL cell lines (Davis et al. 2001; Lam et al. 2005). Our analysis of NF-κB expression in a series of 113 DLBCL samples revealed that the majority of DLBCL tumors express nuclear NF-κB, independently of ABC/GCB subclassification. Surprisingly, we found no significant correlation between ABC/GCB subtype and the expression of any of the five NF-κB members, indicating that NF-κB signaling is present not only in ABC-DLBCL, but also in GCB-DLBCL. To discard the possibility that this observation could be a result of using a suboptimal classification method for ABC/GCB classification, we performed the analysis in two independent series of DLBCL tumors, classified both by immunohistochemistry and gene expression profiling (considered the gold standard for ABC/GCB classification). A concordance of 91.7% was obtained when immunohistochemistry and gene expression profiling were compared, indicating that immunohistochemistry is a valid method for DLBCL classification in our study. These two analyses both showed that NF-κB was expressed equally in ABC- and GCB-DLBCL. In agreement with our observation, previous works analyzing the expression of phopho-p65 and p52 as markers of an activated NF-κB pathway in DLBCL tumors, reported expression of these subunits in both DLBCL subtypes with similar frequencies (Espinosa et al. 2008; Pham

et al. 2011). On the contrary, other studies associated the expression of nuclear p65, p50 and p52 with the ABC-subtype, although they were also present in a considerable fraction of GCB-DLBCL as well (Compagno et al. 2009; Bavi et al. 2011). An important difference between our study and several others, was that EBV-positive cases were excluded from the analysis. Due to their distinct molecular and clinical profile, EBV-positive DLBCL has been suggested as a distinct DLBCL category (Swerdlow et al. 2008). EBV-associated DLBCLs have been characterized by NF-κB activation and they frequently present an ABC-phenotype (Montes-Moreno et al. 2012). Including this category together with EBV-negative DLBCL, probably gives rise to bias with an increased number of NF-κB-positive cases and a stronger association with the ABC-phenotype. Our observation that NF-κB signaling is present in both ABC and GCB subtypes, evokes several questions concerning whether NF-κB is involved in the underlying pathogenesis of GCB as well, and whether NF-κB inhibition could be useful in a subset of GCB-DLBCL. In fact, even though mutations affecting NF-κB regulator genes are more frequent in ABC-DLBCL, amplifications of CREL have been described in GCB (Rosenwald et al. 2002) and at least 23% of GCB tumors harbor somatic mutations in several genes involved in NF-κB signaling, such as CARD11, A20 and TRAF2 (Compagno et al. 2009). Since the ABC and GCB subtypes partly present a distinct pattern of genetic abnormalities and respond differently to therapy (Lenz et al. 2008; Lenz et al. 2010), the mechanisms leading to NF-κB signaling and the subsequent transcriptional response might be different in the two subtypes. Moreover, the majority of published functional studies considering NF-κB in GCB/ABC DLBCL have been conducted in a specific set of DLBCL cell lines, where the GCB cell lines are characterized by a lack of NF-κB (Davis et al. 2001; Lam et al. 2005). In fact, analyzing the expression of nuclear NF-κB in these DLBCL cell lines, we also observed a significant and positive association between NF-κB and ABC subtype (data no shown). Additionally, a study analyzing NF-κB expression in a distinct set of DLBCL cell lines showed that NF-κB signaling was present in both subtypes, although p65 expression was more frequent in ABC-DLBCL(Pham et al. 2011). Having our results in mind, the use of ABC/GCB cell lines might not reflect the actual situation in patient tumors and the extraction of these results to the clinic may be questioned. The presence of NF-κB signaling in both ABC- and GCB-DLBCL is something to contemplate when evaluating molecular mechanisms and putative therapeutic targets in future studies.

5.1.3 The impact of NF-κB on clinical outcome in DLBCL patients

There are only a few previous publications describing NF-κB signaling and its clinical correlation in lymphomas, and the results are contradictive (Espinosa et al. 2008; Curry et al. 2009; Bavi et al. 2011). In this work, we investigated the impact of all NF-κB members on patient overall survival, using nuclear expression as an estimate of NF-κB activation. In DLBCL, nuclear c-Rel expression was seen to be a common feature and identified a subset of patients with enhanced overall survival. The other four transcription factors did not have any significant impact on DLBCL survival, although a trend towards superior overall survival was observed in p52-positive cases as well. Additionally, c-Rel was identified as an independent favorable prognostic factor in DLBCL and had a greater impact on overall survival than had GCB/ABC classification in our series. The fact that c-Rel-positive tumors are associated with a favorable overall survival, does not mean that NF-κB-targeted therapies could not be an attractive molecular target in these malignancies, but the relatively favorable clinical course of these patients in an R-CHOP regimen, should be taken into consideration when evaluating the effects of novel therapeutic strategies. C-Rel is the only NF-kB transcription factor that is frequently amplified in human cancers and has also consistently been shown to have transforming potential in culture (Gilmore et al. 2001; Gilmore et al. 2004). Amplification of the REL locus (encoding c-Rel) (Gilmore et al. 2004) is commonly observed in DLBCL and mainly associated with the GCB phenotype (Rosenwald et al. 2002). In our study, nuclear c-Rel expression is though detected in both ABC- and GCB- DLBCL. However, no correlation between REL amplification and nuclear c-Rel expression was observed in DLBCL in a study by Houldsworth et al (Houldsworth et al. 2004). The fact that only c-Rel expression has prognostic impact on DLBCL suggests that different NF-κB subunits have different roles and activate different transcriptional programs. However, the subunit- specific or dimer-specific functions of NF-κB in regulating transcriptional selectivity are far from understood. Whether c-Rel is required for tumor cell survival in these tumors, is still unknown, and would be a relevant subject for future studies.

In line with our results, NF-κB was also associated with enhanced patient survival in another DLBCL study where phosphorylated p65 was assessed (Espinosa et al. 2008). In contrast to our findings, p65 expression was described as an adverse prognostic marker in DLBCL in another report (Bavi et al. 2011). Moreover, nuclear c-Rel assessed by immunohistochemistry, was associated with worse clinical outcome in GCB-DLBCL in a

previous publication (Curry et al. 2009). Those studies though, were performed in biopsies from patients treated with chemotherapy without Rituximab. Since the addition of Rituximab has markedly improved the overall survival rates in DLBCL (Coiffier et al. 2010), and the outcome of survival analyses depends on the clinical management, this can be a possible explanation for the observed differences. Our study is performed using a cohort of patients that has uniformly been treated with R-CHOP, which is the standard treatment for DLBCL patients nowadays.

5.2 The NF-κB pathway in T cell lymphomas: NIK as a regulator of classical and alternative signaling and cell survival

5.2.1 The expression of NF-κB in PTCL tumors and its clinical impact

Analyzing the expression of the different NF-κB members in patient material from the most common subtypes of PTCL (PTCL-NOS, AITL and ALCL), we found markers of activation of both the classical and alternative pathways in a significant subset of samples, characterized by the nuclear expression of p50, p52, RelB, and c-Rel. As in DLBCL, the nuclear expression of p65 in PTCL was also uncommon and only present in a minority of the cases in our study (see section 5.1.1 for further discussion). A few other publications have also reported NF-κB activation in PTCL (Izban et al. 2000; Martinez-Delgado et al. 2005; Sors et al. 2006), but the trigger of this activation is still unknown. No mutations in the pathway have been described, apart from TNFAIP3 deletions in Sézary Syndrome(Braun et al. 2011) and p100 truncations (Fracchiolla et al. 1993; Derudder et al. 2003), leaving a field of research ahead. Deciphering the molecular mechanisms leading to pathogenic NF-κB activation in PTCL will be important in order to understand its molecular pathology and discover novel therapeutic targets.

In PTCL patients (including PTCL-NOS and AITL), in contrast to DLBCL, nuclear expression of classical or alternative NF-κB factors was significantly associated with worse OS compared to NF-κB-negative tumors. In the ALCL subtype, NF-κB was also associated with inferior overall survival and was negatively correlated with ALK-expression, being more frequent in the more aggressive ALK-negative ALCLs. In PTCL, no specific NF-κB subunit was responsible for the prognostic impact, but when NF-κB was evaluated as a whole, patients lacking nuclear expression of any NF-κB had a favorable outcome. Looking at c-Rel expression alone in PTCL,

as done in DLBCL, positive cases had an extremely unfavorable survival curve, even though the differences were not statistically significant due to the less frequent expression of c-Rel in PTCL (data not shown). In contrast with our results, Martinez-Delgado and colleagues (Martinez-Delgado et al. 2005) associated the expression of NF-κB–related genes, using gene expression microarrays, with a favorable clinical outcome in PTCL. These disparities might be explained by the differences in PTCL subtypes included in our study (PTCL-NOS and AITL, or ALCL alone) and the study performed by Martínez-Delgado (PTCL-NOS, AITL, CTCL and NK/T lymphomas in the same analysis) or by the variation and limitations of each of the employed techniques for NF-κB estimation (discussed in section 5.1.1). A comparison of these two techniques, including the gene expression profile of NF-κB target genes as well as the expression of the five different transcription factors, in the same patient cohort would provide valuable information to clarify this issue. Apart from ALK, prognostic factors and predictive markers for therapy outcome in PTCL are scarce. Our results led to the identification of a group of PTCL with unfavorable clinical outcome, based on NF-κB expression, suggesting that aberrant NF-κB activation may confer enhanced survival or treatment resistance on these tumors. NF-κB was thus an interesting candidate to explore molecular targets for therapy. The different impact of NF-κB in DLBCL and PTCL patients, reflects the heterogeneity of human tumors and the NF-κB signaling network, which is highly dependent on the cell type, cellular context and parallel signaling mechanisms (Oeckinghaus et al. 2009) .

5.2.2 NIK expression in PTCL

NIK captured our attention in T cell lymphomas after the observations that recurrent NF-κB activation was present in PTCL tumor samples and highly expressed NIK levels were detected in PTCL cell lines in an initial screening of different lymphoma cell lines. Even though NIK had been studied in the context of other tumors, such as multiple myeloma(Annunziata et al. 2007), the role of NIK in T cell lymphomagenesis was unknown. Since the pathogenesis of PTCL is largely undiscovered, studies clarifying oncogenic mechanisms and identifying putative molecular targets are urgently required in order to improve their dismal prognosis. The observation that NIK was overexpressed in a subset of T cell lymphoma cell lines and primary Sézary syndrome samples, when compared to healthy T lymphocytes, indicated that NIK might be involved in malignant signaling in PTCL and led us to further investigate its role

in this neoplasm. NIK has previously been found to be overexpressed at the RNA and/or protein level in other cancers, such as melanoma, multiple myeloma, DLBCL, mucosa-associated lymphoid tissue (MALT) lymphoma, and adult T-cell leukemia and Hodgkin lymphoma (Saitoh et al. 2003; Annunziata et al. 2007; Pham et al. 2011; Rosebeck et al. 2011; Ranuncolo et al. 2012; Thu et al. 2012). In some cases, genetic alterations such as gene amplifications, translocations, or mutations in NIK, or alterations in genes regulating the stability of NIK protein (such as TRAF2, TRAF3 and cIAP2/3), are described, emphasizing the role of NIK in tumorigenesis (Annunziata et al. 2007; Keats et al. 2007; Rossi et al. 2011). Interestingly, we did observe an absent or strongly reduced expression of TRAF3, a major negative regulator of NIK protein stability, in cell lines where NIK was highly expressed. This observation suggests that this might be one of the mechanisms regulating NIK signaling in T cell lymphoma cells, as described in other cell types (Keats et al. 2007; Vallabhapurapu et al. 2008). Moreover, whole genome sequencing of four T cell lymphoma cell lines performed in our group (My-La, HuT 78, HH and MJ), revealed a potentially deleterious point mutation affecting TRAF3 in My-La cells, substituting a serine for an asparagine in position 233 (Vaque et al. Submitted). The discovery of a TRAF3 mutation in a T cell lymphoma cell line is novel and of interest, but the heterozygous nature of the mutation however, does not explain the complete absence of TRAF3 protein in My-La cells. Moreover, absence of TRAF3 does not explain the overexpression of NIK that we observed at the transcriptional level. In Hodgkin lymphoma, the simultaneous existence of MAP3K14 amplifications and TRAF3 deletions have been described to occur in tumor samples (Otto et al. 2012), suggesting that both protein stabilization and transcriptional overexpression of NIK might be complementary mechanisms to potentiate NIK signaling. Copy-number studies of both MAP3K14 and TRAF3 would give valuable insight to the mechanisms causing NIK overexpression in PTCL. The upstream mechanisms leading to NIK overexpression in T cell lymphomas are at the moment unidentified. Possible contributions to NF-κB activation in T-cell lymphomas are oncogenic viruses (de Oliveira et al. 2010) and signals from CD30 (Buchan et al. 2012) or the T-cell receptor (Schulze-Luehrmann et al. 2006; Wright et al. 2007), but whether NIK is involved in transmitting these signals is still to be clarified. Recently, mir-31 was reported to be regulating the levels of NIK in tumors, where polycomb-mediated repression of mir-31 led to an overexpression of NIK (Yamagishi et al. 2012). Analyzing the levels of mir-31 in our PTCL cell lines, we observed a lack of mir-31 in several cell lines, but this absence was independent of the levels of NIK (data not shown). It could also be hypothesized that the activation of NIK and NF-κB can be an effect of deregulated signaling of other pathways

linked to T-cell lymphomagenesis, such as the PI3K/AKT, NOTCH, or JAK/STAT pathway, which can all result in NF-κB activation (Oeckinghaus et al. 2009).

A major gap in our study is the inability to detect endogenous NIK protein in tumor samples. A few previous works report the detection of NIK by immunohistochemistry on paraffin-embedded tumors (Pham et al. 2011; Ranuncolo et al. 2012). However, when we tested these antibodies, as well as a range of additional NIK antibodies, none of these showed specificity for NIK when tested in paraffin-embedded cell lines where NIK had previously been genetically depleted. A couple of attempts of generating NIK-specific monoclonal antibodies at the Monoclonal Antibody Unit at the CNIO, have been maid. Unfortunately, these antibodies also failed to detect endogenous NIK levels. Moreover, the detection of NIK by western blot is also complicated, since the pre-treatment of cells with the proteasome inhibitor MG-132 is needed prior to protein extraction in order to obtain detectable levels of the protein. Hence, there is still a need for the development of specific and sensitive NIK antibodies, which will permit us to detect endogenous expression of the protein.

5.2.3 NIK-regulated NF-κB signaling in PTCL

Several approaches were performed demonstrating the role of NIK as a regulator of NF-κB signaling in PTCL. In PTCL tumor samples, we showed that NIK expression was positively and significantly correlated with the expression of NF-κB target genes, indicating that NIK might be involved in NF-κB signaling in PTCL. From previous reports, the role of NIK in the alternative NF-κB pathway is clear, but the involvement of NIK in the regulation of the classical pathway seems to be signal and cell type dependent (Zarnegar et al. 2008; Thu et al. 2010). For example, in melanoma and pancreatic cancer, NIK only affects the alternative pathway (Nishina et al. 2009; Thu et al. 2012), whereas NIK regulates both pathways in DLBCL and multiple myeloma (Annunziata et al. 2007; Pham et al. 2011). Our functional studies based on genetic knockdown of NIK in different PTCL cell lines, were able to demonstrate that NIK regulated the signaling of both the classical and alternative axis in T cell lymphoma. NIK knockdown led to decreased processing of p100 and p105, decreased nuclear levels of p52 and p50, as well as a decreased DNA-binding activity of both classical (p65, p50, and c-Rel) and alternative (p52 and Rel-B) NF-κB transcription factors. Futhermore, silencing of NIK also gave rise to a significant downregulation of NF-κB target genes, as

measured by whole genome expression profiling. Some of these target genes, are commonly associated with classical NF-κB signaling, such as IL6, IL10, and NFKBIA (coding the protein IκBα) (Libermann et al. 1990; Sun et al. 1993). NIK has not previously been reported to regulate the processing of p105. The reduced levels of p50 observed, might be an effect of direct NIK signaling or an indirect effect due to reduced NF-κB target expression (NFKB1, encoding p105, is a NF-κB target). Then again, even though the detection of p50 reduction is a later event than the reduction of p52, the consistent and reproducible upregulation of p105 upon NIK knockdown in My-La and SR-786 cells, suggest that there is a blockage in p105 processing. The mechanisms involved in p105 processing are only partly clarified. P105 is normally constitutively processed to p50 in unstimulated cells (Fan et al. 1991; Palombella et al. 1994). IKKβ have also been reported to phosphorylate p105, which can lead to either p50 formation or complete degradation (Cohen et al. 2004; Oeckinghaus et al. 2009). However, IKKβ knockdown didn't give rise to any consistent reduction of p50 in our cells, proposing that NIK might regulate the processing of p105 independently of IKKβ. If NIK is able to bind directly to p105 and induce its proteolysis, or if this is an indirect effect, is though still to be explored. From our NIK knockdown results, we could also observe that NIK depletion led to a decrease in phosphorylation of both IKKα and IKKβ. Evidences for NIK-induced phosphorylation of IKKα and IKKβ have previously been published in other experimental settings (Woronicz et al. 1997; Ling et al. 1998; Delhase et al. 1999). Interestingly, reduced levels of total IKKα and IKKβ were also detected upon NIK silencing. The transcriptional regulation of the genes encoding IKKα and IKKβ is not known, and they are not described as NF-κB target genes. On the other hand, the fact that NIK knockdown led to a more efficient reduction of p50 and p52 in PTCL, compared with IKKα or IKKβ knockdown, suggests that NIK can, at least in part, regulate the NF-κB pathway by IKK-independent mechanisms. Consistent with these results, direct phosphorylation of p100 in an IKKα-independent manner has been reported (Xiao et al. 2001). The role of NIK in the regulation of NF-κB-induced gene transcription in PTCL, was further confirmed examining the gene expression profile in NIK-silenced T cell lymphoma cells by whole genome expression microarrays, where NF-κB target genes were found significantly downregulated. However, NIK does not seem to be strictly essential for NF-κB activation in all PTCL cells, as we found that nuclear NF-κB was not exclusively expressed in NIK-overexpressing cell lines andcells with absent/low expression of NIK presented at least classical pathway activation. Thus, the pathway may be activated by different mechanisms in these cells. A proper identification of upstream mechanisms is important for efficient NF-κB inhibition. The

alternative pathway however, was only seen to be activated in cell lines expressing NIK or a truncated form of p100, which permits bypassing NIK for alternative pathway activation(Neri et al. 1991; Chang et al. 1995). Taken together, our data show that NIK has a profound effect on NF-κB regulation in PTCL, being a major gate-keeper of the activation of all NF-κB transription factors.

5.2.4 NIK signaling and its effect on PTCL cell survival

The mechanisms underlying T cell lymphomagenesis are poorly defined, partly due to its heterogeneous presentation and lack of representative study models. PTCL is a highly aggressive malignancy where proper targeted therapies are lacking due to the insufficient knowledge about implicated pathologic mechanisms. Hence, studies clarifying its pathobiology and the discovery of candidate molecular targets are needed and are underway. Aberrant signaling of pathways employed by T cells in their normal development and proliferation has been described in T cell neoplasms, such as deregulated signaling of PI3K/AKT, NOTCH, MAPK, JAK/STAT, NF-κB or Calcineurin/Nuclear factor of activated T-cells (NFAT) pathway. (Zhao 2010; Martin-Sanchez et al. 2013), However, most of these evidences, come from reports of Adult T cell leukemia, a T cell neoplasm not included in our work. Hints about malignant mechanisms in PTCL can also be provided from therapeutic studies of novel treatment alternatives. For instance, clinical efficacy has been achieved by histone deacetylase ihibitors, such as Vorinostat and Panobinostat, in CTCL and PTCL, indicating that aberrant epigenetic mechanisms might be involved in T cell lymphoma pathogenesis (Wozniak et al. 2010; Foss 2013). Moreover, the use of monoclonal CD30 antibodies as therapy in ALCL, suggests a role for CD30 in malignant signaling (Forero-Torres et al. 2009; Foss 2013).

PTCL-NOS and AITL are the most common subtypes of PTCL. Nevertheless, evidences for their malignant mechanisms are poor and mainly based on gene expression profiling studies, due to the fact that no PTCL-NOS or AITL cell lines or animal models are available. The functional studies in our work were conducted in T cell lymphoma cell lines representing different PTCL subtypes; Mycosis fungoides, anaplástic T cell lymphoma, Sézary Syndrome and γδ hepatosplenic T cell lymphoma. On the other hand, our expression studies in primary T cell lymphoma samples and the clinical correlation studies, were performed in samples diagnosed as PTCL-NOS, AITL, ALCL and Sézary syndrome. Even though NIK expression in

these samples was demonstrated to correlate with NF-κB activation, the possibility exists that the functional studies performed in this work, might not be fully extrapolated to all of these subtypes. Unfortunately, appropriate models are absent for most PTCL subtypes.

The activated NF-κB pathway reported in some subtypes of T cell lymphoma by us (Wozniak et al. 2009; Odqvist et al. 2013) and others (Martinez-Delgado et al. 2005; Sors et al. 2006), together with studies showing that the inhibition of NF-κB in PTCL cell lines leads to reduced cell survival (Izban et al. 2000; Sors et al. 2006), points toward the possibility that NF-κB might be involved in PTCL pathogenesis. In CTCL cell lines, pharmacological inhibition of IKKβ has been shown to induce apoptosis (Sors et al. 2008). Moreover, Bortezomib has shown clinical efficacy in some PTCL subtypes such as CTCL and PTCL-NOS(Zinzani et al. 2007; Foss 2013), and the antineoplastic activities of Bortezomib have partly been attributed to the ability to block NF-κB activation (McConkey et al. 2008). In order to specifically and properly block NF-κB in tumors, key regulators of the pathological NF-κB activation should be identified. IKKβ inhibitors have been available for several years but have not been able to make their way into the clinical setting, implying that novel targets in the signaling cascade are desirable.

The present study revealed a pivotal role for NIK in the survival of T-cell lymphoma cells. NIK knockdown strongly reduced the cell viability and induced apoptosis in PTCL cell lines. The selective toxicity for siNIK to NIK-overexpressing cells observed in this work, highlights several important issues. First, it confirms the specificity of the siRNA sequences. Second, it provides a tool for identifying potentially targetable tumors. And third, it suggests that NIK-targeting could have a selective effect on NIK-expressing cells, while leaving cells with low NIK levels, like healthy T cells, unaffected. The potent cell-killing effect observed upon NIK depletion in My-La or SR-786 cells, could not be reproduced by knocking down either one or both of its targets, IKKα or IKKβ. Even though the knockdown of these kinases also gave rise to an increase in cell death, comparable or even lower efficiencies of NIK knockdown led to a more profound effect on cell survival. Hence, other or additional mechanisms besides the reduction of IKK activation, seen upon NIK depletion, must be responsible for NIK-induced cell death. Furthermore, the elimination of only the alternative NF-κB factors, RelB and p100, was not able to induce apoptosis in PTCL cell lines. This indicates that NIK-induced survival is not dependent solely on alternative NF-κB activation, in contrast to other studies where RelB has been described as critical for NIK-induced survival in Hodgkin lymphoma (Ranuncolo et

al. 2012). Of the four NF-κB factors expressed in PTCL, only the knockdown of c-Rel showed any significant effect on PTCL survival. As mentioned before, c-Rel has transforming abilities and its locus has been found amplified in several tumors (Martin- Subero et al. 2002; Gilmore et al. 2004). A small subgroup of PTCL-NOS have recently been characterized by chromosomal aberrations with REL locus amplifications(Hartmann et al. 2010). However, its importance and the role of c-Rel in T cell lymphoma pathogenesis have not been investigated. Since NIK reduces the levels of nuclear c-Rel as well as c-Rel DNA- binding activity, the role of NIK in PTCL survival signaling might partly be mediated by c-Rel. The combined effect of other NF-κB members might also be important for PTCL survival, although individual loss did not show any effect. It should also be mentioned that the full-length p100 and p105 proteins can act both as inhibitors of NF-κB and as precursors for p52 and p50 (Oeckinghaus et al. 2009). For that reason, a knockdown of these precursors as performed in our cell lines with siRNA (leading to reduced expression of both the precursors and the processed proteins) might give a different outcome than the blocked processing of p100 and p105 seen after NIK silencing (where the precursors were still expressed).

To investigate the possible downstream effectors of NIK-regulated signaling and tumorigenesis, we conducted whole genome gene expression analysis of NIK-silenced T-cell lymphoma cells. As expected, many of the genes differentially expressed between NIK-silenced and control cells were NF-κB target genes known to be important in the regulation of tumor growth and survival. The expression of anti-apoptotic proteins, such as c-FLIP, Mcl-1, Survivin and Bcl-XL, is one of the mechanisms by which tumor cells manage to survive in the environment and to resist chemotherapy (Kelly et al. 2002). Overexpression of anti-apoptotic proteins has been suggested to be involved in the pathogenesis of PTCL (Jung et al. 2006). For instance, c-FLIP has been described to protect ALCL cells from FAS-induced apoptosis (Oyarzo et al. 2006) and to protect cutaneous T-cell lymphoma cell lines from antitumor treatment (Al-Yacoub et al. 2012). Furthermore, Bcl-2–related anti-apoptotic proteins (Bcl-2, Mcl-1 and Bcl-XL) have been found highly expressed in PTCL tumor tissues and their expression correlated with low apoptotic rate and high proliferation (Rassidakis et al. 2003). Upon NIK knockdown in T cell lymphoma cell lines, we observed a downregulation of several anti-apoptotic genes, such as CFLAR (encoding Bcl-xl), BIRC3 (cIAP2), and BCL2L1 (c-FLIP). The downregulation of these genes, all NF-κB targets (Kreuz et al. 2001; Turner et al. 2007; Pradhan et al. 2012), might explain the strong induction of apoptosis observed in these cells after NIK inhibition. A differential effect on the expression of these genes was

though observed in the cell lines. While, BCL2L1 expression was reduced in My-La and remained unchanged in SR-786 after NIK knockdown, the levels of CFLAR were only reduced in SR-786. In a melanoma cell line, NIK was also shown to regulate the expression of anti-apoptotic factors, but in this case survivin and BCL2, and not the ones affectedin our experimental setting (Thu et al. 2012). In fact, the levels of survivin were unchanged in T cell lymphoma cells after NIK depletion, indicating that NIK and NF-κB can engage different anti-apoptotic players in different cellular contexts.

Other NF-κB target genes that were strongly and consistently downregulated after NIK knockdown in MyLa and SR-786 cells, were the cytokines IL-6 and IL-21. These cytokines are involved in normal B- and T-cell development and a in the proper regulation of the immune response, but have also been widely studied in several tumors owing to their protumorigenic activity and their roles as targets for cancer therapy (Grivennikov et al. 2009; Ma et al. 2011). IL-6 and IL-21 are involved in JAK/STAT signaling and can give rise to both STAT3 and STAT5 phosphorylation (Dien Bard et al. 2009; Sansone et al. 2012; van der Fits et al. 2012). STAT transcription factors regulate cellular processes such as proliferation, cell migration and survival and a deregulated JAK/STAT pathway has been described in several tumors, including T cell lymphomas (Eriksen et al. 2001; Vainchenker et al. 2013). Curiously, in spite of an activated NF-κB pathway in NIK-negative cell lines, only the NIK-positive cell lines expressed high levels of IL-6 and IL-21 as well as pSTAT3 and pSTAT5, indicating a different NF-κB transcriptional program in NIK-positive versus NIK-negative cells. The underrepresentation of JAK/STAT pathway genes in siNIK cells observed in the GSEA analysis gave us a hint that NIK might be involved in the regulation of this pathway as well. To confirm this, we observed reduced levels of both pSTAT3 and pSTAT5 after NIK knockdown in T cell lymphoma cells. We further showed that exogenous IL-21, but not IL-6, was able to induce STAT3 phosphorylation and restore pSTAT3 levels in siNIK cells, proposing IL21 as a possible intermediate between the NF-κB and JAK/STAT pathways. However, further studies, as for example IL21 inhibition or knockdown, should be performed to verify that IL21 is the responsible mediator of STAT activation. The addition of IL21 to siNIK cells was though not sufficient to fully or even partly rescue the apoptosis induced by siNIK. Furthermore, even though STAT3 activation has been proposed as a possible oncogenic mechanism in cutaneous T cell lymphomas(Nielsen et al. 1999), effective silencing of STAT3 in MyLa cells was not able to induce cell death, indicating that STAT3 inhibition alone is not sufficient to induce apoptosis. These results describe for the first time an interesting crosstalk between

NIK and the JAK/STAT pathway, integrating two important survival pathways in T cell lymphomagenesis. IL6 and IL21 were though not the only cytokines with altered expression in siNIK cells, since other cytokines such as IL15 and IL1, also involved in malignant T cell proliferation and survival pathways(Shirakawa et al. 1989; Marzec et al. 2008), were downregulated in both MyLa and SR-786 cells after NIK knockdown as well.

Interestingly, one of the NIK knockdown-sensitive cell lines in our study, SR-786, expresses the oncogenic fusion protein NPM-ALK, as a result of a chromosomal translocation occurring frequently in a subset of ALCL patients (Morris et al. 1994). The critical role of NIK in the survival of SR-786 cells, indicates that NIK is involved either in the downstream signaling of NPM-ALK or in a complementary mechanism required to assure the survival of these cells.

The expression of other genes involved in tumorigenesis, not described as NF-κB targets, was also modulated after NIK knockdown. Unexpectedly, one of the most significantly downregulated gene sets in siNIK cells, was the XBP1 targets. Moreover, XBP1 itself was downregulated in siNIK My-La cells, but not in SR-786. XBP1 (X box-binding protein 1) is a transcription factor involved in the regulation of endoplasmatic reticulum (ER) homeostasis, including protein folding, trafficking and degradation(Acosta-Alvear et al. 2007). It was first described as a transcription factor regulating the major histocompatibility complex (MHC) genes in B cells(Liou et al. 1990) and is also necessary for plasma cell differentiation (Reimold et al. 2001). In the last decade, a role for XBP1 as a key transcription factor in the unfolded protein response (UPR) has been established (He et al. 2010). UPR has been linked to human cancer, where XBP1 has been shown to be activated and act as a survival factor, for instance in multiple myeloma (Romero-Ramirez et al. 2004; Mimura et al. 2012). The activation of XBP1 is controlled by a mRNA splicing reaction, generating a spliced and active form of XBP1(Calfon et al. 2002). To examine whether XBP1 was activated in our T cell lymphoma cell lines, we analyzed the expression of spliced (active) or unspliced XBP1 by semiquantitative PCR. However, only the unspliced variant was detected, suggesting that the XBP-1 pathway is not activated in our panel of cell lines (data not shown). The explanation and link between siNIK and the reduction of XBP1 targets observed in our analysis thus remain unclear.

Another example of tumor-associated genes with altered expression after NIK knockdown is tumor suppressor KLF-2, which was seen strongly upregulated after NIK knockdown. Since

KLF-2 possesses antiproliferative and antitumor characteristics (Taniguchi et al. 2012), we explored the possibility that KLF-2 might be involved in mediating NIK-induced survival. However, the knockdown of KLF-2 together with NIK knockdown, was not able to influence the phenotype induced by siNIK. Yet, only the effect on apoptosis was analyzed and it cannot be excluded that a difference in the proliferative capacity of the cells would be present. The effect of siNIK on non- NF-κB targets could either indicate NF-κB-independent functions of NIK, or the presence of interactions between NF-κB and other signaling pathways. In fact, the involvement of NIK in non-NF-kB-signaling has been described, such as MAPK signaling in neural differentiation(Foehr et al. 2000) and β-catenin signaling in melanoma (Thu et al. 2012).

In summary, NIK knockdown gave rise to reduced NF-κB activation and to the simultaneous deregulation of several important genes and pathways involved in tumorigenesis. We aimed to explore a few of them with the hope to further explain the mechanisms of NIK-induced survival in PTCL. However, the multifunctional role of NIK observed in this analysis, could not be explained or sustained by the modulation of single genes, and the function of NIK is probably dependent on a coordinated network of signaling pathways where NIK acts as a gatekeeper.

5.2.5 The NF-κB pathway and NIK as therapeutic potentials in lymphomas

Since the observation that NF-κB is involved in the pathogenesis of a range of different cancers, (Davis et al. 2001; Annunziata et al. 2007; DiDonato et al. 2012) investigators have been trying to inhibit the pathway in order to achieve anti-tumor activity. The antitumor activity of NF-κB inhibition can be explained by the ability of NF-κB to evade apoptosis and to promote proliferation and survival(DiDonato et al. 2012). Moreover, NF-κB has been shown to block the apoptotic action of cytotoxic agents, suggesting that the addition of NF-κB inhibitors to chemotherapy regimens would be worth exploring (Baldwin 2001; Al-Katib et al. 2010). In spite of tremendous efforts in clarifying the role of NF-κB in normal biology and disease over the past 25-30 years, no specific NF-κB inhibitor has made its way into the clinical practice. Thus, the need remains to identify novel therapeutic targets in the pathway that can be applied in a relevant characterized subtype of tumors. Likewise, the development of specific NF-κB inhibitor molecules has to progress in the same direction. The

proteasome inhibitor Bortezomib has shown clinical efficacy in some tumors and is currently being used in the treatment of multiple myeloma and relapsed / refractory mantle cell lymphoma(Chen et al. 2011). Several studies suggest that NF-κB plays a key role in the mechanism of action and clinical outcome of Bortezomib (Adams 2004; Chen et al. 2011), although this has been debated (Hideshima et al. 2009). Given the diverse effects of proteasome inhibition, it is difficult to define a clinically relevant mechanism of action of this drug and hence, Bortezomib cannot be considered a true NF-κB inhibitor drug. In the preclinical setting, a large number of publications has investigated the rationale for IKKβ inhibition in various tumors, using different synthetic small molecule inhibitors (Lam et al. 2005; Sors et al. 2008; DiDonato et al. 2012). In spite of the demonstrated efficacy in experimental models, no IKKβ inhibitor has though been clinically approved. A few IKKβ inhibitors have been tested in clinical trials against inflammatory diseases showing, however, a concerning toxicity profile, partly due to the induced expression of IL1-β(Liu et al. 2012). Moreover, a compensatory mechanism activating IKKα has been reported after IKKβ inhibition in ABC-DLBCL(Lam et al. 2008). Novel targets in the NF-κB pathway are now emerging with the hope of a safe and specific anti-tumor response. Inhibitors targeting mutated or aberrantly expressed molecular targets in a particular tumor, might be preferable to broad NF-κB inhibition which also abolishes normal NF-κB activation and potentially present more severe adverse effects. The ideal situation would be an arsenal of different compounds directed against specific molecular targets in the NF-κB pathway, each being uniquely suited for the use in a specific subset of tumors, identified by biomarkers. In line with this, NF-κB has been indirectly inhibited by targeting upstream pathological mechanisms, such as Bruton tyrosine kinase (BTK) in ABC-DLBCL with constitutively active BCR signaling(Davis et al. 2010; Honigberg et al. 2010), or by inhibiting interleukin-1 receptor-associated kinase 4 (IRAK4) in Myd88 driven DLBCL(Ngo et al. 2011).

PTCLs are highly aggressive malignancies that currently lack efficient therapies. We showed that PTCL associated with NF-κB activation, was characterized by an even worse clinical outcome. IKKβ inhibition has previously been proposed as putative treatment strategy in PTCL (Sors et al. 2008). Accordingly, we also observed an increase in apoptosis after IKKß knockdown in PTCL cell lines. IKKα depletion also gave rise to a significant increase in T cell lymphoma cell death, but taken together, the effect of IKK knockdown was weak and p50 and p52 expression still remained after IKK knockdown. Moreover, since IKKβ inhibition presents considerable adverse effect in clinical use, other NF-κB targets would be desirable.

C-Rel was also shown to be a mediator of survival in T cell lymphoma cell lines characterized by NIK overexpression. However, since c-Rel is a transcription factor, the development of a specific inhibitor would be challenging. We propose NIK as a promising molecular target in T cell lymphomas for several reasons. First, NIK is overexpressed in a subset of PTCL cell lines and primary samples. Second, targeting NIK by siRNAs in T cell lymphoma cell lines led to a massive induction of apoptosis. Third, reduced survival upon NIK knockdown was only observed in NIK-overexpressing cells. Forth, NIK was found to be a key regulator of NF-κB expression and was also seen to regulate other important pathways in PTCL pathogenesis. Furthermore, since NIK is a kinase, it is druggable, which facilitates the development of a pharmacological inhibitor. There are still no specific NIK inhibitors available today, although they are in the developmental process in several pharmaceutical companies(Mortier et al. 2010). Moreover, although NIK-deficient mice exhibit defects in lymphoid organogenesis, they do not present any gross phenotypic changes (Yin et al. 2001), suggesting that pharmacologic inhibition of NIK might be safer than broad NF-κB inhibition. Interestingly, our group also identified NIK as one of the key markers for poor response in cutaneous T cell lymphoma patients treated with interferon alpha and photo-chemotherapy, where the gene encoding NIK (MAP3K14) was upregulated in non-responders(Wozniak et al. 2009). This observation suggests that NIK targeting could be interesting to further validate in tumors from patients with poor response to conventional therapy. Clearly, additional studies are required to fully explore the therapeutic potential of NIK, involving in vivo and ex vivo models, as well as the use of pharmaceutical NIK inhibitors. Apparently, NIK is only involved in NF-κB activation in a subset of PTCLs, and the upstream mechanisms leading to the activation of NF-κB in other cases remain to be discovered. Our study, will hopefully provide insight into the mechanisms and importance of NF-κB activation in PTCL, and lead to further validation of NIK as a potential target in NIK-overexpressing PTCL.

5.3 Final remarks and perspectives

The work presented in this doctoral thesis integrates expression studies from human tumor samples with functional experimental models, in order to gain a better insight into the role, regulation and targeting potentials of the NF-κB pathway in lymphomas. However, several open questions and areas of future research remain. The complex expression pattern of NF-κB observed in primary lymphoma tumors is an example and an indication that the simplistic view of NF-κB, usually used in functional studies, is ambiguous. The diverse clinical impacts

and functional roles of the distinct NF-κB members observed in this work, indicate the existence of subunit-specific transcriptional programs. It would be interesting to characterize the transcriptional programs induced by different NF-κB factors in these tumors. The heterogeneous behavior of NF-κB in different tumors highlights the importance of investigating signaling pathways in a context-specific manner, and puts forward the difficulty of extrapolating results between particular tumors and settings. The mechanisms leading to NF-κB activation are diverse and NF-κB interfering strategies have to be evaluated in each tumor subtype. In this manner, we believe that options for NF-κB inhibition in GCB- DLBCL should be explored in future studies. The role of NIK in tumorigenesis, shown by us and by others, will hopefully lead to the development of specific NIK inhibitors that will permit us to fully explore its therapeutic potential. Still, further studies are required, including the use of animal models and patient samples, to validate NIK as a target and to maximize its therapeutic possibilities in PTCL. In order to achieve results with a translational character, there is a need for the development of additional representative T cell lymphoma models. In particular, there is a complete lack of experimental models of PTCL-NOS and AITL, the most commonly occurring T cell lymphoma subtypes in humans. It is also crucial to develop a reliable method for NIK detection, especially in tumor samples, to explore its potential as a predictive biomarker. Additionally, studies discovering the mutational landscape of PTCL are underway, and will hopefully give us new insights into the molecular pathogenesis of these tumors in order to more effectively develop targeted therapies.

6. CONCLUSIONS

1. The expression of NF-κB transcription factors in tumor samples from diffuse large B-cell lymphoma (DLBCL) patients shows a complex and heterogeneous pattern, which differs from prototypic NF-κB signaling.

2. The expression of LMP1 in Epstein-Barr virus-positive DLBCL samples, defines tumors with highly frequent NF-κB activation.

3. No significant correlation was observed between NF-κB expression and molecular subtype of DLBCL. Classical and alternative NF-κB members were extensively expressed in both ABC and GCB subtypes.

4. A subcohort of DLBCL with favorable clinical outcome could be identified based on the nuclear expression of the NF-κB member c-Rel.

5. In peripheral T-cell lymphomas (PTCL), nuclear expression of NF-κB defines a subgroup of patients with significantly shorter overall survival.

6. NIK is overexpressed in a subset of T cell lymphoma cell lines and tumor samples.

7. NIK regulates both classical and alternative NF-κB activation in T cell lymphomas. NIK controls NF-κB signaling at least in part, by IKK-independent mechanisms.

8. NIK is required for T cell lymphoma survival. NIK knockdown led to apoptosis in cells presenting high basal levels of NIK, but not in cells with low NIK expression. NIK knockdown produced a more potent and consistent decrease of PTCL cell viability than IKKβ or IKKα knockdown.

9. The NF-κB member c-Rel is required for survival in NIK-positive PTCL cell lines.

10. NIK controls the expression of multiple genes involved in PTCL survival, such as genes encoding the anti-apoptotic proteins Bcl-XL and c-Flip, the cytokines IL-6 and IL-21, and the tumor suppressor KLF-2. NIK signaling also regulates the activation of the JAK/STAT pathway.

REFERENCES

REFERENCES

Acosta-Alvear, D., Y. Zhou, A. Blais, M. Tsikitis, N. H. Lents, C. Arias, C. J. Lennon, Y. Kluger and B. D. Dynlacht (2007). "XBP1 controls diverse cell type- and condition-specific transcriptional regulatory networks." Mol Cell **27(1):** 53-66.

Adams, J. (2004). "The proteasome: a suitable antineoplastic target." Nat Rev Cancer **4(5):** 349-60.

Akiba, H., H. Nakano, S. Nishinaka, M. Shindo, T. Kobata, M. Atsuta, C. Morimoto, C. F. Ware, N. L. Malinin, D. Wallach, H. Yagita and K. Okumura (1998). "CD27, a member of the tumor necrosis factor receptor superfamily, activates NF-kappaB and stress-activated protein kinase/c-Jun N-terminal kinase via TRAF2, TRAF5, and NF-kappaB-inducing kinase." J Biol Chem **273(21):** 13353-8.

Al-Katib, A., A. A. Arnold, A. Aboukameel, A. Sosin, P. Smith, A. N. Mohamed, F. W. Beck and R. M. Mohammad (2010). "I-kappa-kinase-2 (IKK-2) inhibition potentiates vincristine cytotoxicity in non-Hodgkin's lymphoma." Mol Cancer **9:** 228.

Al-Yacoub, N., L. F. Fecker, M. Mobs, M. Plotz, F. K. Braun, W. Sterry and J. Eberle (2012). "Apoptosis induction by SAHA in cutaneous T-cell lymphoma cells is related to downregulation of c-FLIP and enhanced TRAIL signaling." J Invest Dermatol **132(9):** 2263-74.

Alizadeh, A. A., M. B. Eisen, R. E. Davis, C. Ma, I. S. Lossos, A. Rosenwald, J. C. Boldrick, H. Sabet, T. Tran, X. Yu, J. I. Powell, L. Yang, G. E. Marti, T. Moore, J. Hudson, Jr., L. Lu, D. B. Lewis, R. Tibshirani, G. Sherlock, W. C. Chan, T. C. Greiner, D. D. Weisenburger, J. O. Armitage, R. Warnke, R. Levy, W. Wilson, M. R. Grever, J. C. Byrd, D. Botstein, P. O. Brown and L. M. Staudt (2000). "Distinct types of diffuse large B-cell lymphoma identified by gene expression profiling." Nature **403(6769):** 503-11.

Annunziata, C. M., R. E. Davis, Y. Demchenko, W. Bellamy, A. Gabrea, F. Zhan, G. Lenz, I. Hanamura, G. Wright, W. Xiao, S. Dave, E. M. Hurt, B. Tan, H. Zhao, O. Stephens, M. Santra, D. R. Williams, L. Dang, B. Barlogie, J. D. Shaughnessy, Jr., W. M. Kuehl and L. M. Staudt (2007). "Frequent engagement of the classical and alternative NF-kappaB pathways by diverse genetic abnormalities in multiple myeloma." Cancer Cell **12(2):** 115-30.

Armitage, J. O. (2012). "The aggressive peripheral T-cell lymphomas: 2012 update on diagnosis, risk stratification, and management." Am J Hematol **87(5):** 511-9.

Atkinson, P. G., H. J. Coope, M. Rowe and S. C. Ley (2003). "Latent membrane protein 1 of Epstein-Barr virus stimulates processing of NF-kappa B2 p100 to p52." J Biol Chem **278(51):** 51134-42.

Baldwin, A. S. (2001). "Control of oncogenesis and cancer therapy resistance by the transcription factor NF-kappaB." J Clin Invest **107(3):** 241-6.

Barth, T. F., J. I. Martin-Subero, S. Joos, C. K. Menz, C. Hasel, G. Mechtersheimer, R. M. Parwaresch, P. Lichter, R. Siebert and P. Mooller (2003). "Gains of 2p involving the REL locus correlate with nuclear c-Rel protein accumulation in neoplastic cells of classical Hodgkin lymphoma." Blood **101(9):** 3681-6.

Baud, V. and M. Karin (2009). "Is NF-kappaB a good target for cancer therapy? Hopes and

pitfalls." Nat Rev Drug Discov **8(1):** 33-40. 153

Bavi, P., S. Uddin, R. Bu, M. Ahmed, J. Abubaker, V. Balde, Z. Qadri, D. Ajarim, F. Al-Dayel, A. R. Hussain and K. S. Al-Kuraya (2011). "The biological and clinical impact of inhibition of NF-kappaB-initiated apoptosis in diffuse large B cell lymphoma (DLBCL)." J Pathol **224(3):** 355-66.

Beg, A. A. and D. Baltimore (1996). "An essential role for NF-kappaB in preventing TNF-alpha-induced cell death." Science **274(5288):** 782-4.

Berger, C. L., R. Tigelaar, J. Cohen, K. Mariwalla, J. Trinh, N. Wang and R. L. Edelson (2005). "Cutaneous T-cell lymphoma: malignant proliferation of T-regulatory cells." Blood **105(4):** 1640-7.

Bhattacharya, R., S. Senbanerjee, Z. Lin, S. Mir, A. Hamik, P. Wang, P. Mukherjee, D. Mukhopadhyay and M. K. Jain (2005). "Inhibition of vascular permeability factor/vascular endothelial growth factor-mediated angiogenesis by the Kruppel-like factor KLF2." J Biol Chem **280(32):** 28848-51.

Bonizzi, G. and M. Karin (2004). "The two NF-kappaB activation pathways and their role in innate and adaptive immunity." Trends Immunol **25(6):** 280-8.

Bonzheim, I., E. Geissinger, S. Roth, A. Zettl, A. Marx, A. Rosenwald, H. K. Muller-Hermelink and T. Rudiger (2004). "Anaplastic large cell lymphomas lack the expression of T-cell receptor molecules or molecules of proximal T-cell receptor signaling." Blood **104(10):** 3358-60.

Braun, F. C., P. Grabarczyk, M. Mobs, F. K. Braun, J. Eberle, M. Beyer, W. Sterry, F. Busse, J. Schroder, M. Delin, G. K. Przybylski and C. A. Schmidt (2011). "Tumor suppressor TNFAIP3 (A20) is frequently deleted in Sezary syndrome." Leukemia **25(9):** 1494-501.

Buchan, S. L. and A. Al-Shamkhani (2012). "Distinct motifs in the intracellular domain of human CD30 differentially activate canonical and alternative transcription factor NF-kappaB signaling." PLoS One **7(9):** e45244.

Cabannes, E., G. Khan, F. Aillet, R. F. Jarrett and R. T. Hay (1999). "Mutations in the IkBa gene in Hodgkin's disease suggest a tumour suppressor role for IkappaBalpha." Oncogene **18(20):** 3063-70.

Cahir-McFarland, E. D., D. M. Davidson, S. L. Schauer, J. Duong and E. Kieff (2000). "NF-kappa B inhibition causes spontaneous apoptosis in Epstein-Barr virus-transformed lymphoblastoid cells." Proc Natl Acad Sci U S A **97(11):** 6055-60.

Calfon, M., H. Zeng, F. Urano, J. H. Till, S. R. Hubbard, H. P. Harding, S. G. Clark and D. Ron (2002). "IRE1 couples endoplasmic reticulum load to secretory capacity by processing the XBP-1 mRNA." Nature **415(6867):** 92-6.

Claudio, E., K. Brown, S. Park, H. Wang and U. Siebenlist (2002). "BAFF-induced NEMO-independent processing of NF-kappa B2 in maturing B cells." Nat Immunol **3(10):** 958-65.

Cohen, S., H. Achbert-Weiner and A. Ciechanover (2004). "Dual effects of IkappaB kinase beta-mediated phosphorylation on p105 Fate: SCF(beta-TrCP)-dependent degradation and SCF(beta-TrCP)-independent processing." Mol Cell Biol **24(1):** 475-86.

Coiffier, B. (2007). "Rituximab therapy in malignant lymphoma." Oncogene **26(25):** 3603-13.

Coiffier, B., C. Thieblemont, E. Van Den Neste, G. Lepeu, I. Plantier, S. Castaigne, S. Lefort, G. Marit, M. Macro, C. Sebban, K. Belhadj, D. Bordessoule, C. Ferme and H. Tilly (2010). "Long-term outcome of patients in the LNH-98.5 trial, the first randomized study comparing rituximab-CHOP to standard CHOP chemotherapy in DLBCL patients: a study by the Groupe d'Etudes des Lymphomes de l'Adulte." Blood **116(12):** 2040-5.

Compagno, M., W. K. Lim, A. Grunn, S. V. Nandula, M. Brahmachary, Q. Shen, F. Bertoni, M. Ponzoni, M. Scandurra, A. Califano, G. Bhagat, A. Chadburn, R. Dalla-Favera and L. Pasqualucci (2009). "Mutations of multiple genes cause deregulation of NF-kappaB in diffuse large B-cell lymphoma." Nature **459(7247):** 717-21.

Coope, H. J., P. G. Atkinson, B. Huhse, M. Belich, J. Janzen, M. J. Holman, G. G. Klaus, L. H. Johnston and S. C. Ley (2002). "CD40 regulates the processing of NF-kappaB2 p100 to p52." EMBO J **21(20):** 5375-85.

Costello, R., C. Sanchez, T. Le Treut, P. Rihet, J. Imbert and G. Sebahoun (2010). "Peripheral T-cell lymphoma gene expression profiling and potential therapeutic exploitations." Br J Haematol **150(1):** 21-7.

Curry, C. V., A. A. Ewton, R. J. Olsen, B. R. Logan, H. A. Preti, Y. C. Liu, S. L. Perkins and C. C. Chang (2009). "Prognostic impact of C-REL expression in diffuse large B-cell lymphoma." J Hematop **2(1):** 20-6.

Chang, C. C., J. Zhang, L. Lombardi, A. Neri and R. Dalla-Favera (1995). "Rearranged NFKB-2 genes in lymphoid neoplasms code for constitutively active nuclear transactivators." Mol Cell Biol **15(9):** 5180-7.

Chang, K. L., Y. Y. Chen, D. Shibata and L. M. Weiss (1992). "Description of an in situ hybridization methodology for detection of Epstein-Barr virus RNA in paraffin-embedded tissues, with a survey of normal and neoplastic tissues." Diagn Mol Pathol **1(4):** 246-55.

Chen, D., M. Frezza, S. Schmitt, J. Kanwar and Q. P. Dou (2011). "Bortezomib as the first proteasome inhibitor anticancer drug: current status and future perspectives." Curr Cancer Drug Targets **11(3):** 239-53.

Choi, W. W., D. D. Weisenburger, T. C. Greiner, M. A. Piris, A. H. Banham, J. Delabie, R. M. Braziel, H. Geng, J. Iqbal, G. Lenz, J. M. Vose, C. P. Hans, K. Fu, L. M. Smith, M. Li, Z. Liu, R. D. Gascoyne, A. Rosenwald, G. Ott, L. M. Rimsza, E. Campo, E. S. Jaffe, D. L. Jaye, L. M. Staudt and W. C. Chan (2009). "A new immunostain algorithm classifies diffuse large B-cell lymphoma into molecular subtypes with high accuracy." Clin Cancer Res **15(17):** 5494-502.

Davis, R. E., K. D. Brown, U. Siebenlist and L. M. Staudt (2001). "Constitutive nuclear factor kappaB activity is required for survival of activated B cell-like diffuse large B cell lymphoma cells." J Exp Med **194(12):** 1861-74.

Davis, R. E., V. N. Ngo, G. Lenz, P. Tolar, R. M. Young, P. B. Romesser, H. Kohlhammer, L. Lamy, H. Zhao, Y. Yang, W. Xu, A. L. Shaffer, G. Wright, W. Xiao, J. Powell, J. K. Jiang, C. J. Thomas, A. Rosenwald, G. Ott, H. K. Muller-Hermelink, R. D. Gascoyne, J. M. Connors, N. A. Johnson, L. M. Rimsza, E. Campo, E. S. Jaffe, W. H. Wilson, J. Delabie, E. B. Smeland, R. I. Fisher, R. M. Braziel, R. R. Tubbs, J. R. Cook, D. D. Weisenburger, W. C. Chan, S. K. Pierce and L. M. Staudt (2010). "Chronic active B-cell-receptor signalling in diffuse large B-cell

lymphoma." Nature **463(7277):** 88-92.

de Leon-Boenig, G., K. K. Bowman, J. A. Feng, T. Crawford, C. Everett, Y. Franke, A. Oh, M. Stanley, S. T. Staben, M. A. Starovasnik, H. J. Wallweber, J. Wu, L. C. Wu, A. R. Johnson and S. G. Hymowitz (2012). "The crystal structure of the catalytic domain of the NF-kappaB inducing kinase reveals a narrow but flexible active site." Structure **20(10):** 1704-14.

de Leval, L. and P. Gaulard (2011). "Pathology and biology of peripheral T-cell lymphomas." Histopathology **58(1):** 49-68.

de Leval, L., C. Gisselbrecht and P. Gaulard (2010). "Advances in the understanding and management of angioimmunoblastic T-cell lymphoma." Br J Haematol **148(5):** 673-89.

de Oliveira, D. E., G. Ballon and E. Cesarman (2010). "NF-kappaB signaling modulation by EBV and KSHV." Trends Microbiol **18(6):** 248-57.

Dearden, C. E., R. Johnson, R. Pettengell, S. Devereux, K. Cwynarski, S. Whittaker and A. McMillan (2011). "Guidelines for the management of mature T-cell and NK-cell neoplasms (excluding cutaneous T-cell lymphoma)." Br J Haematol **153(4):** 451-85.

Dejardin, E., N. M. Droin, M. Delhase, E. Haas, Y. Cao, C. Makris, Z. W. Li, M. Karin, C. F. Ware and D. R. Green (2002). "The lymphotoxin-beta receptor induces different patterns of gene expression via two NF-kappaB pathways." Immunity **17(4):** 525-35.

Delhase, M., M. Hayakawa, Y. Chen and M. Karin (1999). "Positive and negative regulation of IkappaB kinase activity through IKKbeta subunit phosphorylation." Science **284(5412):** 309-13.

Derudder, E., A. Laferte, V. Ferreira, Z. Mishal, V. Baud, N. Tarantino and M. Korner (2003). "Identification and characterization of p100HB, a new mutant form of p100/NF-kappa B2." Biochem Biophys Res Commun **308(4):** 744-9.

Devergne, O., E. Hatzivassiliou, K. M. Izumi, K. M. Kaye, M. F. Kleijnen, E. Kieff and G. Mosialos (1996). "Association of TRAF1, TRAF2, and TRAF3 with an Epstein-Barr virus LMP1 domain important for B-lymphocyte transformation: role in NF-kappaB activation." Mol Cell Biol **16(12):** 7098-108.

DiDonato, J. A., F. Mercurio and M. Karin (2012). "NF-kappaB and the link between inflammation and cancer." Immunol Rev **246(1):** 379-400.

Dien Bard, J., P. Gelebart, M. Anand, Z. Zak, S. A. Hegazy, H. M. Amin and R. Lai (2009). "IL-21 contributes to JAK3/STAT3 activation and promotes cell growth in ALK-positive anaplastic large cell lymphoma." Am J Pathol **175(2):** 825-34.

Doppler, H., G. Y. Liou and P. Storz (2013). "Downregulation of TRAF2 mediates NIK-induced pancreatic cancer cell proliferation and tumorigenicity." PLoS One **8(1):** e53676.

Dunleavy, K., W. H. Wilson and E. S. Jaffe (2007). "Angioimmunoblastic T cell lymphoma: pathobiological insights and clinical implications." Curr Opin Hematol **14(4):** 348-53.

Elbashir, S. M., J. Harborth, W. Lendeckel, A. Yalcin, K. Weber and T. Tuschl (2001). "Duplexes of 21-nucleotide RNAs mediate RNA interference in cultured mammalian cells." Nature **411(6836):** 494-8.

Eliopoulos, A. G. and L. S. Young (2001). "LMP1 structure and signal transduction." Semin Cancer Biol **11(6):** 435-44.

Emmerich, F., S. Theurich, M. Hummel, A. Haeffker, M. S. Vry, K. Dohner, K. Bommert, H. Stein and B. Dorken (2003). "Inactivating I kappa B epsilon mutations in Hodgkin/Reed-Sternberg cells." J Pathol **201(3):** 413-20.

Eriksen, K. W., K. Kaltoft, G. Mikkelsen, M. Nielsen, Q. Zhang, C. Geisler, M. H. Nissen, C. Ropke, M. A. Wasik and N. Odum (2001). "Constitutive STAT3-activation in Sezary syndrome: tyrphostin AG490 inhibits STAT3-activation, interleukin-2 receptor expression and growth of leukemic Sezary cells." Leukemia **15(5):** 787-93.

Espinosa, I., J. Briones, R. Bordes, S. Brunet, R. Martino, A. Sureda, J. Sierra and J. Prat (2008). "Activation of the NF-kappaB signalling pathway in diffuse large B-cell lymphoma: clinical implications." Histopathology **53(4):** 441-9.

Fan, C. M. and T. Maniatis (1991). "Generation of p50 subunit of NF-kappa B by processing of p105 through an ATP-dependent pathway." Nature **354(6352):** 395-8.

Ferreri, A. J., S. Govi, S. A. Pileri and K. J. Savage (2012). "Anaplastic large cell lymphoma, ALK-positive." Crit Rev Oncol Hematol **83(2):** 293-302.

Foehr, E. D., J. Bohuslav, L. F. Chen, C. DeNoronha, R. Geleziunas, X. Lin, A. O'Mahony and W. C. Greene (2000). "The NF-kappa B-inducing kinase induces PC12 cell differentiation and prevents apoptosis." J Biol Chem **275(44):** 34021-4.

Forero-Torres, A., J. P. Leonard, A. Younes, J. D. Rosenblatt, P. Brice, N. L. Bartlett, A. Bosly, L. Pinter-Brown, D. Kennedy, E. L. Sievers and A. K. Gopal (2009). "A Phase II study of SGN-30 (anti-CD30 mAb) in Hodgkin lymphoma or systemic anaplastic large cell lymphoma." Br J Haematol **146(2):** 171-9.

Fornari, A., R. Piva, R. Chiarle, D. Novero and G. Inghirami (2009). "Anaplastic large cell lymphoma: one or more entities among T-cell lymphoma?" Hematol Oncol **27(4):** 161-70.

Foss, F. M. (2013). "Treatment strategies for peripheral T-cell lymphomas." Best Pract Res Clin Haematol **26(1):** 43-56.

Foss, F. M., P. L. Zinzani, J. M. Vose, R. D. Gascoyne, S. T. Rosen and K. Tobinai (2011). "Peripheral T-cell lymphoma." Blood **117(25):** 6756-67.

Foss, H. D., I. Anagnostopoulos, I. Araujo, C. Assaf, G. Demel, J. A. Kummer, M. Hummel and H. Stein (1996). "Anaplastic large-cell lymphomas of T-cell and null-cell phenotype express cytotoxic molecules." Blood **88(10):** 4005-11.

Fracchiolla, N. S., L. Lombardi, M. Salina, A. Migliazza, L. Baldini, E. Berti, L. Cro, E. Polli, A. T. Maiolo and A. Neri (1993). "Structural alterations of the NF-kappa B transcription factor lyt-10 in lymphoid malignancies." Oncogene **8(10):** 2839-45.

Gilmore, T. D., C. Cormier, J. Jean-Jacques and M. E. Gapuzan (2001). "Malignant transformation of primary chicken spleen cells by human transcription factor c-Rel." Oncogene **20(48):** 7098-103.

Gilmore, T. D., D. Kalaitzidis, M. C. Liang and D. T. Starczynowski (2004). "The c-Rel

transcription factor and B-cell proliferation: a deal with the devil." Oncogene **23(13):** 2275-86.

Grivennikov, S., E. Karin, J. Terzic, D. Mucida, G. Y. Yu, S. Vallabhapurapu, J. Scheller, S. Rose-John, H. Cheroutre, L. Eckmann and M. Karin (2009). "IL-6 and Stat3 are required for survival of intestinal epithelial cells and development of colitis-associated cancer." Cancer Cell **15(2):** 103-13.

Hanahan, D. and R. A. Weinberg (2000). "The hallmarks of cancer." Cell **100(1):** 57-70. Hanahan, D. and R. A. Weinberg (2011). "Hallmarks of cancer: the next generation." Cell

144(5): 646-74.

Hans, C. P., D. D. Weisenburger, T. C. Greiner, R. D. Gascoyne, J. Delabie, G. Ott, H. K. Muller-Hermelink, E. Campo, R. M. Braziel, E. S. Jaffe, Z. Pan, P. Farinha, L. M. Smith, B. Falini, A. H. Banham, A. Rosenwald, L. M. Staudt, J. M. Connors, J. O. Armitage and W. C. Chan (2004). "Confirmation of the molecular classification of diffuse large B-cell lymphoma by immunohistochemistry using a tissue microarray." Blood **103(1):** 275-82.

Hartmann, S., S. Gesk, R. Scholtysik, M. Kreuz, S. Bug, I. Vater, C. Doring, S. Cogliatti, M. Parrens, J. P. Merlio, A. Kwiecinska, A. Porwit, P. P. Piccaluga, S. Pileri, G. Hoefler, R. Kuppers, R. Siebert and M. L. Hansmann (2010). "High resolution SNP array genomic profiling of peripheral T cell lymphomas, not otherwise specified, identifies a subgroup with chromosomal aberrations affecting the REL locus." Br J Haematol **148(3):** 402-12.

Hayden, M. S. and S. Ghosh (2008). "Shared principles in NF-kappaB signaling." Cell **132(3):** 344-62.

Hayden, M. S. and S. Ghosh (2011). "NF-kappaB in immunobiology." Cell Res **21(2):** 223-44. Hayden, M. S. and S. Ghosh (2012). "NF-kappaB, the first quarter-century: remarkable

progress and outstanding questions." Genes Dev **26(3):** 203-34.

He, J. Q., B. Zarnegar, G. Oganesyan, S. K. Saha, S. Yamazaki, S. E. Doyle, P. W. Dempsey and G. Cheng (2006). "Rescue of TRAF3-null mice by p100 NF-kappa B deficiency." J Exp Med **203(11):** 2413-8.

He, Y., S. Sun, H. Sha, Z. Liu, L. Yang, Z. Xue, H. Chen and L. Qi (2010). "Emerging roles for XBP1, a sUPeR transcription factor." Gene Expr **15(1):** 13-25.

He, Z., B. Xin, X. Yang, C. Chan and L. Cao (2000). "Nuclear factor-kappaB activation is involved in LMP1-mediated transformation and tumorigenesis of rat-1 fibroblasts." Cancer Res **60(7):** 1845-8.

Hernandez-Ilizaliturri, F. J., G. Deeb, P. L. Zinzani, S. A. Pileri, F. Malik, W. R. Macon, A. Goy, T. E. Witzig and M. S. Czuczman (2011). "Higher response to lenalidomide in relapsed/refractory diffuse large B-cell lymphoma in nongerminal center B-cell-like than in germinal center B-cell-like phenotype." Cancer **117(22):** 5058-66.

Herreros, B., A. Sanchez-Aguilera and M. A. Piris (2008). "Lymphoma microenvironment: culprit or innocent?" Leukemia **22(1):** 49-58.

Hideshima, T., H. Ikeda, D. Chauhan, Y. Okawa, N. Raje, K. Podar, C. Mitsiades, N. C. Munshi,

P. G. Richardson, R. D. Carrasco and K. C. Anderson (2009). "Bortezomib induces canonical nuclear factor-kappaB activation in multiple myeloma cells." Blood **114(5):** 1046-52.

Hoffmann, A. and D. Baltimore (2006). "Circuitry of nuclear factor kappaB signaling." Immunol Rev **210:** 171-86.

Hoffmann, A., G. Natoli and G. Ghosh (2006). "Transcriptional regulation via the NF-kappaB signaling module." Oncogene **25(51):** 6706-16.

Honigberg, L. A., A. M. Smith, M. Sirisawad, E. Verner, D. Loury, B. Chang, S. Li, Z. Pan, D. H. Thamm, R. A. Miller and J. J. Buggy (2010). "The Bruton tyrosine kinase inhibitor PCI-32765 blocks B-cell activation and is efficacious in models of autoimmune disease and B-cell malignancy." Proc Natl Acad Sci U S A **107(29):** 13075-80.

Honma, K., S. Tsuzuki, M. Nakagawa, H. Tagawa, S. Nakamura, Y. Morishima and M. Seto (2009). "TNFAIP3/A20 functions as a novel tumor suppressor gene in several subtypes of non-Hodgkin lymphomas." Blood **114(12):** 2467-75.

Hostager, B. S., S. A. Haxhinasto, S. L. Rowland and G. A. Bishop (2003). "Tumor necrosis factor receptor-associated factor 2 (TRAF2)-deficient B lymphocytes reveal novel roles for TRAF2 in CD40 signaling." J Biol Chem **278(46):** 45382-90.

Houldsworth, J., A. B. Olshen, G. Cattoretti, G. B. Donnelly, J. Teruya-Feldstein, J. Qin, N. Palanisamy, Y. Shen, K. Dyomina, M. Petlakh, Q. Pan, A. D. Zelenetz, R. Dalla-Favera and R. S. Chaganti (2004). "Relationship between REL amplification, REL function, and clinical and biologic features in diffuse large B-cell lymphomas." Blood **103(5):** 1862-8.

Hu, S., Z. Y. Xu-Monette, A. Balasubramanyam, G. C. Manyam, C. Visco, A. Tzankov, W. M. Liu, R. N. Miranda, L. Zhang, S. Montes-Moreno, K. Dybkaer, A. Chiu, A. Orazi, Y. Zu, G. Bhagat, K. L. Richards, E. D. Hsi, W. W. Choi, J. Han van Krieken, Q. Huang, J. Huh, W. Ai, M. Ponzoni, A. J. Ferreri, X. Zhao, J. N. Winter, M. Zhang, L. Li, M. B. Moller, M. A. Piris, Y. Li, R. S. Go, L. Wu, L. J. Medeiros and K. H. Young (2013). "CD30 expression defines a novel subgroup of diffuse large B-cell lymphoma with favorable prognosis and distinct gene expression signature: a report from the International DLBCL Rituximab-CHOP Consortium Program Study." Blood **121(14):** 2715-24.

Huang, S., C. A. Pettaway, H. Uehara, C. D. Bucana and I. J. Fidler (2001). "Blockade of NF-kappaB activity in human prostate cancer cells is associated with suppression of angiogenesis, invasion, and metastasis." Oncogene **20(31):** 4188-97.

Hwang, S. T., J. E. Janik, E. S. Jaffe and W. H. Wilson (2008). "Mycosis fungoides and Sezary syndrome." Lancet **371(9616):** 945-57.

Iqbal, J., D. D. Weisenburger, T. C. Greiner, J. M. Vose, T. McKeithan, C. Kucuk, H. Geng, K. Deffenbacher, L. Smith, K. Dybkaer, S. Nakamura, M. Seto, J. Delabie, F. Berger, F. Loong, W. Y. Au, Y. H. Ko, I. Sng, J. O. Armitage and W. C. Chan (2010). "Molecular signatures to improve diagnosis in peripheral T-cell lymphoma and prognostication in angioimmunoblastic T-cell lymphoma." Blood **115(5):** 1026-36.

Izban, K. F., M. Ergin, J. Z. Qin, R. L. Martinez, R. J. Pooley, S. Saeed and S. Alkan (2000). "Constitutive expression of NF-kappa B is a characteristic feature of mycosis fungoides: implications for apoptosis resistance and pathogenesis." Hum Pathol **31(12):** 1482-90.

Jost, P. J. and J. Ruland (2007). "Aberrant NF-kappaB signaling in lymphoma: mechanisms, consequences, and therapeutic implications." Blood **109(7):** 2700-7.

Joyce, D., C. Albanese, J. Steer, M. Fu, B. Bouzahzah and R. G. Pestell (2001). "NF-kappaB and cell-cycle regulation: the cyclin connection." Cytokine Growth Factor Rev **12(1):** 73-90.

Jung, J. T., D. H. Kim, E. K. Kwak, J. G. Kim, T. I. Park, S. K. Sohn, Y. R. Do, K. Y. Kwon, H. S. Song, E. H. Park and K. B. Lee (2006). "Clinical role of Bcl-2, Bax, or p53 overexpression in peripheral T-cell lymphomas." Ann Hematol **85(9):** 575-81.

Kajiura, F., S. Sun, T. Nomura, K. Izumi, T. Ueno, Y. Bando, N. Kuroda, H. Han, Y. Li, A. Matsushima, Y. Takahama, S. Sakaguchi, T. Mitani and M. Matsumoto (2004). "NF-kappa B-inducing kinase establishes self-tolerance in a thymic stroma-dependent manner." J Immunol **172(4):** 2067-75.

Kallioniemi, O. P., U. Wagner, J. Kononen and G. Sauter (2001). "Tissue microarray technology for high-throughput molecular profiling of cancer." Hum Mol Genet **10(7):** 657-62.

Karin, M. and Y. Ben-Neriah (2000). "Phosphorylation meets ubiquitination: the control of NF-[kappa]B activity." Annu Rev Immunol **18:** 621-63.

Kaye, K. M., K. M. Izumi and E. Kieff (1993). "Epstein-Barr virus latent membrane protein 1 is essential for B-lymphocyte growth transformation." Proc Natl Acad Sci U S A **90(19):** 9150-4.

Keats, J. J., R. Fonseca, M. Chesi, R. Schop, A. Baker, W. J. Chng, S. Van Wier, R. Tiedemann, C. X. Shi, M. Sebag, E. Braggio, T. Henry, Y. X. Zhu, H. Fogle, T. Price-Troska, G. Ahmann, C. Mancini, L. A. Brents, S. Kumar, P. Greipp, A. Dispenzieri, B. Bryant, G. Mulligan, L. Bruhn, M. Barrett, R. Valdez, J. Trent, A. K. Stewart, J. Carpten and P. L. Bergsagel (2007). "Promiscuous mutations activate the noncanonical NF-kappaB pathway in multiple myeloma." Cancer Cell **12(2):** 131-44.

Keller, S. A., D. Hernandez-Hopkins, J. Vider, V. Ponomarev, E. Hyjek, E. J. Schattner and E. Cesarman (2006). "NF-kappaB is essential for the progression of KSHV- and EBV-infected lymphomas in vivo." Blood **107(8):** 3295-302.

Kelly, S., Z. J. Zhang, H. Zhao, L. Xu, R. G. Giffard, R. M. Sapolsky, M. A. Yenari and G. K. Steinberg (2002). "Gene transfer of HSP72 protects cornu ammonis 1 region of the hippocampus neurons from global ischemia: influence of Bcl-2." Ann Neurol **52(2):** 160-7.

Kreuz, S., D. Siegmund, P. Scheurich and H. Wajant (2001). "NF-kappaB inducers upregulate cFLIP, a cycloheximide-sensitive inhibitor of death receptor signaling." Mol Cell Biol **21(12):** 3964-73.

Kutok, J. L. and F. Wang (2006). "Spectrum of Epstein-Barr virus-associated diseases." Annu Rev Pathol **1:** 375-404.

Lam, L. T., R. E. Davis, V. N. Ngo, G. Lenz, G. Wright, W. Xu, H. Zhao, X. Yu, L. Dang and L. M. Staudt (2008). "Compensatory IKKalpha activation of classical NF-kappaB signaling during IKKbeta inhibition identified by an RNA interference sensitization screen." Proc Natl Acad Sci U S A **105(52):** 20798-803.

Lam, L. T., R. E. Davis, J. Pierce, M. Hepperle, Y. Xu, M. Hottelet, Y. Nong, D. Wen, J. Adams, L.

Dang and L. M. Staudt (2005). "Small molecule inhibitors of IkappaB kinase are selectively toxic for subgroups of diffuse large B-cell lymphoma defined by gene expression profiling." Clin Cancer Res **11(1):** 28-40.

Lamant, L., A. de Reynies, M. M. Duplantier, D. S. Rickman, F. Sabourdy, S. Giuriato, L. Brugieres, P. Gaulard, E. Espinos and G. Delsol (2007). "Gene-expression profiling of systemic anaplastic large-cell lymphoma reveals differences based on ALK status and two distinct morphologic ALK+ subtypes." Blood **109(5):** 2156-64.

Landau, D. A., S. L. Carter, P. Stojanov, A. McKenna, K. Stevenson, M. S. Lawrence, C. Sougnez, C. Stewart, A. Sivachenko, L. Wang, Y. Wan, W. Zhang, S. A. Shukla, A. Vartanov, S. M. Fernandes, G. Saksena, K. Cibulskis, B. Tesar, S. Gabriel, N. Hacohen, M. Meyerson, E. S. Lander, D. Neuberg, J. R. Brown, G. Getz and C. J. Wu (2013). "Evolution and impact of subclonal mutations in chronic lymphocytic leukemia." Cell **152(4):** 714-26.

Lenz, G., R. E. Davis, V. N. Ngo, L. Lam, T. C. George, G. W. Wright, S. S. Dave, H. Zhao, W. Xu, A. Rosenwald, G. Ott, H. K. Muller-Hermelink, R. D. Gascoyne, J. M. Connors, L. M. Rimsza, E. Campo, E. S. Jaffe, J. Delabie, E. B. Smeland, R. I. Fisher, W. C. Chan and L. M. Staudt (2008). "Oncogenic CARD11 mutations in human diffuse large B cell lymphoma." Science **319(5870):** 1676-9.

Lenz, G. and L. M. Staudt (2010). "Aggressive lymphomas." N Engl J Med **362(15):** 1417-29.

Lenz, G., G. W. Wright, N. C. Emre, H. Kohlhammer, S. S. Dave, R. E. Davis, S. Carty, L. T. Lam, A. L. Shaffer, W. Xiao, J. Powell, A. Rosenwald, G. Ott, H. K. Muller-Hermelink, R. D. Gascoyne, J. M. Connors, E. Campo, E. S. Jaffe, J. Delabie, E. B. Smeland, L. M. Rimsza, R. I. Fisher, D. D. Weisenburger, W. C. Chan and L. M. Staudt (2008). "Molecular subtypes of diffuse large B-cell lymphoma arise by distinct genetic pathways." Proc Natl Acad Sci U S A **105(36):** 13520-5.

Li, Q. and I. M. Verma (2002). "NF-kappaB regulation in the immune system." Nat Rev Immunol **2(10):** 725-34.

Li, Z. W., W. Chu, Y. Hu, M. Delhase, T. Deerinck, M. Ellisman, R. Johnson and M. Karin (1999). "The IKKbeta subunit of IkappaB kinase (IKK) is essential for nuclear factor kappaB activation and prevention of apoptosis." J Exp Med **189(11):** 1839-45.

Liang, C., M. Zhang and S. C. Sun (2006). "beta-TrCP binding and processing of NF-kappaB2/p100 involve its phosphorylation at serines 866 and 870." Cell Signal **18(8):** 1309-17.

Liao, G., M. Zhang, E. W. Harhaj and S. C. Sun (2004). "Regulation of the NF-kappaB-inducing kinase by tumor necrosis factor receptor-associated factor 3-induced degradation." J Biol Chem **279(25):** 26243-50.

Libermann, T. A. and D. Baltimore (1990). "Activation of interleukin-6 gene expression through the NF-kappa B transcription factor." Mol Cell Biol **10(5):** 2327-34.

Lin, S. C., J. Y. Chung, B. Lamothe, K. Rajashankar, M. Lu, Y. C. Lo, A. Y. Lam, B. G. Darnay and H. Wu (2008). "Molecular basis for the unique deubiquitinating activity of the NF-kappaB inhibitor A20." J Mol Biol **376(2):** 526-40.

Lin, X., Y. Mu, E. T. Cunningham, Jr., K. B. Marcu, R. Geleziunas and W. C. Greene (1998). "Molecular determinants of NF-kappaB-inducing kinase action." Mol Cell Biol **18(10):** 5899-

907.

Ling, L., Z. Cao and D. V. Goeddel (1998). "NF-kappaB-inducing kinase activates IKK-alpha by phosphorylation of Ser-176." Proc Natl Acad Sci U S A **95(7):** 3792-7.

Liou, H. C., M. R. Boothby, P. W. Finn, R. Davidon, N. Nabavi, N. J. Zeleznik-Le, J. P. Ting and L. H. Glimcher (1990). "A new member of the leucine zipper class of proteins that binds to the HLA DR alpha promoter." Science **247(4950):** 1581-4.

Liu, F., Y. Xia, A. S. Parker and I. M. Verma (2012). "IKK biology." Immunol Rev **246(1):** 239-53.

Liu, J., A. Sudom, X. Min, Z. Cao, X. Gao, M. Ayres, F. Lee, P. Cao, S. Johnstone, O. Plotnikova, N. Walker, G. Chen and Z. Wang (2012). "Structure of the nuclear factor kappaB-inducing kinase (NIK) kinase domain reveals a constitutively active conformation." J Biol Chem **287(33):** 27326-34.

Lohr, J. G., P. Stojanov, M. S. Lawrence, D. Auclair, B. Chapuy, C. Sougnez, P. Cruz-Gordillo, B. Knoechel, Y. W. Asmann, S. L. Slager, A. J. Novak, A. Dogan, S. M. Ansell, B. K. Link, L. Zou, J. Gould, G. Saksena, N. Stransky, C. Rangel-Escareno, J. C. Fernandez-Lopez, A. Hidalgo-Miranda, J. Melendez-Zajgla, E. Hernandez-Lemus, A. Schwarz-Cruz y Celis, I. Imaz-Rosshandler, A. I. Ojesina, J. Jung, C. S. Pedamallu, E. S. Lander, T. M. Habermann, J. R. Cerhan, M. A. Shipp, G. Getz and T. R. Golub (2012). "Discovery and prioritization of somatic mutations in diffuse large B-cell lymphoma (DLBCL) by whole-exome sequencing." Proc Natl Acad Sci U S A **109(10):** 3879-84.

Lowry, O. H., N. J. Rosebrough, A. L. Farr and R. J. Randall (1951). "Protein measurement with the Folin phenol reagent." J Biol Chem **193(1):** 265-75.

Lucas, P. C., M. Yonezumi, N. Inohara, L. M. McAllister-Lucas, M. E. Abazeed, F. F. Chen, S. Yamaoka, M. Seto and G. Nunez (2001). "Bcl10 and MALT1, independent targets of chromosomal translocation in malt lymphoma, cooperate in a novel NF-kappa B signaling pathway." J Biol Chem **276(22):** 19012-9.

Luftig, M., T. Yasui, V. Soni, M. S. Kang, N. Jacobson, E. Cahir-McFarland, B. Seed and E. Kieff (2004). "Epstein-Barr virus latent infection membrane protein 1 TRAF-binding site induces NIK/IKK alpha-dependent noncanonical NF-kappaB activation." Proc Natl Acad Sci U S A **101(1):** 141-6.

Ma, J., D. Ma and C. Ji (2011). "The role of IL-21 in hematological malignancies." Cytokine **56(2):** 133-9.

Malinin, N. L., M. P. Boldin, A. V. Kovalenko and D. Wallach (1997). "MAP3K-related kinase involved in NF-kappaB induction by TNF, CD95 and IL-1." Nature **385(6616):** 540-4.

Mandelbaum, J., G. Bhagat, H. Tang, T. Mo, M. Brahmachary, Q. Shen, A. Chadburn, K. Rajewsky, A. Tarakhovsky, L. Pasqualucci and R. Dalla-Favera (2010). "BLIMP1 is a tumor suppressor gene frequently disrupted in activated B cell-like diffuse large B cell lymphoma." Cancer Cell **18(6):** 568-79.

Martin-Sanchez, E., S. M. Rodriguez-Pinilla, M. Sanchez-Beato, L. Lombardia, B. Dominguez-Gonzalez, D. Romero, L. Odqvist, P. Garcia-Sanz, M. B. Wozniak, G. Kurz, C. Blanco-Aparicio, M. Mollejo, F. J. Alves, J. Menarguez, F. Gonzalez-Palacios, J. L. Rodriguez-Peralto, P. L. Ortiz-

Romero, J. F. Garcia, J. R. Bischoff and M. A. Piris (2013). "Simultaneous inhibition of pan-phosphatidylinositol-3-kinases and MEK as a potential therapeutic strategy in peripheral T-cell lymphomas." Haematologica **98(1):** 57-64.
Martin-Subero, J. I., S. Gesk, L. Harder, T. Sonoki, P. W. Tucker, B. Schlegelberger, W. Grote, F. J. Novo, M. J. Calasanz, M. L. Hansmann, M. J. Dyer and R. Siebert (2002). "Recurrent involvement of the REL and BCL11A loci in classical Hodgkin lymphoma." Blood **99(4):** 1474-7.

Martinez-Delgado, B., M. Cuadros, E. Honrado, A. Ruiz de la Parte, G. Roncador, J. Alves, J. M. Castrillo, C. Rivas and J. Benitez (2005). "Differential expression of NF-kappaB pathway genes among peripheral T-cell lymphomas." Leukemia **19(12):** 2254-63.

Marzec, M., K. Halasa, M. Kasprzycka, M. Wysocka, X. Liu, J. W. Tobias, D. Baldwin, Q. Zhang, N. Odum, A. H. Rook and M. A. Wasik (2008). "Differential effects of interleukin-2 and interleukin-15 versus interleukin-21 on CD4+ cutaneous T-cell lymphoma cells." Cancer Res **68(4):** 1083-91.

McConkey, D. J. and K. Zhu (2008). "Mechanisms of proteasome inhibitor action and resistance in cancer." Drug Resist Updat **11(4-5):** 164-79.

McCusker, M. E., M. Garifallou and S. A. Bogen (1997). "Sezary lineage cells can be induced to proliferate via CD28-mediated costimulation." J Immunol **158(10):** 4984-91.

Meier, C., S. Hoeller, C. Bourgau, P. Hirschmann, J. Schwaller, P. Went, S. A. Pileri, A. Reiter, S. Dirnhofer and A. Tzankov (2009). "Recurrent numerical aberrations of JAK2 and deregulation of the JAK2-STAT cascade in lymphomas." Mod Pathol **22(3):** 476-87.

Mimura, N., M. Fulciniti, G. Gorgun, Y. T. Tai, D. Cirstea, L. Santo, Y. Hu, C. Fabre, J. Minami, H. Ohguchi, T. Kiziltepe, H. Ikeda, Y. Kawano, M. French, M. Blumenthal, V. Tam, N. L. Kertesz, U. M. Malyankar, M. Hokenson, T. Pham, Q. Zeng, J. B. Patterson, P. G. Richardson, N. C. Munshi and K. C. Anderson (2012). "Blockade of XBP1 splicing by inhibition of IRE1alpha is a promising therapeutic option in multiple myeloma." Blood **119(24):** 5772-81.

Montes-Moreno, S., L. Odqvist, J. A. Diaz-Perez, A. B. Lopez, S. G. de Villambrosia, F. Mazorra, M. E. Castillo, M. Lopez, R. Pajares, J. F. Garcia, M. Mollejo, F. I. Camacho, C. Ruiz- Marcellan, M. Adrados, N. Ortiz, R. Franco, C. Ortiz-Hidalgo, A. Suarez-Gauthier, K. H. Young and M. A. Piris (2012). "EBV-positive diffuse large B-cell lymphoma of the elderly is an aggressive post-germinal center B-cell neoplasm characterized by prominent nuclear factor- kB activation." Mod Pathol **25(7):** 968-82.

Morales, D., B. Beltran, F. H. De Mendoza, L. Riva, A. Yabar, P. Quinones, J. N. Butera and J. Castillo (2010). "Epstein-Barr virus as a prognostic factor in de novo nodal diffuse large B-cell lymphoma." Leuk Lymphoma **51(1):** 66-72.

Morin, R. D., M. Mendez-Lago, A. J. Mungall, R. Goya, K. L. Mungall, R. D. Corbett, N. A. Johnson, T. M. Severson, R. Chiu, M. Field, S. Jackman, M. Krzywinski, D. W. Scott, D. L. Trinh, J. Tamura-Wells, S. Li, M. R. Firme, S. Rogic, M. Griffith, S. Chan, O. Yakovenko, I. M. Meyer, E. Y. Zhao, D. Smailus, M. Moksa, S. Chittaranjan, L. Rimsza, A. Brooks-Wilson, J. J. Spinelli, S. Ben-Neriah, B. Meissner, B. Woolcock, M. Boyle, H. McDonald, A. Tam, Y. Zhao, A. Delaney,T. Zeng, K. Tse, Y. Butterfield, I. Birol, R. Holt, J. Schein, D. E. Horsman, R. Moore, S. J. Jones, J. M. Connors, M. Hirst, R. D. Gascoyne and M. A. Marra (2011). "Frequent mutation of histone-modifying genes in non-Hodgkin lymphoma." Nature **476(7360):** 298-303.

Morris, S. W., M. N. Kirstein, M. B. Valentine, K. G. Dittmer, D. N. Shapiro, D. L. Saltman and A. T. Look (1994). "Fusion of a kinase gene, ALK, to a nucleolar protein gene, NPM, in non-Hodgkin's lymphoma." Science **263(5151):** 1281-4.

Mortier, J., B. Masereel, C. Remouchamps, C. Ganeff, J. Piette and R. Frederick (2010). "NF-kappaB inducing kinase (NIK) inhibitors: identification of new scaffolds using virtual screening." Bioorg Med Chem Lett **20(15):** 4515-20.

Morton, L. M., S. S. Wang, S. S. Devesa, P. Hartge, D. D. Weisenburger and M. S. Linet (2006). "Lymphoma incidence patterns by WHO subtype in the United States, 1992-2001." Blood **107(1):** 265-76.

Nadiminty, N., J. Y. Chun, Y. Hu, S. Dutt, X. Lin and A. C. Gao (2007). "LIGHT, a member of the TNF superfamily, activates Stat3 mediated by NIK pathway." Biochem Biophys Res Commun **359(2):** 379-84.

Navas, I. C., P. L. Ortiz-Romero, R. Villuendas, P. Martinez, C. Garcia, E. Gomez, J. L. Rodriguez, D. Garcia, F. Vanaclocha, L. Iglesias, M. A. Piris and P. Algara (2000). "p16(INK4a) gene alterations are frequent in lesions of mycosis fungoides." Am J Pathol **156(5):** 1565-72.

Neri, A., C. C. Chang, L. Lombardi, M. Salina, P. Corradini, A. T. Maiolo, R. S. Chaganti and R. Dalla-Favera (1991). "B cell lymphoma-associated chromosomal translocation involves candidate oncogene lyt-10, homologous to NF-kappa B p50." Cell **67(6):** 1075-87.

Ngo, V. N., R. M. Young, R. Schmitz, S. Jhavar, W. Xiao, K. H. Lim, H. Kohlhammer, W. Xu, Y. Yang, H. Zhao, A. L. Shaffer, P. Romesser, G. Wright, J. Powell, A. Rosenwald, H. K. Muller-Hermelink, G. Ott, R. D. Gascoyne, J. M. Connors, L. M. Rimsza, E. Campo, E. S. Jaffe, J. Delabie, E. B. Smeland, R. I. Fisher, R. M. Braziel, R. R. Tubbs, J. R. Cook, D. D. Weisenburger, W. C. Chan and L. M. Staudt (2011). "Oncogenically active MYD88 mutations in human lymphoma." Nature **470(7332):** 115-9.

Nielsen, M., C. G. Kaestel, K. W. Eriksen, A. Woetmann, T. Stokkedal, K. Kaltoft, C. Geisler, C. Ropke and N. Odum (1999). "Inhibition of constitutively activated Stat3 correlates with altered Bcl-2/Bax expression and induction of apoptosis in mycosis fungoides tumor cells." Leukemia **13(5):** 735-8.

Nishina, T., N. Yamaguchi, J. Gohda, K. Semba and J. Inoue (2009). "NIK is involved in constitutive activation of the alternative NF-kappaB pathway and proliferation of pancreatic cancer cells." Biochem Biophys Res Commun **388(1):** 96-101.

Novack, D. V. (2011). "Role of NF-kappaB in the skeleton." Cell Res **21(1):** 169-82.

Novack, D. V., L. Yin, A. Hagen-Stapleton, R. D. Schreiber, D. V. Goeddel, F. P. Ross and S. L. Teitelbaum (2003). "The IkappaB function of NF-kappaB2 p100 controls stimulated osteoclastogenesis." J Exp Med **198(5):** 771-81.

Novelli, S., J. Briones and J. Sierra (2013). "Epidemiology of lymphoid malignancies: last decade update." Springerplus **2(1):** 70.

Odqvist, L., M. Sanchez-Beato, S. Montes-Moreno, E. Martin-Sanchez, R. Pajares, L. Sanchez-Verde, P. L. Ortiz-Romero, J. Rodriguez, S. M. Rodriguez-Pinilla, F. Iniesta-Martinez, J. C. Solera-Arroyo, R. Ramos-Asensio, T. Flores, J. M. Palanca, F. G. Bragado, P. D. Franjo and M. A. Piris (2013). "NIK controls classical and alternative NF-kappaB activation and is necessary

for the survival of human T-cell lymphoma cells." Clin Cancer Res **19(9):** 2319-30.

Oeckinghaus, A. and S. Ghosh (2009). "The NF-kappaB family of transcription factors and its regulation." Cold Spring Harb Perspect Biol **1(4):** a000034.

Otto, C., M. Giefing, A. Massow, I. Vater, S. Gesk, M. Schlesner, J. Richter, W. Klapper, M. L. Hansmann, R. Siebert and R. Kuppers (2012). "Genetic lesions of the TRAF3 and MAP3K14 genes in classical Hodgkin lymphoma." Br J Haematol **157(6):** 702-8.

Oyarzo, M. P., L. J. Medeiros, C. Atwell, M. Feretzaki, V. Leventaki, E. Drakos, H. M. Amin and G. Z. Rassidakis (2006). "c-FLIP confers resistance to FAS-mediated apoptosis in anaplastic large-cell lymphoma." Blood **107(6):** 2544-7.

Palombella, V. J., O. J. Rando, A. L. Goldberg and T. Maniatis (1994). "The ubiquitin-proteasome pathway is required for processing the NF-kappa B1 precursor protein and the activation of NF-kappa B." Cell **78(5):** 773-85.

Park, S., J. Lee, Y. H. Ko, A. Han, H. J. Jun, S. C. Lee, I. G. Hwang, Y. H. Park, J. S. Ahn, C. W. Jung, K. Kim, Y. C. Ahn, W. K. Kang, K. Park and W. S. Kim (2007). "The impact of Epstein-Barr virus status on clinical outcome in diffuse large B-cell lymphoma." Blood **110(3):** 972-8.

Pasqualucci, L., O. Bereschenko, H. Niu, U. Klein, K. Basso, R. Guglielmino, G. Cattoretti and R. Dalla-Favera (2003). "Molecular pathogenesis of non-Hodgkin's lymphoma: the role of Bcl-6." Leuk Lymphoma **44 Suppl 3:** S5-12.

Pasqualucci, L., V. Trifonov, G. Fabbri, J. Ma, D. Rossi, A. Chiarenza, V. A. Wells, A. Grunn, M. Messina, O. Elliot, J. Chan, G. Bhagat, A. Chadburn, G. Gaidano, C. G. Mullighan, R. Rabadan and R. Dalla-Favera (2011). "Analysis of the coding genome of diffuse large B-cell lymphoma." Nat Genet **43(9):** 830-7.

Pescarmona, E., P. Pignoloni, M. Puopolo, M. Martelli, M. Addesso, C. Guglielmi and C. D. Baroni (2001). "p53 over-expression identifies a subset of nodal peripheral T-cell lymphomas with a distinctive biological profile and poor clinical outcome." J Pathol **195(3):** 361-6.

Pham, L. V., L. Fu, A. T. Tamayo, C. Bueso-Ramos, E. Drakos, F. Vega, L. J. Medeiros and R. J. Ford (2011). "Constitutive BR3 receptor signaling in diffuse, large B-cell lymphomas stabilizes nuclear factor-kappaB-inducing kinase while activating both canonical and alternative nuclear factor-kappaB pathways." Blood **117(1):** 200-10.

Piccaluga, P. P., C. Agostinelli, A. Califano, A. Carbone, L. Fantoni, S. Ferrari, A. Gazzola, A. Gloghini, S. Righi, M. Rossi, E. Tagliafico, P. L. Zinzani, S. Zupo, M. Baccarani and S. A. Pileri (2007). "Gene expression analysis of angioimmunoblastic lymphoma indicates derivation from T follicular helper cells and vascular endothelial growth factor deregulation." Cancer Res **67(22):** 10703-10.

Piccaluga, P. P., C. Agostinelli, A. Califano, M. Rossi, K. Basso, S. Zupo, P. Went, U. Klein, P. L. Zinzani, M. Baccarani, R. Dalla Favera and S. A. Pileri (2007). "Gene expression analysis of peripheral T cell lymphoma, unspecified, reveals distinct profiles and new potential therapeutic targets." J Clin Invest **117(3):** 823-34.

Piccaluga, P. P., C. Agostinelli, C. Tripodo, A. Gazzola, F. Bacci, E. Sabattini and S. A. Pileri (2011). "Peripheral T-cell lymphoma classification: the matter of cellular derivation." Expert Rev Hematol **4(4):** 415-25.

Pradhan, M., S. C. Baumgarten, L. A. Bembinster and J. Frasor (2012). "CBP mediates NF-kappaB-dependent histone acetylation and estrogen receptor recruitment to an estrogen response element in the BIRC3 promoter." Mol Cell Biol **32(2):** 569-75.

Puente, X. S., M. Pinyol, V. Quesada, L. Conde, G. R. Ordonez, N. Villamor, G. Escaramis, P. Jares, S. Bea, M. Gonzalez-Diaz, L. Bassaganyas, T. Baumann, M. Juan, M. Lopez-Guerra, D. Colomer, J. M. Tubio, C. Lopez, A. Navarro, C. Tornador, M. Aymerich, M. Rozman, J. M. Hernandez, D. A. Puente, J. M. Freije, G. Velasco, A. Gutierrez-Fernandez, D. Costa, A. Carrio, S. Guijarro, A. Enjuanes, L. Hernandez, J. Yague, P. Nicolas, C. M. Romeo-Casabona, H. Himmelbauer, E. Castillo, J. C. Dohm, S. de Sanjose, M. A. Piris, E. de Alava, J. San Miguel, R. Royo, J. L. Gelpi, D. Torrents, M. Orozco, D. G. Pisano, A. Valencia, R. Guigo, M. Bayes, S. Heath, M. Gut, P. Klatt, J. Marshall, K. Raine, L. A. Stebbings, P. A. Futreal, M. R. Stratton, P. J. Campbell, I. Gut, A. Lopez-Guillermo, X. Estivill, E. Montserrat, C. Lopez-Otin and E. Campo (2011). "Whole-genome sequencing identifies recurrent mutations in chronic lymphocytic leukaemia." Nature **475(7354):** 101-5.

Quintanilla-Martinez, L., S. Kumar, F. Fend, E. Reyes, J. Teruya-Feldstein, D. W. Kingma, L. Sorbara, M. Raffeld, S. E. Straus and E. S. Jaffe (2000). "Fulminant EBV(+) T-cell lymphoproliferative disorder following acute/chronic EBV infection: a distinct clinicopathologic syndrome." Blood **96(2):** 443-51.

Ramakrishnan, P., W. Wang and D. Wallach (2004). "Receptor-specific signaling for both the alternative and the canonical NF-kappaB activation pathways by NF-kappaB-inducing kinase." Immunity **21(4):** 477-89.

Ranuncolo, S. M., S. Pittaluga, M. O. Evbuomwan, E. S. Jaffe and B. A. Lewis (2012). "Hodgkin lymphoma requires stabilized NIK and constitutive RelB expression for survival." Blood **120(18):** 3756-63.

Rassidakis, G. Z., D. Jones, R. Lai, P. Ramalingam, A. H. Sarris, T. J. McDonnell and L. J. Medeiros (2003). "BCL-2 family proteins in peripheral T-cell lymphomas: correlation with tumour apoptosis and proliferation." J Pathol **200(2):** 240-8.

Razani, B., A. D. Reichardt and G. Cheng (2011). "Non-canonical NF-kappaB signaling activation and regulation: principles and perspectives." Immunol Rev **244(1):** 44-54.

Reimold, A. M., N. N. Iwakoshi, J. Manis, P. Vallabhajosyula, E. Szomolanyi-Tsuda, E. M. Gravallese, D. Friend, M. J. Grusby, F. Alt and L. H. Glimcher (2001). "Plasma cell differentiation requires the transcription factor XBP-1." Nature **412(6844):** 300-7.

Robson, A. (2010). "Immunocytochemistry and the diagnosis of cutaneous lymphoma." Histopathology **56(1):** 71-90.

Rodriguez-Abreu, D., V. B. Filho and E. Zucca (2008). "Peripheral T-cell lymphomas, unspecified (or not otherwise specified): a review." Hematol Oncol **26(1):** 8-20.

Romero-Ramirez, L., H. Cao, D. Nelson, E. Hammond, A. H. Lee, H. Yoshida, K. Mori, L. H. Glimcher, N. C. Denko, A. J. Giaccia, Q. T. Le and A. C. Koong (2004). "XBP1 is essential for survival under hypoxic conditions and is required for tumor growth." Cancer Res **64(17):** 5943-7.

Rosebeck, S., L. Madden, X. Jin, S. Gu, I. J. Apel, A. Appert, R. A. Hamoudi, H. Noels, X. Sagaert, P. Van Loo, M. Baens, M. Q. Du, P. C. Lucas and L. M. McAllister-Lucas (2011).

"Cleavage of NIK by the API2-MALT1 fusion oncoprotein leads to noncanonical NF-kappaB activation." Science **331(6016):** 468-72.

Rosenwald, A., G. Wright, W. C. Chan, J. M. Connors, E. Campo, R. I. Fisher, R. D. Gascoyne, H. K. Muller-Hermelink, E. B. Smeland, J. M. Giltnane, E. M. Hurt, H. Zhao, L. Averett, L. Yang, W. H. Wilson, E. S. Jaffe, R. Simon, R. D. Klausner, J. Powell, P. L. Duffey, D. L. Longo, T. C. Greiner, D. D. Weisenburger, W. G. Sanger, B. J. Dave, J. C. Lynch, J. Vose, J. O. Armitage, E. Montserrat, A. Lopez-Guillermo, T. M. Grogan, T. P. Miller, M. LeBlanc, G. Ott, S. Kvaloy, J. Delabie, H. Holte, P. Krajci, T. Stokke and L. M. Staudt (2002). "The use of molecular profiling to predict survival after chemotherapy for diffuse large-B-cell lymphoma." N Engl J Med **346(25):** 1937-47.

Rossi, D., S. Deaglio, D. Dominguez-Sola, S. Rasi, T. Vaisitti, C. Agostinelli, V. Spina, A. Bruscaggin, S. Monti, M. Cerri, S. Cresta, M. Fangazio, L. Arcaini, M. Lucioni, R. Marasca, C. Thieblemont, D. Capello, F. Facchetti, I. Kwee, S. A. Pileri, R. Foa, F. Bertoni, R. Dalla-Favera, L. Pasqualucci and G. Gaidano (2011). "Alteration of BIRC3 and multiple other NF-kappaB pathway genes in splenic marginal zone lymphoma." Blood **118(18):** 4930-4.

Rudiger, T., D. D. Weisenburger, J. R. Anderson, J. O. Armitage, J. Diebold, K. A. MacLennan, B. N. Nathwani, F. Ullrich and H. K. Muller-Hermelink (2002). "Peripheral T-cell lymphoma (excluding anaplastic large-cell lymphoma): results from the Non-Hodgkin's Lymphoma Classification Project." Ann Oncol **13(1):** 140-9.

Saha, A. and E. S. Robertson (2011). "Epstein-Barr virus-associated B-cell lymphomas: pathogenesis and clinical outcomes." Clin Cancer Res **17(10):** 3056-63.

Saitoh, T., M. Nakayama, H. Nakano, H. Yagita, N. Yamamoto and S. Yamaoka (2003). "TWEAK induces NF-kappaB2 p100 processing and long lasting NF-kappaB activation." J Biol Chem **278(38):** 36005-12.

Saitoh, Y., N. Yamamoto, M. Z. Dewan, H. Sugimoto, V. J. Martinez Bruyn, Y. Iwasaki, K. Matsubara, X. Qi, T. Saitoh, I. Imoto, J. Inazawa, A. Utsunomiya, T. Watanabe, T. Masuda, N. Yamamoto and S. Yamaoka (2008). "Overexpressed NF-kappaB-inducing kinase contributes to the tumorigenesis of adult T-cell leukemia and Hodgkin Reed-Sternberg cells." Blood **111(10):** 5118-29.

Salaverria, I., S. Bea, A. Lopez-Guillermo, V. Lespinet, M. Pinyol, B. Burkhardt, L. Lamant, A. Zettl, D. Horsman, R. Gascoyne, G. Ott, R. Siebert, G. Delsol and E. Campo (2008). "Genomic profiling reveals different genetic aberrations in systemic ALK-positive and ALK-negative anaplastic large cell lymphomas." Br J Haematol **140(5):** 516-26.

Sansone, P. and J. Bromberg (2012). "Targeting the interleukin-6/Jak/stat pathway in human malignancies." J Clin Oncol **30(9):** 1005-14.

Sasaki, Y., D. P. Calado, E. Derudder, B. Zhang, Y. Shimizu, F. Mackay, S. Nishikawa, K. Rajewsky and M. Schmidt-Supprian (2008). "NIK overexpression amplifies, whereas ablation of its TRAF3-binding domain replaces BAFF:BAFF-R-mediated survival signals in B cells." Proc Natl Acad Sci U S A **105(31):** 10883-8.

Savage, K. J. (2011). "Therapies for peripheral T-cell lymphomas." Hematology Am Soc Hematol Educ Program **2011:** 515-24.

Scarisbrick, J. J., A. J. Woolford, R. Russell-Jones and S. J. Whittaker (2000). "Loss of heterozygosity on 10q and microsatellite instability in advanced stages of primary cutaneous

T-cell lymphoma and possible association with homozygous deletion of PTEN." Blood **95(9):** 2937-42.

Schmitz, R., M. L. Hansmann, V. Bohle, J. I. Martin-Subero, S. Hartmann, G. Mechtersheimer, W. Klapper, I. Vater, M. Giefing, S. Gesk, J. Stanelle, R. Siebert and R. Kuppers (2009). "TNFAIP3 (A20) is a tumor suppressor gene in Hodgkin lymphoma and primary mediastinal B cell lymphoma." J Exp Med **206(5):** 981-9.

Schulze-Luehrmann, J. and S. Ghosh (2006). "Antigen-receptor signaling to nuclear factor kappa B." Immunity **25(5):** 701-15.

Sen, R. and D. Baltimore (1986). "Multiple nuclear factors interact with the immunoglobulin enhancer sequences." Cell **46(5):** 705-16.

Senftleben, U., Y. Cao, G. Xiao, F. R. Greten, G. Krahn, G. Bonizzi, Y. Chen, Y. Hu, A. Fong, S. C. Sun and M. Karin (2001). "Activation by IKKalpha of a second, evolutionary conserved, NF-kappa B signaling pathway." Science **293(5534):** 1495-9.

Shinkura, R., K. Kitada, F. Matsuda, K. Tashiro, K. Ikuta, M. Suzuki, K. Kogishi, T. Serikawa and T. Honjo (1999). "Alymphoplasia is caused by a point mutation in the mouse gene encoding Nf-kappa b-inducing kinase." Nat Genet **22(1):** 74-7.

Shirakawa, F., Y. Tanaka, S. Oda, S. Eto and U. Yamashita (1989). "Autocrine stimulation of interleukin 1 alpha in the growth of adult human T-cell leukemia cells." Cancer Res **49(5):** 1143-7.

Smale, S. T. (2011). "Hierarchies of NF-kappaB target-gene regulation." Nat Immunol **12(8):** 689-94.

Sors, A., F. Jean-Louis, E. Begue, L. Parmentier, L. Dubertret, M. Dreano, G. Courtois, H. Bachelez and L. Michel (2008). "Inhibition of IkappaB kinase subunit 2 in cutaneous T-cell lymphoma down-regulates nuclear factor-kappaB constitutive activation, induces cell death, and potentiates the apoptotic response to antineoplastic chemotherapeutic agents." Clin Cancer Res **14(3):** 901-11.

Sors, A., F. Jean-Louis, C. Pellet, L. Laroche, L. Dubertret, G. Courtois, H. Bachelez and L. Michel (2006). "Down-regulating constitutive activation of the NF-kappaB canonical pathway overcomes the resistance of cutaneous T-cell lymphoma to apoptosis." Blood **107(6):** 2354-63.

Staudt, L. M. (2010). "Oncogenic activation of NF-kappaB." Cold Spring Harb Perspect Biol **2(6):** a000109.

Staudt, L. M. and S. Dave (2005). "The biology of human lymphoid malignancies revealed by gene expression profiling." Adv Immunol **87:** 163-208.

Stein, H., D. Y. Mason, J. Gerdes, N. O'Connor, J. Wainscoat, G. Pallesen, K. Gatter, B. Falini, G. Delsol, H. Lemke and et al. (1985). "The expression of the Hodgkin's disease associate antigen Ki-1 in reactive and neoplastic lymphoid tissue: evidence that Reed-Sternberg cells and histiocytic malignancies are derived from activated lymphoid cells." Blood **66(4):** 848-58.

Streubel, B., U. Vinatzer, M. Willheim, M. Raderer and A. Chott (2006). "Novel t(5;9)(q33;q22) fuses ITK to SYK in unspecified peripheral T-cell lymphoma." Leukemia **20(2):**

313-8.

Subramanian, A., P. Tamayo, V. K. Mootha, S. Mukherjee, B. L. Ebert, M. A. Gillette, A. Paulovich, S. L. Pomeroy, T. R. Golub, E. S. Lander and J. P. Mesirov (2005). "Gene set enrichment analysis: a knowledge-based approach for interpreting genome-wide expression profiles." Proc Natl Acad Sci U S A **102(43):** 15545-50.

Sun, S. C. (2011). "Non-canonical NF-kappaB signaling pathway." Cell Res **21(1):** 71-85.

Sun, S. C., P. A. Ganchi, D. W. Ballard and W. C. Greene (1993). "NF-kappa B controls expression of inhibitor I kappa B alpha: evidence for an inducible autoregulatory pathway." Science **259(5103):** 1912-5.

Swerdlow, S. H., E. Campo, N. L. Harris, E. S. Jaffe, A. Pileri, Jr., H. Stein, J. Thiele and J. W. Vardiman (2008). WHO classification of tumours of haematopoietic and lymphoid tissue, WHO Press IARC.

Swerdlow, S. H., E. Campo, N. L. Harris, E. S. Jaffe, A. Pileri, Jr., H. Stein, J. Thiele and J. W. Vardiman (2008). WHO classification of tumours of haematopoietic and lymphoid tissue.

Sylla, B. S., S. C. Hung, D. M. Davidson, E. Hatzivassiliou, N. L. Malinin, D. Wallach, T. D. Gilmore, E. Kieff and G. Mosialos (1998). "Epstein-Barr virus-transforming protein latent infection membrane protein 1 activates transcription factor NF-kappaB through a pathway that includes the NF-kappaB-inducing kinase and the IkappaB kinases IKKalpha and IKKbeta." Proc Natl Acad Sci U S A **95(17):** 10106-11.

Talwalkar, S. S., J. R. Valbuena, L. V. Abruzzo, J. H. Admirand, S. N. Konoplev, C. E. Bueso-Ramos and L. J. Medeiros (2006). "MALT1 gene rearrangements and NF-kappaB activation involving p65 and p50 are absent or rare in primary MALT lymphomas of the breast." Mod Pathol **19(11):** 1402-8.

Tan, B. T., R. A. Warnke and D. A. Arber (2006). "The frequency of B- and T-cell gene rearrangements and epstein-barr virus in T-cell lymphomas: a comparison between angioimmunoblastic T-cell lymphoma and peripheral T-cell lymphoma, unspecified with and without associated B-cell proliferations." J Mol Diagn **8(4):** 466-75; quiz 527.

Taniguchi, H., F. V. Jacinto, A. Villanueva, A. F. Fernandez, H. Yamamoto, F. J. Carmona, S. Puertas, V. E. Marquez, Y. Shinomura, K. Imai and M. Esteller (2012). "Silencing of Kruppel-like factor 2 by the histone methyltransferase EZH2 in human cancer." Oncogene **31(15):** 1988-94.

Thakur, S., H. C. Lin, W. T. Tseng, S. Kumar, R. Bravo, F. Foss, C. Gelinas and A. B. Rabson (1994). "Rearrangement and altered expression of the NFKB-2 gene in human cutaneous T-lymphoma cells." Oncogene **9(8):** 2335-44.

Thornburg, N. J., W. Kulwichit, R. H. Edwards, K. H. Shair, K. M. Bendt and N. Raab-Traub (2006). "LMP1 signaling and activation of NF-kappaB in LMP1 transgenic mice." Oncogene **25(2):** 288-97. 169

Thu, Y. M. and A. Richmond (2010). "NF-kappaB inducing kinase: a key regulator in the immune system and in cancer." Cytokine Growth Factor Rev **21(4):** 213-26.

Thu, Y. M., Y. Su, J. Yang, R. Splittgerber, S. Na, A. Boyd, C. Mosse, C. Simons and A.

Richmond (2012). "NF-kappaB inducing kinase (NIK) modulates melanoma tumorigenesis by regulating expression of pro-survival factors through the beta-catenin pathway." Oncogene **31(20):** 2580-92.

Turner, D. J., S. M. Alaish, T. Zou, J. N. Rao, J. Y. Wang and E. D. Strauch (2007). "Bile salts induce resistance to apoptosis through NF-kappaB-mediated XIAP expression." Ann Surg **245(3):** 415-25.

Vainchenker, W. and S. N. Constantinescu (2013). "JAK/STAT signaling in hematological malignancies." Oncogene **32(21):** 2601-13.

Vallabhapurapu, S. and M. Karin (2009). "Regulation and function of NF-kappaB transcription factors in the immune system." Annu Rev Immunol **27:** 693-733.

Vallabhapurapu, S., A. Matsuzawa, W. Zhang, P. H. Tseng, J. J. Keats, H. Wang, D. A. Vignali, P. L. Bergsagel and M. Karin (2008). "Nonredundant and complementary functions of TRAF2 and TRAF3 in a ubiquitination cascade that activates NIK-dependent alternative NF-kappaB signaling." Nat Immunol **9(12):** 1364-70.

van der Fits, L., J. J. Out-Luiting, M. A. van Leeuwen, J. N. Samsom, R. Willemze, C. P. Tensen and M. H. Vermeer (2012). "Autocrine IL-21 stimulation is involved in the maintenance of constitutive STAT3 activation in Sezary syndrome." J Invest Dermatol **132(2):** 440-7.

Varettoni, M., L. Arcaini, S. Zibellini, E. Boveri, S. Rattotti, R. Riboni, A. Corso, E. Orlandi, M. Bonfichi, M. Gotti, C. Pascutto, S. Mangiacavalli, G. Croci, V. Fiaccadori, L. Morello, M. L. Guerrera, M. Paulli and M. Cazzola (2013). "Prevalence and clinical significance of the MYD88 (L265P) somatic mutation in Waldenstrom's macroglobulinemia and related lymphoid neoplasms." Blood.

Varfolomeev, E., J. W. Blankenship, S. M. Wayson, A. V. Fedorova, N. Kayagaki, P. Garg, K. Zobel, J. N. Dynek, L. O. Elliott, H. J. Wallweber, J. A. Flygare, W. J. Fairbrother, K. Deshayes, V. M. Dixit and D. Vucic (2007). "IAP antagonists induce autoubiquitination of c-IAPs, NF-kappaB activation, and TNFalpha-dependent apoptosis." Cell **131(4):** 669-81.

Vose, J., J. Armitage and D. Weisenburger (2008). "International peripheral T-cell and natural killer/T-cell lymphoma study: pathology findings and clinical outcomes." J Clin Oncol **26(25):** 4124-30.

Wang, C., L. Deng, M. Hong, G. R. Akkaraju, J. Inoue and Z. J. Chen (2001). "TAK1 is a ubiquitin-dependent kinase of MKK and IKK." Nature **412(6844):** 346-51.

Wang, F., Y. Zhu, Y. Huang, S. McAvoy, W. B. Johnson, T. H. Cheung, T. K. Chung, K. W. Lo, S. F. Yim, M. M. Yu, H. Y. Ngan, Y. F. Wong and D. I. Smith (2005). "Transcriptional repression of WEE1 by Kruppel-like factor 2 is involved in DNA damage-induced apoptosis." Oncogene **24(24):** 3875-85.

Wilcox, R. A. (2011). "Cutaneous T-cell lymphoma: 2011 update on diagnosis, risk-stratification, and management." Am J Hematol **86(11):** 928-48.

Wong, H. K., A. Mishra, T. Hake and P. Porcu (2011). "Evolving insights in the pathogenesis and therapy of cutaneous T-cell lymphoma (mycosis fungoides and Sezary syndrome)." Br J Haematol **155(2):** 150-66.

Woronicz, J. D., X. Gao, Z. Cao, M. Rothe and D. V. Goeddel (1997). "IkappaB kinase-beta: NF-kappaB activation and complex formation with IkappaB kinase-alpha and NIK." Science **278(5339):** 866-9.

Wozniak, M. B., L. Tracey, P. L. Ortiz-Romero, S. Montes, M. Alvarez, J. Fraga, J. Fernandez Herrera, S. Vidal, J. L. Rodriguez-Peralto, M. A. Piris and R. Villuendas Deceased (2009). "Psoralen plus ultraviolet A +/- interferon-alpha treatment resistance in mycosis fungoides: the role of tumour microenvironment, nuclear transcription factor-kappaB and T-cell receptor pathways." Br J Dermatol **160(1):** 92-102.

Wozniak, M. B., R. Villuendas, J. R. Bischoff, C. B. Aparicio, J. F. Martinez Leal, P. de La Cueva, M. E. Rodriguez, B. Herreros, D. Martin-Perez, M. I. Longo, M. Herrera, M. A. Piris and P. L. Ortiz-Romero (2010). "Vorinostat interferes with the signaling transduction pathway of T-cell receptor and synergizes with phosphoinositide-3 kinase inhibitors in cutaneous T-cell lymphoma." Haematologica **95(4):** 613-21.

Wright, C. W., J. M. Rumble and C. S. Duckett (2007). "CD30 activates both the canonical and alternative NF-kappaB pathways in anaplastic large cell lymphoma cells." J Biol Chem **282(14):** 10252-62.

Wright, G., B. Tan, A. Rosenwald, E. H. Hurt, A. Wiestner and L. M. Staudt (2003). "A gene expression-based method to diagnose clinically distinct subgroups of diffuse large B cell lymphoma." Proc Natl Acad Sci U S A **100(17):** 9991-6.

Wu, J. and J. B. Lingrel (2004). "KLF2 inhibits Jurkat T leukemia cell growth via upregulation of cyclin-dependent kinase inhibitor p21WAF1/CIP1." Oncogene **23(49):** 8088-96.

Wullaert, A., M. C. Bonnet and M. Pasparakis (2011). "NF-kappaB in the regulation of epithelial homeostasis and inflammation." Cell Res **21(1):** 146-58.

Xiao, G., M. E. Cvijic, A. Fong, E. W. Harhaj, M. T. Uhlik, M. Waterfield and S. C. Sun (2001). "Retroviral oncoprotein Tax induces processing of NF-kappaB2/p100 in T cells: evidence for the involvement of IKKalpha." EMBO J **20(23):** 6805-15.

Xiao, G., A. Fong and S. C. Sun (2004). "Induction of p100 processing by NF-kappaB-inducing kinase involves docking IkappaB kinase alpha (IKKalpha) to p100 and IKKalpha-mediated phosphorylation." J Biol Chem **279(29):** 30099-105.

Xiao, G., E. W. Harhaj and S. C. Sun (2001). "NF-kappaB-inducing kinase regulates the processing of NF-kappaB2 p100." Mol Cell **7(2):** 401-9.

Yamada, T., T. Mitani, K. Yorita, D. Uchida, A. Matsushima, K. Iwamasa, S. Fujita and M. Matsumoto (2000). "Abnormal immune function of hemopoietic cells from alymphoplasia (aly) mice, a natural strain with mutant NF-kappa B-inducing kinase." J Immunol **165(2):** 804-12.

Yamagishi, M., K. Nakano, A. Miyake, T. Yamochi, Y. Kagami, A. Tsutsumi, Y. Matsuda, A. Sato-Otsubo, S. Muto, A. Utsunomiya, K. Yamaguchi, K. Uchimaru, S. Ogawa and T. Watanabe (2012). "Polycomb-mediated loss of miR-31 activates NIK-dependent NF-kappaB pathway in adult T cell leukemia and other cancers." Cancer Cell **21(1):** 121-35.

Yang, J., Y. Lin, Z. Guo, J. Cheng, J. Huang, L. Deng, W. Liao, Z. Chen, Z. Liu and B. Su (2001). "The essential role of MEKK3 in TNF-induced NF-kappaB activation." Nat Immunol **2(7):** 620-

Yang, Y., A. L. Shaffer, 3rd, N. C. Emre, M. Ceribelli, M. Zhang, G. Wright, W. Xiao, J. Powell, J. Platig, H. Kohlhammer, R. M. Young, H. Zhao, Y. Yang, W. Xu, J. J. Buggy, S. Balasubramanian, L. A. Mathews, P. Shinn, R. Guha, M. Ferrer, C. Thomas, T. A. Waldmann and L. M. Staudt (2012). "Exploiting synthetic lethality for the therapy of ABC diffuse large B cell lymphoma." Cancer Cell **21(6):** 723-37.

Yin, L., L. Wu, H. Wesche, C. D. Arthur, J. M. White, D. V. Goeddel and R. D. Schreiber (2001). "Defective lymphotoxin-beta receptor-induced NF-kappaB transcriptional activity in NIK-deficient mice." Science **291(5511):** 2162-5.

Zarnegar, B., S. Yamazaki, J. Q. He and G. Cheng (2008). "Control of canonical NF-kappaB activation through the NIK-IKK complex pathway." Proc Natl Acad Sci U S A **105(9):** 3503-8.

Zarnegar, B. J., Y. Wang, D. J. Mahoney, P. W. Dempsey, H. H. Cheung, J. He, T. Shiba, X. Yang, W. C. Yeh, T. W. Mak, R. G. Korneluk and G. Cheng (2008). "Noncanonical NF-kappaB activation requires coordinated assembly of a regulatory complex of the adaptors cIAP1, cIAP2, TRAF2 and TRAF3 and the kinase NIK." Nat Immunol **9(12):** 1371-8.

Zettl, A., T. Rudiger, M. A. Konrad, A. Chott, I. Simonitsch-Klupp, R. Sonnen, H. K. Muller-Hermelink and G. Ott (2004). "Genomic profiling of peripheral T-cell lymphoma, unspecified, and anaplastic large T-cell lymphoma delineates novel recurrent chromosomal alterations." Am J Pathol **164(5):** 1837-48.

Zhang, J., V. Grubor, C. L. Love, A. Banerjee, K. L. Richards, P. A. Mieczkowski, C. Dunphy, W. Choi, W. Y. Au, G. Srivastava, P. L. Lugar, D. A. Rizzieri, A. S. Lagoo, L. Bernal-Mizrachi, K. P. Mann, C. Flowers, K. Naresh, A. Evens, L. I. Gordon, M. Czader, J. I. Gill, E. D. Hsi, Q. Liu, A. Fan, K. Walsh, D. Jima, L. L. Smith, A. J. Johnson, J. C. Byrd, M. A. Luftig, T. Ni, J. Zhu, A. Chadburn, S. Levy, D. Dunson and S. S. Dave (2013). "Genetic heterogeneity of diffuse large B-cell lymphoma." Proc Natl Acad Sci U S A **110(4):** 1398-403.

Zhao, W. L. (2010). "Targeted therapy in T-cell malignancies: dysregulation of the cellular signaling pathways." Leukemia **24(1):** 13-21.

Zhou, Y., A. D. Attygalle, S. S. Chuang, T. Diss, H. Ye, H. Liu, R. A. Hamoudi, P. Munson, C. M. Bacon, A. Dogan and M. Q. Du (2007). "Angioimmunoblastic T-cell lymphoma: histological progression associates with EBV and HHV6B viral load." Br J Haematol **138(1):** 44-53.

Zinzani, P. L., G. Musuraca, M. Tani, V. Stefoni, E. Marchi, M. Fina, C. Pellegrini, L. Alinari, E. Derenzini, A. de Vivo, E. Sabattini, S. Pileri and M. Baccarani (2007). "Phase II trial of proteasome inhibitor bortezomib in patients with relapsed or refractory cutaneous T-cell lymphoma." J Clin Oncol **25(27):** 4293-7.

APPENDIX I

Supplementary Figure 1

Supplementary Table 1

Summary in spanish

SUPPLEMENTARY FIGURES AND TABLES

Supplementary Figure 1. Validation of NIK knockdown for gene expression studies in cell lines. NIK protein expression after NIK knockdown in My-La and SR-786 in the three independent experiments performed for the gene expression analysis. The first lane in each membrane represent the non-template control. The second lane is loaded with cells transfected with siNIK1 and the third lane with siNIK2.

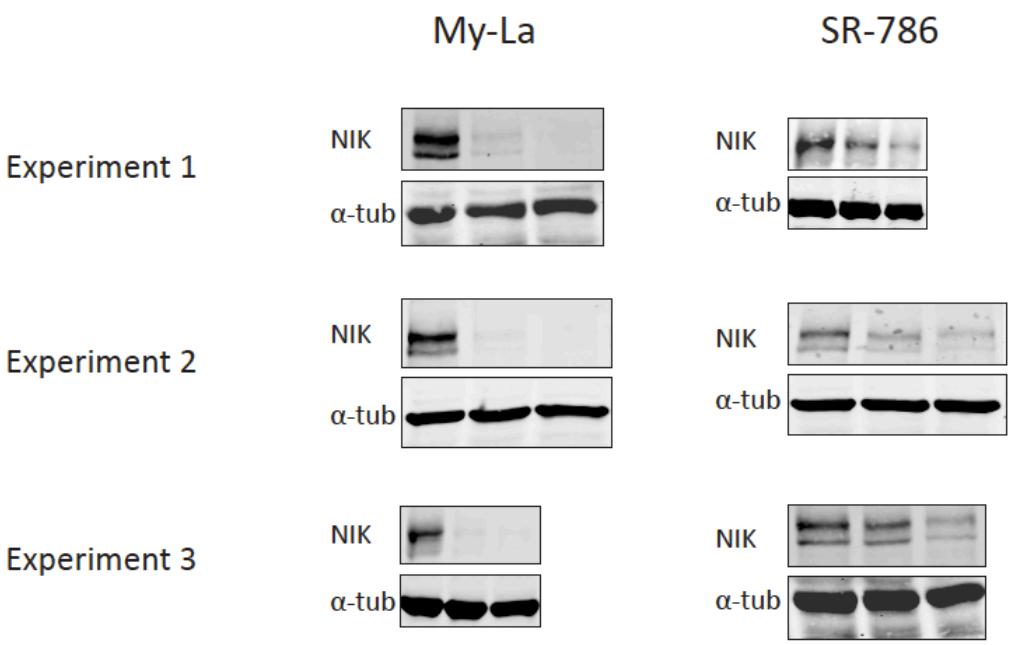

Supplementary Table 1. Genes with altered expression after NIK knockdown

List of genes differentially expressed (paired t-test) between control and NIK knockdown cells. Genes with FDR <0.05 and $\log_2$ foldchange >±0.6 are shown.

My-La		
NAME	siNIK Average foldchange (log2)	FDR
PON2	-1.935	0.000
YAP1	-1.922	0.000
CTH	-1.852	0.011
HOXB9	-1.554	0.004
DDIT3	-1.516	0.012
BTN3A3	-1.515	0.000
RGS16	-1.463	0.000
LARGE	-1.452	0.002
NCRNA00176	-1.450	0.000
TNFSF4	-1.427	0.000
ATP8A2	-1.419	0.001
ADAM8	-1.354	0.004
RAB9A	-1.323	0.001
OTOA	-1.321	0.000
EDN2	-1.314	0.002
LOC284561	-1.314	0.004
TIFA	-1.254	0.001
WARS	-1.240	0.003
IL3RA	-1.239	0.000
IL6	-1.235	0.000
IL15	-1.232	0.001
XBP1	-1.222	0.003
LOC339047	-1.217	0.007
PFKM	-1.214	0.000
ATF3	-1.213	0.003
NFKBIA	-1.211	0.000
IFRD1	-1.210	0.004
IL21	-1.178	0.001
RAB9P1	-1.175	0.001
SQRDL	-1.162	0.000
OLAH	-1.161	0.002
NCRNA00158	-1.157	0.001
IL9	-1.138	0.006
EMR1	-1.129	0.001
PSAT1	-1.119	0.009
C6orf105	-1.114	0.001
GLUD1	-1.111	0.002
RAI14	-1.099	0.002
ZNF643	-1.092	0.003
JMY	-1.070	0.001
IFIH1	-1.066	0.002
BBS12	-1.066	0.014
AMICA1	-1.061	0.000
C10orf116	-1.059	0.000
GLUD2	-1.055	0.001
GSDMB	-1.046	0.001
PTP4A3	-1.024	0.001
FHL2	-1.021	0.012
ATF5	-1.012	0.020
SH2B3	-1.008	0.002
COL15A1	-1.008	0.001
PGLYRP4	-0.999	0.002
GARS	-0.995	0.005
PLXDC2	-0.993	0.001
CLIP2	-0.992	0.004
LTA	-0.991	0.004
LOR	-0.987	0.001
CHAC1	-0.973	0.011
RNGTT	-0.972	0.004
DDX4	-0.969	0.001
STRA6	-0.967	0.002
FERMT2	-0.965	0.003
MARS	-0.959	0.004
GFPT2	-0.956	0.000
CCL5	-0.954	0.000
SLC26A9	-0.951	0.002
SERPINB8	-0.947	0.001
IL1R2	-0.943	0.001
HYAL4	-0.942	0.004
CARS	-0.937	0.007
TRERF1	-0.934	0.005
SHMT2	-0.933	0.001
DARS2	-0.932	0.008
ZG16B	-0.931	0.005
HLA-F	-0.930	0.001
GPT2	-0.930	0.014
PCK2	-0.929	0.007
GAS7	-0.925	0.000
MAP2K1	-0.920	0.000
BEST1	-0.912	0.038
IL1A	-0.910	0.000
FAS	-0.907	0.002
SLC1A5	-0.907	0.004
DDR2	-0.906	0.002
VDR	-0.906	0.003
ICAM1	-0.892	0.000
PLEKHG1	-0.891	0.001
ZBED2	-0.887	0.003
UBD	-0.881	0.034
CCDC50	-0.878	0.012
RHEBL1	-0.878	0.001
CD302	-0.874	0.000
PSME2	-0.874	0.000

FSCN1	-0.872	0.000	**SNHG5**	-0.718	0.009
CD44	-0.861	0.002	**ENOX1**	-0.716	0.003
CCNB1IP1	-0.861	0.002	**EXTL2**	-0.715	0.001
INSIG1	-0.857	0.002	**ADARB2**	-0.714	0.003
INHBA	-0.851	0.001	**RUNDC3B**	-0.710	0.011
TNFAIP6	-0.850	0.001	**BTNL8**	-0.707	0.035
MIR155HG	-0.844	0.001	**IL18R1**	-0.707	0.003
FCER2	-0.830	0.003	**ITLN2**	-0.704	0.003
TTC25	-0.828	0.026	**PRR5L**	-0.704	0.001
C7orf68	-0.818	0.007	**VIM**	-0.704	0.034
SGCA	-0.818	0.008	**ASNS**	-0.703	0.021
TUBE1	-0.818	0.007	**C10orf10**	-0.703	0.006
TJP2	-0.814	0.008	**BTN3A1**	-0.702	0.002
ERMN	-0.813	0.001	**SLC39A9**	-0.700	0.012
GLT25D2	-0.808	0.025	**GNPDA1**	-0.698	0.002
IGSF3	-0.805	0.008	**PYCR1**	-0.696	0.001
FDFT1	-0.805	0.004	**KIAA1147**	-0.694	0.001
PSMB9	-0.802	0.000	**FKBP14**	-0.692	0.001
MID1IP1	-0.798	0.004	**IL23R**	-0.688	0.008
DHCR7	-0.797	0.001	**CFLAR**	-0.682	0.001
FKBP11	-0.794	0.004	**LPIN2**	-0.678	0.002
RAD23A	-0.794	0.004	**UPK1B**	-0.678	0.004
DNAJC5B	-0.791	0.010	**LY75**	-0.676	0.002
KIF21B	-0.788	0.006	**MGST3**	-0.673	0.009
EHD4	-0.788	0.005	**SLC3A2**	-0.673	0.010
IARS	-0.788	0.013	**ACAD11**	-0.672	0.004
GBE1	-0.786	0.014	**EEF1A1**	-0.671	0.016
RILPL2	-0.785	0.002	**TPTE**	-0.670	0.003
AARS	-0.785	0.009	**PLA1A**	-0.669	0.002
LOC374491	-0.785	0.036	**RFX5**	-0.666	0.004
SARS	-0.782	0.014	**MVK**	-0.666	0.003
CHRNA6	-0.780	0.007	**SEMA4A**	-0.661	0.036
EIF4EBP1	-0.777	0.007	**HAX1**	-0.660	0.016
B4GALT4	-0.776	0.001	**ATF4**	-0.659	0.008
PSME1	-0.775	0.002	**VPS29**	-0.654	0.017
ST8SIA1	-0.773	0.001	**FAM122B**	-0.652	0.015
BIRC3	-0.772	0.001	**DNAJC12**	-0.652	0.004
GEM	-0.771	0.001	**BAZ2A**	-0.652	0.007
ALPK1	-0.771	0.004	**C20orf112**	-0.652	0.005
CLDN16	-0.769	0.001	**ACSM3**	-0.650	0.032
LONP1	-0.768	0.013	**LIPA**	-0.648	0.045
CNR1	-0.762	0.001	**IL4I1**	-0.648	0.004
NFKBIE	-0.761	0.004	**CD80**	-0.646	0.001
DHRS2	-0.759	0.001	**DENND5A**	-0.646	0.001
WIPI1	-0.752	0.020	**ALDOC**	-0.642	0.012
LGTN	-0.750	0.007	**C13orf23**	-0.642	0.002
MYO5C	-0.749	0.007	**CD83**	-0.641	0.001
YARS	-0.748	0.005	**HLA-H**	-0.640	0.002
FASN	-0.747	0.001	**NPIP**	-0.639	0.034
SLC7A11	-0.746	0.036	**NUDT15**	-0.637	0.001
KCNH8	-0.744	0.012	**TCAM1**	-0.634	0.007
DNAJC7	-0.735	0.008	**C5orf23**	-0.633	0.015
LTB	-0.731	0.046	**LOC645676**	-0.627	0.002
RASGRF2	-0.730	0.008	**GADD45A**	-0.626	0.022
KDM4A	-0.730	0.007	**GPR87**	-0.626	0.025
SESN2	-0.726	0.004	**HERPUD1**	-0.624	0.011

APOBEC3H	-0.624	0.004	**CDH1**	0.639	0.002
EPRS	-0.622	0.019	**C9orf62**	0.639	0.049
C18orf58	-0.622	0.032	**ANKRD13C**	0.640	0.012
CT45A5	-0.620	0.002	**TP53INP1**	0.640	0.015
MST1R	-0.619	0.003	**FAM176A**	0.642	0.002
IL22	-0.618	0.023	**HCN4**	0.643	0.018
SLC7A5	-0.618	0.004	**ITGB1**	0.644	0.001
SCD	-0.618	0.001	**CDKN1C**	0.645	0.027
MAGEB2	-0.618	0.003	**NKAIN1**	0.645	0.029
BCL2L1	-0.616	0.001	**CD96**	0.646	0.019
CT45A1	-0.615	0.003	**IFI6**	0.647	0.012
KIF2C	-0.615	0.013	**RELL1**	0.647	0.004
WDR65	-0.614	0.005	**SH3GL3**	0.648	0.032
PDAP1	-0.613	0.010	**MTSS1**	0.649	0.001
XPOT	-0.611	0.012	**DEXI**	0.650	0.003
TTC39A	-0.606	0.001	**RNF149**	0.650	0.001
DHRS11	-0.605	0.017	**TMTC2**	0.653	0.003
HLA-J	-0.605	0.002	**GPR78**	0.654	0.041
CPNE5	-0.604	0.002	**WDR81**	0.655	0.005
CHST12	0.600	0.006	**LOC338620**	0.655	0.001
IGFBP1	0.602	0.022	**PIP5K1B**	0.657	0.007
TPSG1	0.603	0.031	**GRIN2D**	0.658	0.022
F5	0.603	0.020	**GPR153**	0.661	0.019
MKL2	0.604	0.002	**LOC439951**	0.666	0.023
ZNF579	0.604	0.022	**NCDN**	0.668	0.004
ASPRV1	0.604	0.002	**SOX2**	0.670	0.006
OXCT1	0.605	0.002	**HOMER3**	0.674	0.000
PPP1R9A	0.605	0.006	**FAM116A**	0.675	0.014
SFRS6	0.607	0.038	**PM20D2**	0.675	0.007
MEGF6	0.607	0.019	**COX6A2**	0.675	0.022
C6orf225	0.608	0.001	**UTS2D**	0.677	0.002
CD7	0.608	0.025	**C9orf135**	0.679	0.002
ABR	0.609	0.001	**IL7R**	0.679	0.005
AMY1C	0.611	0.013	**C1orf53**	0.681	0.002
C10orf140	0.612	0.003	**GMNN**	0.686	0.015
CACNA1E	0.614	0.039	**TIMM8B**	0.690	0.010
GRK5	0.617	0.003	**DKFZP434I0714**	0.691	0.021
MAF	0.619	0.019	**CACNA1H**	0.691	0.008
ZMYND11	0.622	0.003	**KIF25**	0.697	0.007
C18orf50	0.622	0.009	**ITM2A**	0.697	0.001
FLJ22184	0.624	0.031	**FAIM**	0.698	0.002
WFDC1	0.626	0.005	**FBXL17**	0.699	0.004
CABYR	0.628	0.003	**SOBP**	0.702	0.006
DAZAP2	0.628	0.002	**ARL4C**	0.704	0.001
JAZF1	0.629	0.010	**PODXL**	0.706	0.008
TFPI	0.629	0.003	**TNFRSF18**	0.714	0.001
SLC19A2	0.630	0.008	**IFITM5**	0.718	0.024
E2F3	0.631	0.006	**KLHDC7B**	0.718	0.008
LOC100131998	0.632	0.006	**PPP2CB**	0.719	0.001
FRAT2	0.633	0.004	**VNN2**	0.722	0.003
SESN3	0.633	0.014	**GPR150**	0.723	0.018
ATP6V1G1	0.634	0.001	**GPR65**	0.725	0.009
PNMA1	0.636	0.001	**ARHGAP12**	0.725	0.001
HSPA2	0.636	0.012	**XYLT1**	0.732	0.001
CSGALNACT1	0.637	0.006	**GPR137B**	0.734	0.001
UTS2R	0.638	0.016	**DUX4**	0.735	0.017
ZSCAN10	0.638	0.021	**ITM2C**	0.736	0.002

HCN2	0.742	0.020
ENTPD1	0.754	0.001
LOC644246	0.756	0.013
RTP4	0.762	0.002
KCNJ13	0.762	0.000
ITGB7	0.770	0.004
CORO2A	0.771	0.005
NUCB2	0.777	0.022
CEP70	0.778	0.001
TTC18	0.779	0.002
FAM46C	0.782	0.000
PGBD2	0.785	0.001
ZNF670	0.789	0.014
TXNDC3	0.793	0.001
NTNG2	0.808	0.019
TSHZ3	0.809	0.002
MUC20	0.814	0.007
MUC6	0.817	0.031
SLC26A11	0.821	0.001
ITM2B	0.824	0.001
SATB1	0.824	0.006
PSKH1	0.830	0.000
LIMA1	0.837	0.000
PTPRC	0.842	0.006
IRS1	0.843	0.004
CRABP2	0.848	0.011
GLCCI1	0.853	0.000
LAMB1	0.863	0.001
TULP4	0.864	0.006
CD28	0.869	0.000
KCNJ12	0.879	0.012
LOC541471	0.880	0.004
SLC44A1	0.899	0.000
TIPARP	0.904	0.007
CDKN2C	0.905	0.029
CASP7	0.935	0.005
FRY	0.944	0.001
SCG2	0.961	0.001
RGS9	0.964	0.017
CCR3	0.964	0.000
DMBT1	0.970	0.001
SLC9A9	0.974	0.001
SAMD9	0.983	0.000
KIAA1618	0.994	0.003
SLC7A8	0.996	0.007
BZRAP1	1.008	0.001
SLC39A10	1.014	0.005
HIST1H4A	1.024	0.007
SLC38A6	1.047	0.001
GZMB	1.048	0.008
RBP4	1.088	0.006
BFSP1	1.117	0.000
TOX2	1.125	0.000
TRBV5-4	1.149	0.000
NME7	1.160	0.000
F2R	1.183	0.000
GPR15	1.199	0.004
FAM9B	1.215	0.000
LOC150759	1.271	0.000
ENPP2	1.301	0.003
ENC1	1.319	0.000
IER5L	1.327	0.004
CCR5	1.380	0.000
LOC283143	1.415	0.031
SMCR5	1.467	0.008
SAMD9L	1.507	0.000
ARNT2	1.537	0.000
HTR2B	1.547	0.000
CFHR3	1.556	0.000
MGC42105	1.586	0.001
KLF2	1.639	0.000
ANKRD55	1.642	0.001
LGR4	1.728	0.000
CFH	1.743	0.000
PMCHL1	2.355	0.000
PMCH	3.078	0.000

SR-786		
NAME	**siNIK Average foldchange (log2)**	**FDR**
IL6	-1.568	0.000
IL21	-1.343	0.001
ENOX1	-1.063	0.002
ZBED2	-1.039	0.006
HYAL4	-1.034	0.003
OCA2	-1.025	0.000
COL15A1	-1.006	0.001
EDN2	-1.003	0.007
IL22	-0.939	0.033
ADAM8	-0.939	0.006
OTOA	-0.929	0.001
C7orf68	-0.911	0.023
C6orf105	-0.868	0.002
YAP1	-0.847	0.002
RILPL2	-0.841	0.005
SQRDL	-0.837	0.008
DDIT3	-0.829	0.040
IL26	-0.806	0.002
PGLYRP4	-0.797	0.007
GFPT2	-0.789	0.002
CCL17	-0.778	0.005
IL4I1	-0.770	0.002
NEURL3	-0.758	0.002
CNR1	-0.757	0.001
HSD11B1	-0.754	0.050
IFIH1	-0.742	0.003
SLC2A14	-0.733	0.008
C10orf116	-0.731	0.002
BTN3A3	-0.719	0.007

RGS16	-0.718	0.033	**SLC9A9**	0.654	0.013
IL1A	-0.714	0.002	**POU2AF1**	0.666	0.011
MIR155HG	-0.713	0.007	**BFSP1**	0.668	0.007
LOR	-0.709	0.005	**MGC42105**	0.685	0.008
PLXDC2	-0.698	0.012	**GLCCI1**	0.686	0.008
BBS12	-0.687	0.007	**TRBV5-4**	0.688	0.008
TNFSF4	-0.685	0.007	**UTS2D**	0.692	0.009
EXTL2	-0.678	0.002	**LGR4**	0.714	0.008
CYP1A1	-0.675	0.001	**SLC26A11**	0.734	0.009
EEF1A2	-0.674	0.007	**PIM2**	0.734	0.007
INHBA	-0.674	0.003	**SLC39A10**	0.752	0.007
MGST3	-0.663	0.007	**SLC38A6**	0.768	0.005
PLEKHG1	-0.661	0.007	**IRS1**	0.769	0.013
IL9	-0.656	0.026	**KCNJ12**	0.771	0.007
TNFAIP6	-0.646	0.004	**RASGRP3**	0.807	0.007
KCNQ2	-0.643	0.005	**NME7**	0.808	0.002
VDR	-0.641	0.003	**ENPP2**	0.819	0.001
LTA	-0.638	0.008	**SAMD9**	0.837	0.003
TIFA	-0.636	0.009	**RTP4**	0.864	0.005
NRCAM	-0.631	0.002	**GPR15**	0.922	0.012
BTNL8	-0.631	0.026	**ARNT2**	0.935	0.002
WARS	-0.630	0.027	**SAMD9L**	1.065	0.001
NFKBIA	-0.618	0.004	**ENC1**	1.100	0.003
NCRNA00176	-0.613	0.014	**IGHM**	1.129	0.000
SLC45A3	-0.609	0.011	**DNAH12**	1.144	0.001
ATP8A2	-0.608	0.007	**KLF2**	1.217	0.002
IL15	-0.605	0.002	**F2R**	1.336	0.001
JMY	-0.605	0.016	**FAM9B**	1.506	0.003
BIRC3	-0.603	0.002	**HTR2B**	1.663	0.002
DAZAP2	0.606	0.007	**PMCHL1**	2.370	0.001
TMTC2	0.619	0.014	**PMCH**	3.062	0.000
CCR5	0.629	0.013			
CDKN2C	0.633	0.018			
CARHSP1	0.647	0.046			

RESUMEN EN ESPAÑOL

Caracterización e inhibición de la ruta de NF-κB en linfomas no-Hodgkin

INTRODUCCION

Los linfomas constituyen un grupo amplio de neoplasias linfoproliferativas con comportamiento y respuesta al tratamiento variados. En la actualidad, la terapia de los linfomas está basada en fármacos citotóxicos o anticuerpos monoclonales dirigidos contra marcadores de superficie de los linfocitos. En muchos casos, el tratamiento estándar no es capaz de curar a los pacientes y presentan un porcentaje de recidivas muy alto. En esta tesis doctoral se han estudiado principalmente dos tipos de linfomas: linfoma B difuso de célula grande (LBDCG) y linfoma periférico de células T (LPCT). El LBDCG se caracteriza por una proliferación descontrolada de linfocitos B maduros y es el linfoma más común en el adulto, representando alrededor del 30-40 % de todos los linfomas no-Hodgkin (Lenz et al. 2010).

Basándose en el perfil de expresión génica, los LBDCGs se pueden dividir en dos subtipos diferentes según la "supuesta" célula de origen: el subtipo ABC (por las siglas en inglés de "Activated B-cell") que se caracteriza por un perfil de expresión génica parecido a los linfocitos B activados, y el subtipo GCB (por las siglas en inglés de "Germinal Center C-cell"), definido por la expresión de genes típicamente expresados por las células B del centro germinal (Alizadeh et al. 2000). Los LBDCGs del tipo ABC presentan un curso clínico más agresivo que los GCB y se ha propuesto que estos linfomas dependen de la activación de la vía de NF-κB para su supervivencia (Alizadeh et al. 2000; Staudt et al. 2005; Davis et al. 2001).

Los LPCTs forman un grupo muy heterogéneo de tumores caracterizados por una proliferación maligna de los linfocitos T. Los LPCT constituyen alrededor del 12% de todos los linfomas no-Hodgkin y el conocimiento de su origen y biología es escaso (Piccaluga et al. 2011; Vose et al. 2008). Los LPCTs son tumores muy agresivos que hoy en día carecen de terapias eficaces (Foss et al. 2013).

Con el objetivo de buscar nuevas dianas terapéuticas para el desarrollo de terapias dirigidas efectivas en los pacientes de linfomas, es necesario identificar y caracterizar rutas de

señalización que alimentan a estos tumores. Una de las rutas de señalización asociadas a los tumores hematológicos es la vía de NF-κB. La ruta de NF-κB se ha encontrado activada en varios tipos de linfomas, entre ellos linfoma de Hodgkin, LBDCG y linfomas de células T. Se han descrito varias alteraciones genéticas en diferentes componentes de la vía, dando lugar a su activación en estos tumores (Compagno et al. 2009; Keats et al. 2007; Schmitz et al 2009). Como consecuencia, terapias basadas en la inhibición de NF-κB aparecen como una estrategia terapéutica prometedora en ensayos preclínicos. Para llevar estas estrategias adelante, es necesario realizar estudios adicionales que permitan identificar dianas moleculares y tumores con mayor probabilidad de respuesta a estas terapias.

NF-κB es una familia de factores de transcripción constituida por cinco miembros; RelA (p65), RelB, c-Rel, p50 (con su precursor p105), y p52 (con su precursor p100) (Vallabhapurapu et al. 2009). Estos factores de transcripción regulan la expresión de cientos de genes implicados en la regulación de la respuesta inmune, proliferación celular, apoptosis y supervivencia celular (Hayden et al. 2011). Por este motivo, una activación descontrolada de NF-κB puede resultar en el desarrollo de tumores. Existen dos cascadas principales de activación de NF-κB: la vía clásica/canónica y la vía alternativa/no canónica. Varios estímulos pueden activar la vía, como la estimulación de los receptores de TNF (*tumor necrosis factor*), los receptores de interleuquinas, los TLR (*Toll-like receptors*) y los receptores de antígenos BCR (el receptor de células B) y TCR (el receptor de células T) (Vallabhapurapu et al. 2009). Resumido, una activación de dichos receptores da lugar a la activación de un complejo IKK, que incluye varias quinasas. Estas quinasas (IKKα y IKKβ) son capaces de fosforilar inhibidores de NF-κB, permitiendo así que dímeros de NF-κB que se encuentran retenidos en el citoplasma por estos inhibidores, se desplacen al núcleo y se unan al ADN (Oeckinghaus et al. 2009). La vía clásica de NF-κB, se caracteriza por la activación de la quinasa IKKβ y la translocación nuclear de los factores RelA, c-Rel y p50. La vía alternativa por otro lado, necesita la activación de las quinasas NIK y IKKα y termina en la translocación nuclear de RelB y p52 (Hayden et al. 2008). En esta tesis doctoral, gran parte del trabajo está enfocado en el estudio del papel de NIK como regulador de NF-κB en linfomas. NIK es una serina-treonina quinasa capaz de activar tanto la vía clásica como la vía alternativa de NF-κB. Aún así, la presencia de NIK sólo es esencial para la activación de la vía alternativa, a diferencia de la vía clásica que puede ser activada sin la presencia de NIK (Zarnegar et al. 2008a; Zarnetar et al. 2008b). NIK actúa fosforilando a IKKα, dando lugar a la fosforilación de p100, permitiendo de este modo su procesamiento a p52 y su posterior translocación al núcleo

donde regula la transcripción (Xiao et al. 2001; Senftleben et al. 2001). NIK está implicado en la regulación de la vía de NF-κB sólo en ciertos tipos celulares y en respuesta a un reducido número de estímulos. La función de NIK en los LPCTs no está descrita. Sin embargo, NIK se encuentra sobre-expresado e implicado en la supervivencia tumoral en otras neoplasias, y se ha propuesto como posible diana terapéutica en mieloma múltiple (Annunziata et al. 2007; Pham et al. 2011; Thu et al. 2012). Aunque la vía de NF-κB se ha estudiado ampliamente durante los últimos 20 años, su regulación y aplicación en el desarrollo de estrategias antitumorales todavía no está clara. Tampoco está completamente claro como funciona la señalización de NF-κB en tumores primarios, su correlación clínica, y la relevancia clínica de los hallazgos encontrados en líneas celulares y modelos animales. Actualmente no existen inhibidores específicos para NF-κB en la práctica clínica, lo que hace necesario realizar estudios que permitan identificar nuevas dianas terapéuticas en esta vía.

OBJETIVOS

El objetivo global de este trabajo es caracterizar la expresión de NF-κB en linfomas e identificar nuevas dianas moleculares con el fin de encontrar nuevos abordajes para inhibir la activación maligna de NF-κB en estos tumores. Los objetivos específicos en las dos partes del proyecto son los siguientes:

- Caracterizar la expresión de NF-κB en muestras de pacientes de linfoma B difuso de célula grande y establecer su correlación clínica y asociación a diferentes subtipos.

- Analizar el papel de NIK en la regulación de NF-κB y en la supervivencia celular con el fin de testar NIK como posible diana molecular en los linfomas periféricos de células T.

MATERIAL Y MÉTODOS

Series amplias de muestras de pacientes diagnosticados con diferentes subtipos de linfomas (LBDCG, LPCT del tipo no especificado, linfoma T angioinmunoblástico, linfoma anaplásico de células grandes, linfoma de manto, linfoma esplénico de células marginales, linfoma folicular, y linfoma de Hodgkin) fueron recogidas en varios hospitales de España. Para evaluar la

expresión de las distintas subunidades de NF-κB en estas muestras, se han empleado técnicas de inmunohistoquímica sobre muestras parafinadas. También se han utilizado micromatrices de expresión génica del genoma completo para estudiar el perfil de expresión génica en estos tumores. Los estudios funcionales para la investigación del papel de NIK en linfomas T se han llevado a cabo en un panel de líneas celulares, representando diferentes tipos de LPTC. Para silenciar NIK u otros componentes de la vía de NF-κB en líneas celulares linfoides, se ha utilizado una técnica de electroporación, la microporación, para introducir secuencias de ARN de interferencia en las células. Para estudiar los efectos moleculares producidos en las células tras el silenciamiento de NIK, se han empleado técnicas de expresión de ARN (PCR cuantitativa, micromatrices de expresión génica) y técnicas de expresión de proteína (western blot, inmunohistoquímica, inmunofluorescencia, ELISA). Los efectos sobre muerte celular se han evaluado utilizando citometría de flujo midiendo marcadores de viabilidad celular y apoptosis.

RESULTADOS

La vía de NF-κB ha sido ampliamente estudiada en LBDCG en modelos experimentales y se ha descrito como un mecanismo fundamental en la patogénesis del subtipo ABC, pero no del subtipo GCB (Davis et al. 2001). Sin embargo, la relevancia clínica de estas observaciones no está clara, y la expresión real de NF-κB en muestras tumorales no está bien definida. En la primera parte del trabajo, la expresión nuclear de los cinco factores de NF-κB se evaluó por inmunohistoquímica en 113 muestras de pacientes con LBDCG. Este estudio reveló un perfil de expresión de los subunidades de NF-κB complejo, mostrando gran heterogeneidad, siendo la mayoría de tumores positivos para alguno de los factores de la familia. Se encontró una correlación significativa entre la expresión de subunidades de la vía clásica y la alternativa, sugiriendo que ambas vías frecuentemente se encuentran activadas en el mismo tumor. Notablemente, la expresión nuclear de NF-κB, se detectó tanto en los LBDCGs tipo GCB, como en los tipo ABC. Esta observación se confirmó en dos series independientes, donde la clasificación GCB/ABC se hizo utilizando dos abordajes diferentes: por micromatrices de expresión génica, o por inmunohistoquímia. Además, se detectó expresión nuclear de c-Rel en una gran parte de los tumores (65%), siendo su patrón de expresión diferente a la de los otros miembros de la familia ya que una tercera parte de los tumores eran positivos únicamente para c-Rel. La expresión nuclear de c-Rel también mostró ser un

marcador pronóstico favorable, asociado a una supervivencia más largo, en pacientes de LBDCG tratados con R-CHOP.

En LBDCG asociado a VEB, vimos que la expresión de la proteína viral LMP1 se correlacionaba significativamente con una activación de NF-κB, siendo el 85.7% de los casos positivos para marcadores de la vía clásica, y 92.8% positivos para marcadores de la vía alternativa.

En una serie de 77 muestras de pacientes con LPTC, al contrario que en las muestras de pacientes con LBDCG, la expresión de NF-κB se asoció de forma significativa con una supervivencia global más corta. Aunque los mecanismos moleculares de los LPTCs son desconocidos en su mayor parte, se ha sugerido que la ruta de NF-κB es uno de los mecanismos que confieren supervivencia a las células T tumorales (Sors et al. 2008; Zhao et al. 2010). Nuestra observación de que la vía de NF-κB está activada en un subgrupo de LPTCs con un curso clínico muy agresivo, nos llevó a investigar cómo interferir la activación de NF-κB de forma específica actuando sobre proteínas claves en la activación de la vía.

Se analizó el papel de la quinasa NIK en los LPTCs con el fin de investigar su función en la regulación de la vía de NF-κB y en la supervivencia de células de LPTC. Para ello, se midió la expresión de NIK a nivel de ARNm por PCR cuantitativa en líneas celulares de LPTC y en células T de pacientes con síndrome de Sézary (un subtipo de LPTC). Se observó que NIK se encontraba muy sobre-expresado en un grupo de tumores y líneas celulares, comparado con linfocitos T de donantes sanos. Esta sobre-expresión de NIK a nivel de ARNm se correlacionaba también con niveles más altos de la proteína NIK. Utilizando datos de expresión génica de micromatrices, en una serie de 27 casos de LPTC, vimos que la expresión de NIK en estos tumores se correlacionaba significativamente con la expresión de los genes diana de NF-κB, sugiriendo que NIK pueda estar implicado en la regulación de NF-κB en LPTC.

Esta observación se confirmó también en estudios funcionales. Utilizando ARN de interferencia, silenciamos NIK en dos líneas celulares derivadas de LPTC. El silenciamiento de NIK dio lugar a una reducción de los niveles de expresión tanto de p52 (vía alternativa) como de p50 (vía clásica). Un ensayo ELISA específico para evaluar la actividad de unión al ADN de los factores de NF-κB, confirmó que la reducción observada de NF-κB se correspondía a una disminución de actividad tanto de la vía alternativa (p52 y RelB) como de la vía clásica (p50,

p65 y c-Rel). Estos resultados indican que NIK está implicado en la regulación de ambas vías. Notablemente, sólo el silenciamiento de NIK y no el silenciamiento de IKKα o/y IKKβ, resultó en una reducción fuerte de los niveles de p50 y p52, indicando que la función de NIK en la vía de NF-κB está, al menos en parte, regulada por mecanismos independientes de IKKα y IKKβ.

Para validar NIK como posible diana terapéutica en LPTC, medimos el efecto del silenciamiento de NIK sobre la apoptosis y la viabilidad celular. El silenciamiento de NIK resultó en un incremento en muerte celular en células de LPTC, medido con AnnexinaV/DAPI por citometría de flujo. Siete días tras la transfección con siNIK (el ARN de interferencia usados para silenciar NIK), apenas el 2% de las células permanecían vivas. La detección de caspasa 3 y PARP procesadas, confirmó la inducción de apoptosis. Sólo las líneas celulares con niveles basales altos de NIK se vieron afectadas por siNIK, mientras que las células con bajos niveles de NIK no presentaban cambios en su viabilidad. El silenciamiento de otros componentes de la ruta de NF-κB, como IKKα y β, no dio lugar a una respuesta apoptótica tan profunda como tras el silenciamiento de NIK, sugiriendo que NIK pueda ser una diana terapéutica más eficaz incluso que IKK, la diana de inhibición de NF-κB habitualmente utilizada hasta ahora.

Al silenciar las subunidades de NF-κB expresados en LPTC (c-Rel, RelB, p52 y p50), observamos que únicamente el silenciamiento de c-Rel provocó una inducción de apoptosis en las líneas celulares que eran sensibles para siNIK. La reducción de los niveles nucleares de c-Rel después de tratar las células con siNIK, sugiere que al menos parte de la supervivencia inducida por NIK, podría ser mediada por c-Rel. En cambio, la pérdida de la actividad alternativa de NF-κB, mediante ARN de interferencia contra RelB y p52, no pudo explicar los efectos de siNIK sobre la viabilidad celular, descartando que el efecto de NIK esté mediado únicamente por la vía alternativa.

Para conocer mejor los mecanismos de supervivencia regulados por NIK, utilizamos la técnica de micromatrices de expresión génica para comparar los perfiles de expresión entre células control y células silenciadas con siNIK en dos líneas celulares. Utilizando *Gene Set Enrichment Analysis* (GSEA) confirmamos que la expresión de los genes dianas de NF-κB se perdía tras el silenciamiento de NIK, validando el papel de NIK en la activación funcional de la vía. Otras vías alteradas tras la inhibición de NIK fueron la vía de JAK/Stat, las dianas del

factor de transcripción XBP1 y la señalización por interleuquinas. Entre los genes perdidos en las células transfectadas con siNIK, se encontraban los genes anti-apoptoticos BCL2L1 (Bcl-x(L)) y CFLAR (c-FLIP) y las interleuquinas relacionadas con cáncer, IL6 y IL21. Otros genes alterados no relacionados con NF-κB fueron los oncogenes PON2 y YAP1 y el supresor tumoral KLF2. Por lo tanto, el perfil génico tras silenciar NIK en estos linfomas, altera la expresión de múltiples genes y rutas de señalización implicados en proliferación y supervivencia. El efecto de siNIK sobre la vía de JAK/Stat se confirmó por western blot, detectando niveles reducidos de las formas fosforilados de STAT3 y STAT5. También se vio que la adición de IL21 al medio de cultivo tras el silenciamiento de NIK, provoca un re-establecimiento de los niveles de p-STAT3 y p-STAT5, proponiendo un posible enlace entre NIK y la activación de JAK/Stat en estos tumores.

DISCUSIÓN

La mayoría de los estudios publicados sobre la vía de NF-κB, se han realizado utilizando líneas celulares o modelos animales. Nuestro estudio, al haberse realizado sobre muestras de pacientes de linfoma, establece un enlace translacional de gran relevancia para futuros estudios. También es el primer estudio que analiza el papel de los cinco subunidades de NF-κB en linfomas humanos, aportando así una visión más completa de la vía. La heterogeneidad y complejidad observada en la expresión de los distintos factores de transcripción, pone de manifiesto la diversidad que existe en la señalización por NF-κB e indica que la expresión real de NF-κB en los tumores, no refleja el patrón de señalización habitualmente descrito. Aún así, la formación de dímeros entre una variedad de subunidades de NF-κB y entre NF-κB y factores atípicos, han sido descritos previamente (24). Así mismo, la activación de la transcripción mediada por dímeros formados por CD40 y c-Rel, ya habían sido descritos en LBDCG (Zhou et al. 2007). Nuestra observación de que c-Rel se detecta frecuentemente en el núcleo en ausencia de otros factores de NF-κB, podría explicarse por este motivo, y la futura evaluación de CD40 en esta serie de muestras de LBDCG sería de gran interés. Estos resultados también nos demuestran que la evaluación de sólo una o un par de subunidades de la familia de NF-κB, llevaría a una subestimación de la expresión real de NF-κB. La observación de que la expresión de NF-κB no sólo es una característica del subtipo ABC, sino también del GCB, está apoyada por estudios previos que también muestran que hay activación de NF-κB en el subtipo GCB (Pham et al. 2011; Espinosa et al. 2008). Otros estudios demuestran datos opuestos, correlacionando la

activación de NF-κB con el subtipo ABC (Compagno et al. 2009; Bavi et al. 2011). Una diferencia importante entre nuestro trabajo y estudios previos, es que en nuestro estudio, se han excluido los casos positivos para el virus de Epstein-Barr (VEB), pero no en otros estudios publicados. Los LBDCG asociados a VEB presentan un curso clínico y características moleculares distintos a los casos VEB negativos, por lo que se ha propuesto que LBDCG asociado a VEB ha de ser considerado como un subtipo de linfoma distinto (Swerdlow et al. 2008). Como los LBDCG asociados a EBV se caracterizan por una activación de NF-κB y un fenotipo ABC (Montes-Moreno et al. 2012), la inclusión de estos casos en el análisis puede modificar significativamente los resultados. Existen pocas publicaciones sobre la correlación clínica de NF-κB, y los estudios que hay son contradictorios. En nuestra serie de pacientes, c-Rel es capaz de identificar a un subgrupo de casos asociado a supervivencia global mayor. La expresión de c-Rel se ha descrito anteriormente como un factor de pronóstico desfavorable en una serie de pacientes de DLBCL tipo GCB (Curry et al. 2009). Sin embargo, ese estudio se realizó en pacientes tratados con CHOP, mientras que el presente análisis incluye solamente pacientes tratados con R-CHOP, la terapia estándar utilizada hoy en día.

El linfoma periférico de células T es un tipo de linfoma con un curso clínico altamente desfavorable para el que actualmente no existen terapias efectivas. Nuestra observación de que la expresión nuclear de NF-κB puede distinguir un subgrupo de estos tumores con una supervivencia aún peor, junto con publicaciones previas indicando la implicación de NF-κB en la patogénesis de LPCT (Sors et al. 2006; Foss et al. 2011), nos llevó a investigar nuevos abordajes para inhibir la activación de NF-κB en estos tumores. La sobre-expresión de NIK en un grupo de líneas celulares y muestras de pacientes con LPCT, nos hizo centramos en el estudio del papel de NIK. Utilizando varias técnicas diferentes, demostramos el papel fundamental de NIK en la regulación tanto de la vía clásica como de la alternativa de NF-κB en LPCT. El silenciamiento de NIK indujo apoptosis en líneas celulares de LPCT de manera selectiva, afectando sólo a las líneas caracterizadas por una sobre-expresión de NIK. La función fundamental de NIK en la supervivencia de estas células, viene reflejada por los genes cuya expresión se alteró por el silenciamiento de NIK, incluyendo genes que codifican para proteínas anti-apoptoticas implicadas en el patogénesis de PTCL, como c-Flip y Bcl-XL (Rassidakis et al. 2003; Al-Yacoub et al. 2012), y las interleuquinas pro-tumorales IL-6 y IL21 (Grivennikov et al. 2009; Ma et al. 2011). NIK también manifestó ser un regulador de la vía de JAK/STAT ya que el silenciamiento de NIK resultó en una pérdida de expresión de genes incluidos en la ruta de señalización de JAK/STAT (identificados por micromatrices de

expresión génica), y en una disminución de los niveles de fosforilación de STAT3 y STAT5. Nuestros datos sugieren que un posible mediador entre NIK y la vía de JAK/STAT es IL21. Aunque hemos demostrado que IL21 puede inducir la fosforilación de STAT3 y STAT5 en estos tumores, se necesitan estudios adicionales para verificar su papel en la señalización de NIK. Además, la supervivencia inducida por NIK, se puede explicar en parte por su regulación del factor de transcripción c-Rel, cuya inhibición por sí sola produjo apoptosis en estas líneas celulares. Por tanto, proponemos NIK como una posible diana terapéutica en LPCT por varios motivos. Primero, el silenciamiento de NIK induce una fuerte respuesta de apoptosis en células de LPCT. Segundo, el efecto citotóxico es selectivo sobre las células que expresan altos niveles de NIK, lo que indica que NIK no es necesario para la supervivencia de los linfocitos T normales y limitaría posibles efectos secundarios. Tercero, la inhibición de NIK sería una buena estrategia para interferir la actividad de vías de supervivencia claves en el patogénesis de varios tipos de LPCT, como son la vía de NF-κB y la vía de JAK/STAT. Además, el silenciamiento de NIK demostró ser más efectivo en la inducción de muerte celular que el silenciamiento de IKKβ o IKKα. Y por último, aunque el *knockout* de NIK en ratones altera el desarrollo de los órganos linfáticos, el fenotipo global no presenta mayores incompatibilidades en las funciones vitales normales (Yin et al. 2001), sugiriendo que una inhibición de NIK puede ser un abordaje seguro. Distintos mecanismos dan lugar a una activación de NF-κB en los diferentes tipos tumorales, y la identificación de estos mecanismos es fundamental para poder desarrollar estrategias terapéuticas seguras que permitan interferir de forma selectiva en la actividad maligna de NF-κB.

CONCLUSIONES

1. La expresión de NF-κB en tejidos tumorales de LBDCG presenta un patrón complejo y heterogéneo que no refleja la cascada prototípica de señalización de NF-κB.

2. La expresión de LMP1 en LBDCG asociado al virus de Epstein-Barr, define tumores con activación de NF-κB.

3. No existe ninguna correlación significativa entre la expresión de NF-κB y los subtipos ABC o GCB de LGDCG. Componentes de la vía alternativa y clásica se expresan en ambos subtipos.

4. La expresión nuclear de c-Rel identifica un grupo de pacientes de LGDCG con un pronóstico favorable.

En la segunda parte del proyecto, dedicada al estudio de NIK y NF-κB en linfomas periféricos de células T, podemos concluir lo siguientes:

5. Los pacientes cuyos tumores expresan NF-κB nuclear, presentan un curso clínico desfavorable con una supervivencia más corta que los pacientes con tumores negativos para NF-κB.

6. NIK está sobreexpresado en un grupo de líneas celulares y muestras tumorales de LPCT.

7. NIK regula la activación de la vía clásica y alternativa de NF-κB in LPCT. NIK controla la señalización de NF-κB, al menos en parte, mediante mecanismos independientes de IKK.

8. NIK es necesario para la supervivencia de células de LPCT. El silenciamiento de NIK resultó en apoptosis en células con niveles basales altos de NIK, pero no en células con baja expresión de NIK. El silenciamiento de NIK dio lugar una reducción de viabilidad celular más potente que el silenciamiento de IKKβ o IKKα.

9. C-Rel es necesario para la supervivencia de células de LPCT positivas para NIK.

10. NIK regula la expresión de múltiples genes implicados en supervivencia de LPCT, como son los genes que codifican para las proteínas anti-apoptoticas Bcl-XL y c-Flip, las citoquinas IL-6 y IL-21, y el supresor tumoral KLF-2. NIK también está implicado en la ruta de señalización de JAK/STAT.